REMARKS

Claims 7-12, 15-17, 22-25 and 29-37 are currently pending in this application, where claims 22-25 are withdrawn as being directed to non-elected subject matter and claims 30-37 are indicated as allowable.

Claims 1 -6, 13-14, 26-28 and 38 were previously cancelled and claims 18-21 are presently cancelled without prejudice or disclaimer to the subject matter contained therein.

Claims 7, 12 and 17 are amended. Claim 7 is amended to incorporate the limitation "a infectious RNA transcript of JEV is transcribed directly from the cDNA clone," claim 12 is amended to remove non-elected subject matter, and claim 17 is amended to be consistent with claim 15 from which claim 17 depends. Support for the amendments can be found throughout the present specification as originally filed, including, for example, previous claim 18 now cancelled.

The amendment and the cancellation of the claims are solely for advancing prosecution. Applicants, by amending or canceling any claims herein, make no admission as to the validity of any rejection made by the Examiner against any of these claims. Applicants reserve the right to reassert the original claim scope of any claim amended herein, in a continuing application.

Applicants thank the Examiner for reinstating and examining the previously withdrawn claims 34-37, and for the indication that claims 30-37 are allowable. Applicants also thank the Examiner for an indication of allowability of claims 12 and 15-17, although they remain objected to a being dependent on a rejected claim.

The Specification is amended with regard to the section "Brief description of the drawings." In particular, the Specification is amended in the paragraph at page 36, line 4 to page 37, line 13 as originally filed, which describes Figure 3. The paragraph as amended contains sequence identifiers SEQ ID NOs. 68-71 for the sequences described in Figure 3 as originally filed.

The Sequence Listing is substituted with the ninety-five (95) pages of substitute sheets for Sequence Listing. In the substitute sheets, the sequence listing has been amended to provide sections <210> - <213>, <220>, <223> and <400> for each of the sequences presented in the original Figure 3.

No new matter is introduced in the claims and the specification within the meaning of 35 U.S.C. §132. Accordingly, entry of the amendments to the claims and the specification is respectfully requested.

Further, no new matter is introduced in the amendment to the sequence listing within the meaning of 35 U.S.C. §132. The submission, attached hereto in accordance with the relevant sections of 37 CFR 1.821, does not include new matter and the content of the attached paper copy; and the attached computer readable copy of the Sequence Listing are the same. Therefore, entry of the amendment is respectfully requested.

I. At page 5 of the Official Action, the specification is objected to for the informalities that Figure 3 includes sequences which are not properly indentified by sequence identifier.

Applicants submit that the sequences as presented in Figure 3 are identified in the substitute sheets of Sequence Listing as SEQ ID NOs. 68-71, respectively. Also, the Specification as amended describes in the section "Brief description of the

Applicants submit that the sequences as presented in Figure 3 are identified in the substitute sheets of Sequence Listing as SEQ ID NOs. 68-71, respectively. Also, the Specification as amended describes in the section "Brief description of the drawings" the four sequences presented in Figure 3 using sequence identifier SEQ ID NO. 68 for the 5' termini of full-length JEV cDNA clone, tatagagaag; SEQ ID NO. 69 for the 3' termini of SP6- or T7-driven JEV cDNA template digested with XhoI, aggatccgag; SEQ ID NO. 70 for the 3' termini of SP6- or T7-driven JEV cDNA templated digested with XbaI, aggatctcta ga; and SEQ ID NO. 71 for the 3' termini of JEV cDNA template treated with mung bean nuclease, aggatct.

Accordingly, Applicants submit that each of the sequences in Figure 3 is properly described using sequence identifiers SEQ ID NOs. 68-71, respectively, in the description of Figure 3, as required by 37 CFR §1.821.

Accordingly, withdrawal of this objection is respectfully requested.

II. At page 5 of the Official Action, claims 12 is objected for the informalities that it contains multiple sequence identifiers drawn to non-elected subject matter.

Applicants submit that presently pending claim 12, as amended, does not contain multiple sequence identifiers drawn to non-elected subject matter. Accordingly, withdrawal of this objection is respectfully requested.

Applicants note that at page 3 the Official Action states that the objection to claim 15 has been maintained. However, considering that claim 15 has been previously amended not to contain multiple sequence identifiers and the same objection is not presented under the title "New Objections" in the Official Action, Applicants believe that

the previous objection to claim 15 is withdrawn in this Official Action. *See* page 3 1st and 2nd paragraphs under the title "Claim Objections."

III. At page 5 of the Official Action, claim 7-11, 18-19, 21 and 29 are rejected as being unpatentable over Zhang et al. (Journal of Virological Methods, Aug.2001, Vol. 96, No. 2, pp. 171-182) in view of Venugopal et al. (Vaccine, 1995, Vol. 13, No.11, pp. 1000-1005).

As a basis for the rejection, the Official Action states in relevant part:

> ...Zhang et al. (hereinafter Zhang) teaches a technique to produce genome length cDNA stable clone from Japanese encephalitis virus (Abstract). The cDNA has a T7 promoter at the 5' end and a "run-off' transcript with vector sequences at either end (Abstract). The full-length amplicon was cloned into a vector under the SP6 promoter (Abstract). The RNA transcript was synthesized from the clone (page 174-175, connecting paragraph). Zhang teaches Japanese encephalitis virus genome lacks a poly-A tail at the 3'-terminus (page 176, 1st column). Zhang teaches RNA transcripts were transfected into BHK-21 cells (page 175, 1st column, 1st paragraph). Zhang teaches Japanese encephalitis virus has short untranslated regions (page 172, 1st column, 1st paragraph). Zhang teaches amplification of the full-length JEV genome by novel long RT-PCR protocol, transcription of infectious RNA directly from the amplicon and construction of a stable full-length JEV cDNA clone (page 173, 1st column, 2nd paragraph). Zhang also teaches the transcript from the clone was non-infectious, however, the transcript from the amplicon of the clone was infectious (page 180, top of 2nd col.).
>
> ... Zhang does not teach the cDNA of JEV cloned into a BAC vector. Venugopal et al. (herein after Venugopal) teaches protective immunogens of flaviviruses produced in a recombinant baculovirus expression system has been shown to be successful in animal models (Abstract). Venugopal teaches the cDNA clone was transcribed into the baculovirus vector (p. 1001, 1st col. 2nd para.). Venugopal teaches the recombinant baculovirus vector expressing St. Louis encephalitis (SLE) virus proteins showed significant protective immune responses against SLE virus in mice (60% survival) (p. 1003, 1st col. 2nd full para.). Therefore Venugopal teaches using a BAC vector with another encephalitis virus of the flavivirus family. It would have been prima facie obvious to the person of ordinary skill in the art at the time of the invention was made to use a baculovirus vector. The person of ordinary skill in the art would have been motivated to use a BAC vector because it is a common vector used in the rat and Venugopal teaches the BAC vector provided protective immune response with a flavivirus, and reasonably would have expected success because of the teachings of Zhang and Venugopal.

Applicants respectfully traverse this rejection with regard to presently pending claims 7-11, 21 and 29. Applicants note that to establish a *prima facie* case of obviousness, the PTO must satisfy three requirements. First, as the U.S. Supreme Court recently held in *KSR International Co. v. Teleflex Inc., 550 U.S. 398 (2007)*, "a court must ask whether the improvement is more than the predictable use of prior art elements according to their established functions. ... it can be important to identify a reason that would have prompted a person of ordinary skill in the relevant field to combine the elements in the way the claimed new invention does... because inventions in most, if not all, instances rely upon building blocks long since uncovered, and claimed discoveries almost of necessity will be combinations of what, in some sense, is already known." Second, the proposed modification of the prior art must have had a reasonable expectation of success, determined from the vantage point of the skilled artisan at the time the invention was made. *Amgen Inc.* v. *Chugai Pharm. Co.*, 18 USPQ 1016, 1023 (C.C.P.A 1970). Lastly, the prior art references must teach or suggest all the limitations of the claims. *In re Wilson*, 165 USPQ 494, 496 (C.C.P.A. 1970).

Further, Applicants note that a *prima facie* case of obviousness can be rebutted if the claimed invention yields unexpectedly improved properties or properties not presented in the prior art. *In re Dillon*, 919 F.2d at 692-93, 16 USPQ2d at 1901.

In the present application, Applicants submit that not only a *prima facie* case of obviousness has not been established by the Examiner since all of the limitations of the present claims are not disclosed or taught by the prior art, but also any *prima facie* case of obviousness, if established, is rebutted by the unexpected results of the presently claimed subject matter, as follows:

Presently claimed subject matter

As clearly presented in the broadest claim 7 as amended, the present subject matter is drawn to "A full length ***infectious*** and genetically stable cDNA clone of Japanese encephalitis virus (JEV), wherein a full length cDNA of JEV is cloned into a ***bacterial artificial chromosome (BAC)*** and an infectious RNA transcript of JEV is transcribed directly from the cDNA clone."

All of pending claims 8-11, 21 and 29 directly or indirectly, dependent from claim 7 and thus contain all the limitations of claim 7 as above. If an independent claim is nonobvious under 35 U.S.C. §103, then any claim depending therefrom is nonobvious. *In re Fine*, 837 F.2d 1071, 5 USPQ2d 1596 (Fed. Cir. 1988).

Zhang et al. not only fail to teach "infectious" cDNA clone of JEV, but also fail to teach use of "bacterial" artificial chromosome (BAC) vector.

Zhang et al. describes a genetically stable cDNA clone of JEV which is ***non-infectious***. In Zhang et al., what is described as infectious is only an amplicon (a cDNA molecule ***not a clone***) produced by long RT-PCR using the cDNA clone as a template and RNA transcripts transcribed from the amplicon.

In this regard, Applicants would draw the Examiner's attention to the fact that ***an infectious cDNA clone is distinguished from an infectious cDNA molecule*** since the former is capable of self-replicating but the latter isn't. Actually, an infectious cDNA molecule of JEV which is not cloned is well known in the art. Indeed, the infectious cDNA molecule can be produced using direct RT-PCR without cloning. *See* Zhang et al., lines 38-42, right column of p. 172. However, no one succeeded in producing an infectious cDNA clone of JEV, including Zhang et al., prior to the presently claimed subject matter. As supported by the references, which are attached hereto as Exhibit A

to D, of which Exhibit B is the work of the present inventors, it has been recognized in the art that an infectious cDNA clone of a particular RNA virus is a cloned cDNA capable of producing infectious RNA transcripts transcribed therefrom. *See* Exhibit A: Mendez *et al.*, *J. Virol.*, 1998, 72(6): 4737-4745, particularly at page 4743, right column; Exhibit B: Yun *et al., J. Virol.*, 2003, 77(11): 6450-6465, particularly at page 6450, Abstract part, right column, lines 6-7, and left column, lines 22-26; Exhibit C: Rice *et al.*, *J. Virol.*, 1987, 61(12): 3809-3819); and Exhibit D: Lai *et al.*, *Proc. Nati. Acad. Sci. USA* , 1991, 88: 5139-5143, particularly at page 5139, right col., lines 16-20 and 29-33. These references are also submitted as Information Disclosure Statement herewith. Indeed, nowhere do Zhang et al. describe that they produced an infectious cDNA clone of JEV. Rather, they describe that they constructed a stable genome-size cDNA clone of JEV. Accordingly, Zhang et al. recognize the difference between an infectious cDNA clone of JEV and a simple full-length cDNA clone of JEV.

Further, Zhang et al. ***fail to teach the bacterial artificial chromosome (BAC)*** vector, as the Examiner admits in the Official Action. *See*, last line of page 6, the Official Action.

Venugopal et al. do not remedy the deficiencies of Zhang et al.

Venugopal et al. do not remedy the lack of teaching of "infectious" cDNA clone of JEV in Zhang et al., nor teach or suggest BAC (bacterial artificial chromosome) vector. In particular, regarding BAC, Venugopal *et al.* rather describe a baculovirus vector, which is different from BAC vector as required by the presently claimed subject matter. Applicants draw the Examiner's attention to that the ***baculovirus described in Venugopal et al., is a kind of "insect" viruses which is used for transfecting***

insect cells. Whereas, the BAC vector used in the presently claimed subject matter is a "***bacterial***" vector.

Further, Venugopal et al. did not clone a full-length cDNA of flavivirus. Rather, Venugopal et al. cloned some genes encoding particular viral peptides. Accordingly, Venugopal et al., taken alone or in combination with Zhang et al., do not remedy the deficiencies of Zhang et al.

As such, each of Zhang et al. and Venugopal et al., taken alone or in combination, fails to teach or suggest all of the limitations of the presently claimed subject matter, as required by *In re Wilson*. Applicants respectfully assert that a *prima facie* case of obviousness has not been established in this application.

The presently claimed subject matter shows unexpected results from the prior arts.

As described above, only in the present application the production of an infectious cDNA clone of JEV has been achieved. This cannot be expected from prior art. No prior arts could succeed in producing an infectious cDNA clone of JEV - all of prior art being failure cases for producing an infectious cDNA clone of JEV. The prior arts instead used two separate clones (which is not a clone, rather are clones) and then ligated fragments derived from the separate clones.

Further, infectious RNA transcripts produced either by conventional methods (i.e., cloning JEV cDNA as 2 fragments and producing RNA transcripts using *in vitro* transcription after *in vitro* ligation of the two fragments) or by the method of Zhang et al., are less effective for infecting mammalian cells. The RNA transcripts produced by the instant cDNA clone of JEV showed very high infectivity (exceeding PFU/ml) which is over 10^4-fold higher than that of conventional methods. Accordingly, Applicants submit

that any *prima facie* case of obviousness, if established, is rebutted by the unexpected results of the presently claimed subject matter.

In view of the foregoing, Zhang et al. fails to teach or suggest the construction of an ***infectious*** cDNA ***clone*** of JEV, as well as a bacterial artificial chromosome (BAC), and Venugopal et al. neither remedy the deficiencies of Zhang et al. Further, the presently claimed subject matter shows remarkable effects which are not expected from prior arts of record.

Accordingly, nothing in Zhang et al. and Venugopal et al., each of reference being taken alone or in combination, can render the presently claimed subject matter obvious under the meaning of 35 USC 103(a).

IV. At page 5 of the Official Action, claim 20 is rejected as being unpatentable over Zhang et al. (Journal of Virological Methods, Aug.2001, Vol. 96, No. 2, pp. 171-182) in view of Venugopal et al. (Vaccine, 1995, Vol. 13, No.11, pp. 1000-1005) and further in view of Sumiyoshi et al. (Journal of Virology, 1992, Vol. 66, No. 9, pp. 5425-5431).

Applicants submit that the rejected claim 20 has been canceled in the pending claims and this rejection is moot.

CONCLUSION

Based upon the above remarks, the presently claimed subject matter is believed to be patentably distinguishable over the prior art of record. The Examiner is therefore respectfully requested to reconsider and withdraw the rejections of claims 7-11, 21 and 29 and allow all pending claims presented herein for reconsideration. Favorable action with an early allowance of the claims pending in this application is earnestly solicited. The Examiner is invited to contact the undersigned attorney if it is believed that such contact will expedite the prosecution of the application.

Respectfully submitted,

THE NATH LAW GROUP

Date: October 19, 2009

By _____

Gary M. Nath
Registration No. 26,965
Tanya E. Harkins
Registration No. 52,993
Customer No. 20529

THE NATH LAW GROUP
112 S. West Street
Alexandria, VA 22314
(703) 548-6284

GMN/TEH/MSK.froa

MAIL STOP AMENDMENT
Attorney Docket No. 26689U

IN THE UNITED STATES PATENT AND TRADEMARK OFFICE

In re Application of:

Lee, et al. Confirmation No.:2581

Serial No.: 10/529,169 Group Art Unit: 1648

Filed: March 24, 2005 Examiner: HURT, Sharon L.

For: **NOVEL FULL-LENGTH GENOMIC RNA OF JAPANESE ENCEPHALITIS VIRUS, INFECTIOUS JEV CDNA THEREFROM, AND USE THEREOF**

APPENDIX

Exhibit A to D

Exhibit A: Mendez *et al.*, *J. Virol.*, 1998, 72(6): 4737-4745.

Exhibit B: Yun *et al., J. Virol.*, 2003, 77(11): 6450-6465.

Exhibit C: Rice *et al.*, *J. Virol.*, 1987, 61(12): 3809-3819).

Exhibit D: Lai *et al.*, *Proc. Nati. Acad. Sci. USA* , 1991, 88: 5139-5143,

JOURNAL OF VIROLOGY, June 1998, p. 4737–4745
0022-538X/98/$04.00+0

Vol. 72, No. 6

Infectious Bovine Viral Diarrhea Virus (Strain NADL) RNA from Stable cDNA Clones: a Cellular Insert Determines NS3 Production and Viral Cytopathogenicity

ERNESTO MENDEZ,[1]† NICOLAS RUGGLI,[1] MARC S. COLLETT,[2] AND CHARLES M. RICE[1]*

Department of Molecular Microbiology, Washington University School of Medicine, St. Louis, Missouri 63110-1093,[1] and ViroPharma Incorporated, Exton, Pennsylvania 19341[2]

Received 31 July 1997/Accepted 10 February 1998

Bovine viral diarrhea virus (BVDV), strain NADL, was originally isolated from an animal with fatal mucosal disease. This isolate is cytopathic in cell culture and produces two forms of NS3-containing proteins: uncleaved NS2-3 and mature NS3. For BVDV NADL, the production of NS3, a characteristic of cytopathic BVDV strains, is believed to be a consequence of an in-frame insertion of a 270-nucleotide cellular mRNA sequence (called cIns) in the NS2 coding region. In this study, we constructed a stable full-length cDNA copy of BVDV NADL in a low-copy-number plasmid vector. As assayed by transfection of MDBK cells, uncapped RNAs transcribed from this template were highly infectious (>10^5 PFU/μg). The recovered virus was similar in plaque morphology, growth properties, polyprotein processing, and cytopathogenicity to the BVDV NADL parent. Deletion of cIns abolished processing at the NS2/NS3 site and produced a virus that was no longer cytopathic for MDBK cells. This deletion did not affect the efficiency of infectious virus production or viral protein production, but it reduced the level of virus-specific RNA synthesis and accumulation. Thus, cIns not only modulates NS3 production but also upregulates RNA replication relative to an isogenic noncytopathic derivative lacking the insert. These results raise the possibility of a linkage between enhanced BVDV NADL RNA replication and virus-induced cytopathogenicity.

Bovine viral diarrhea virus (BVDV), classical swine fever virus (CSFV), and border disease virus are members of the pestivirus genus, a group of important animal pathogens in the family *Flaviviridae* (24, 32). The spread and maintenance of BVDV in cattle involves two kinds of infections (1, 32). Most infections are acute and self-limiting, with effective clearance of the virus. In contrast, infection of pregnant animals early in gestation can lead to efficient transplacental transmission of the virus to the fetus and birth of a persistently infected, BVDV-immunotolerant calf. Such animals are the main reservoir for BVDV, shedding virus for the life of the animal. Sporadically, these animals develop a uniformly fatal pathology called mucosal disease (MD). Two types of BVDV, distinguishable by their ability to cause cytopathic effect (CPE) in cell culture, can be isolated from animals with MD. Strains responsible for establishing persistent infections are typically noncytopathic (non-CP), whereas both non-CP and CP strains can be isolated from animals exhibiting MD. Considerable data suggest that CP strains are derived from non-CP strains by rare RNA recombination events (17).

The typical non-CP pestivirus genome is approximately 12.5 kb in length and consists of a 5′ nontranslated region (NTR), a single open reading frame encoding all viral polypeptides, and a nonpolyadenylated 3′ NTR (17). Uncapped pestivirus mRNA is translated via internal initiation (23, 26) to produce a polyprotein that is cleaved into 11 to 12 polypeptides by host and viral proteases (17). The first protein, N^{pro}, possesses an autoproteolytic activity responsible for cleavage at its own C terminus. Downstream cleavages producing the structural components of the virion, C, E^{rns}, E1, and E2, are mediated mainly by cellular signal peptidase (although the enzyme responsible for cleavage at the E^{rns}/E1 junction has not been defined). The nonstructural (NS) portion of the polyprotein is processed at four sites (3/4A, 4A/4B, 4B/5A, and 5A/5B) by a BVDV-encoded serine protease activity (29, 35, 36). The catalytic domain of this enzyme resides in the NS3 region and requires the NS4A protein as a cofactor for cleavage of at least two sites (4B/5A and 5A/5B) (36).

Surprisingly, processing of the NS2-3 region differs between non-CP and CP BVDV isolates (see reference 17 for a review). Cleavage at the NS2/NS3 junction is not observed for non-CP BVDV. In contrast, a discrete NS3 protein is observed for all CP BVDV strains studied to date (10, 11). Depending on the CP isolate, processing at the NS2/NS3 junction is accomplished by several different strategies, but most appear to involve RNA recombinational events. These observations have led to the hypothesis that MD pathogenesis is linked to the generation of CP BVDV and, in particular, to the recombination events which lead to NS3 production. RNA recombination events linked to NS3 production include duplication and rearrangement of pestivirus sequences, insertion of cellular sequences, and large in-frame deletions resulting in subgenomic defective interfering (DI) RNAs (see reference 17 for a review). For some CP isolates, the mechanism by which NS3 is produced is clear. In several strains, in-frame insertion of cellular ubiquitin (Ub) sequences adjacent to the NS3 N terminus provides a processing site for cellular Ub carboxyl-terminal hydrolase. In other cases, a duplicated N^{pro} autoprotease sequence fused to NS3 mediates the cleavage producing the NS3 N terminus. Recently, subgenomic (~7.5-kb) CP BVDV DI RNAs with large in-frame deletions were identified (14, 31). These CP DI RNAs require a non-CP helper virus for spread and/or repli-

* Corresponding author. Mailing address: Department of Molecular Microbiology, Washington University School of Medicine, 660 S. Euclid Ave., St. Louis, MO 63110-1093. Phone: (314) 362-2842. Fax: (314) 362-1232. E-mail: rice@borcim.wustl.edu.

† Permanent address: Departamento de Genética y Fisiología Molecular, Instituto de Biotecnología/UNAM, Cuernavaca, Morelos, 52271, Mexico.

Exhibit A

cation. For CP9, the sequences encompassing the coding region of C through NS2 have been deleted such that N^{pro} is fused directly to NS3 (31). In CP13, two deletions have resulted in the fusion of 13 N^{pro} residues and 10 E1 residues to NS3, with the NS3 N terminus truncated by five residues relative to the Ub- and N^{pro}-NS3 fusion junctions (14). A CP DI RNA for CSFV in which all sequences between the methionine initiating the open reading frame and NS3 have been deleted has also been identified (18–20).

For two CP strains, CP7 and NADL, the mechanism(s) by which NS3 is produced remains obscure. Both isolates contain insertions in the NS2 region, apparently upstream of the NS2/NS3 (2/3) cleavage site. For CP7, the insertion is a duplicated viral sequence of 27 nucleotides which somehow promotes processing at the 2/3 site, NS3 production, and cytopathogenicity in cell culture (16, 30). In the case of the American prototype CP BVDV strain, NADL, the insert is a 270-base portion of a bovine mRNA of unknown function (called cIns [cellular insertion]) that results in an in-frame insertion of 90 amino acid residues.

To investigate the mechanism of NS3 production and cytopathogenicity by BVDV NADL, we constructed a stable, functional cDNA clone for this virus. Using this clone, we have gone on to engineer an isogenic derivative in which cIns has been deleted. Virus production, NS2-3 protein processing, accumulation of virus-specific proteins and RNA, and cytopathogenicity were then assessed. Our results indicate that cIns is necessary for NS3 production and the CP phenotype.

MATERIALS AND METHODS

Cells and viruses. MDBK cells were propagated in Dulbecco's modified minimal essential medium (DMEM) supplemented with sodium pyruvate and heat-inactivated 10% horse serum (HS). Cells were maintained at 37°C with 5% CO_2.

The NADL strain of BVDV was obtained from the American Type Culture Collection, plaque purified, and amplified by growth in MDBK cells. For infection of MDBK cells, virus dilutions made in DMEM-HS were adsorbed for 1 h at 37°C; then the inoculum was removed and replaced with fresh DMEM-HS. Cultures were incubated at 37°C for 48 h, or until CPE was observed. Virus stocks were prepared by three freeze-thaw cycles of cells in their culture medium and clarified by centrifugation at 1,000 × *g* for 5 min.

BVDV plaque and focus-forming assays. MDBK cells (70 to 80% confluent) were infected with 10-fold dilutions of virus as described above. Following 1 h of adsorption at 37°C, cells were washed once with DMEM, overlaid with 1.5% low-melting-point (LMP) agarose (Gibco-BRL) in MEM containing 5% HS, and incubated at 37°C. To assay for plaque-forming virus, after 3 days monolayers were fixed with 3.7% formaldehyde for 2 h at room temperature, the agarose plugs were removed, and the monolayers were stained with crystal violet (25). Foci produced by non-CP BVDV were visualized by immunostaining. After fixation with formaldehyde, agarose plugs were removed, and cells were permeabilized with Triton X-100 (0.25% in phosphate-buffered saline [PBS]) for 10 min, washed once with PBS, and then incubated with a bovine polyclonal anti-BVDV serum (α49; 1/1,000 dilution in PBS) (5) for 1.5 h. Monolayers were washed two times with PBS, incubated with peroxidase-conjugated rabbit anti-bovine immunoglobulin (1/1,000 dilution in PBS; catalog no. A-5295; Sigma Chemical Co.). After 1.5 h, excess second antibody was removed by washing the monolayer two times with PBS, and foci of BVDV-specific antigens were visualized by using the peroxidase substrate 3-amino-9-ethylcarbazole (catalog no. A-5754; Sigma).

Construction of a full-length BVDV NADL cDNA clone in a low-copy-number plasmid. Initial attempts to assemble stable full-length BVDV NADL cDNA clones in medium-copy-number pBR322-derived vectors were unsuccessful. By using the low-copy-number plasmid vector pACNR1180 (27), standard recombinant DNA techniques and a series of intermediate plasmids were used to successfully assemble a full-length functional clone, called pACNR/NADL. Details of the assembly steps are available upon request. The salient features of the plasmid include a T7 promoter sequence fused to the BVDV 5′ terminus and the full-length BVDV cDNA sequence followed by an engineered *Sse*8387I site for production of runoff RNA transcripts corresponding to the precise BVDV genome RNA 3′ terminus. The T7-5′ and 3′-*Sse*8387I junction sequences are shown in Fig. 1. The clone was assembled by using previously constructed and sequenced NADL cDNA clones (5, 6, 35) or synthetic oligonucleotides and PCR (5′ and 3′ ends and an internal region to correct a single-base deletion at nucleotide 2702) (2). These regions and the clones from which they were derived include 1 to 223 (pBV-B55; by PCR), 224 to 1291 (pBV-18; *Xho*I-*Msc*I fragment), 1292 to 2479 (pBV-116b; *Msc*I-*Eco*RI), 2480 to 2826 (reverse transcription-PCR [RT-PCR] of NADL RNA; *Eco*RI-*Rsr*II), 2827 to 3200 (pBV-116b; *Rsr*II-*Msc*I), 3201 to 4175 (pBV-D79; *Msc*I-*Mun*I), 4176 to 5173 (pBV-F2; *Mun*I-*Eco*RV), 5174 to 12537 (pBV-SD2-3′; *Eco*RV-*Aat*II), and 12538 to 12578 (pBV-C37; by PCR). Regions amplified by PCR were verified by sequence analysis. At nucleotide position 2653, a G residue was found in multiple independent clones instead of the previously reported A residue (6). This change is silent and was present in the BVDV NADL RNA preparation used for RT-PCR, as shown by direct sequencing of the PCR product. The full-length BVDV cDNA is positioned (sense orientation) in the pACNR-*Dra*III$^-$ backbone (created by filling in the unique *Dra*III site in pACNR1180 and religating) between the *Aat*II and *Xho*I sites in the polylinker (which were treated with T4 DNA polymerase prior to cloning).

We consistently found that bacterial colonies harboring the correct full-length plasmid were tiny and required 18 to 20 h to become visible. Of several bacterial hosts analyzed (see Results), *Escherichia coli* SURE cells (Stratagene) were most reliable for pACNR/NADL propagation. This host was therefore used for subsequent plasmid constructions. Large-scale DNA preparations were obtained from bacterial cultures grown in Terrific broth with carbenicillin (28), and plasmids were purified either by CsCl banding or by using Nucleobond AX columns (catalog no. 740-574; The Nest Group).

pACNR/cIns$^-$NADL derivative. This deletion construct was produced by using specific oligonucleotide pairs (Table 1) (based on the BVDV/NADL nucleotide sequence [6]) to PCR amplify subregions of pACNR/NADL and produce a convenient restriction site at or near the deletion breakpoint. These junctions are detailed in Fig. 1B. Fragments were then subcloned into pACNR/NADL to produce the desired deletion mutants. All regions amplified by PCR were verified by sequence analysis.

For pACNR/cIns$^-$NADL, in which the cIns sequence between nucleotides 4994 and 5263 was deleted, oligonucleotides 343 and 346 were used to amplify the 4509–4993 region; oligonucleotides 345 and 344 were used to amplify the 5264–5835 region. Oligonucleotides 345 and 346 contained silent nucleotide changes (underlined in Fig. 1B) to create an *Apa*I site at the deletion breakpoint. PCR-amplified fragments were digested with *Apa*I, ligated with T4 DNA ligase, digested with *Bgl*II, purified by separation on an LMP agarose gel, and cloned into *Bgl*II-digested pACNR/NADL that had been treated with calf intestinal alkaline phosphatase. Potentially correct clones were first identified by supercoiled plasmid size (28) and then by digestion with appropriate restriction enzymes and finally were verified by sequence analysis.

Standard in vitro transcription reaction. pACNR/NADL or pACNR/cIns$^-$NADL were digested to completion with *Sse*8387I, extracted with phenol and then chloroform, and precipitated with ethanol. One microgram of linearized plasmid DNA was transcribed in 20 μl, using the T7-MEGAscript kit (Ambion) with 0.5 μCi of added [^{3}H]UTP (Dupont). Reaction mixtures were incubated at 37°C for 2 h in the absence of the cap analog. After transcription, the template DNA was degraded by using DNase I (2 U per 20-μl reaction; 37°C for 20 min) followed by extraction and precipitation as described above. RNAs were quantified on the basis of [^{3}H]UTP incorporation and resuspended at a concentration of 2 μg/μl. The fraction of full-length RNA transcripts was checked by agarose gel electrophoresis, and aliquots for transfection were stored at −80°C.

Transfection of MDBK cells. MDBK cells (70 to 80% confluent) were trypsinized, washed three times with ice-cold RNase-free PBS, and resuspended at 2 × 10^7 cells/ml in PBS. Unless otherwise indicated, 1 to 5 μg of transcribed RNA was mixed with 0.4 ml of the cell suspension and immediately pulsed with a Bio-Rad Gene Pulser (1.5 kV, 25 μF, infinite resistance, 2 pulses) or a BTX ElectroSquarePorator (0.9 kV, 99-μs pulse length, 10 pulses). The electroporated mixture was diluted with 10 ml of DMEM-HS. Depending on the particular experiment, samples were diluted further and plated in multiple wells or tissue culture dishes. An infectious center assay (12), with slight modifications, was used to quantify RNA specific infectivity. Tenfold dilutions of electroporated MDBK cells (in DMEM-HS) were plated (2 ml per 35-mm-diameter well) on monolayers of MDBK cells grown to 50 to 60% confluence. To permit recovery and attachment of the electroporated cells, plates were incubated for 4 h at 37°C, after which the medium was replaced with a 1.5% LMP agarose overlay as described above. Plates were incubated for 3 days at 37°C, and infectious centers were visualized and counted by staining for plaques or foci as described above.

Radioimmunoprecipitation and SDS-PAGE. Rabbit polyclonal antiserum specific for BVDV NS3 (G40) or bovine anti-BVDV antiserum (α49) have been described elsewhere (5, 7). Depending on the antiserum, sodium dodecyl sulfate (SDS) (G40)- or Triton X-100 (α49)-solubilized cell lysates were used for immunoprecipitations. Following labeling of MDBK cells, the medium was removed, cells were washed twice with ice-cold PBS, and cell extracts were prepared by lysis (0.3 ml per 35-mm-diameter well) with either 0.5% SDS or 0.5% Triton X-100 in TNE (50 mM Tris-Cl [pH 7.5], 1 mM EDTA, 0.15 M NaCl, 20 μg of phenylmethylsulfonyl fluoride). SDS-solubilized lysates were sheared, heated to 75°C for 10 min, and clarified by centrifugation at 12,000 × *g* for 10 min. Triton X-100-solubilized lysates were also clarified. Clarified lysates were diluted 1:5 in TNE containing 0.5% Triton X-100, 2.5 μl (G40) or 5 μl (α49) of antiserum was added, and then the mixture was incubated overnight at 4°C with rocking. Protein A-agarose (Sigma), washed five times with TNE containing 0.1% Triton X-100, was added, and incubation was continued for 2 h at 4°C.

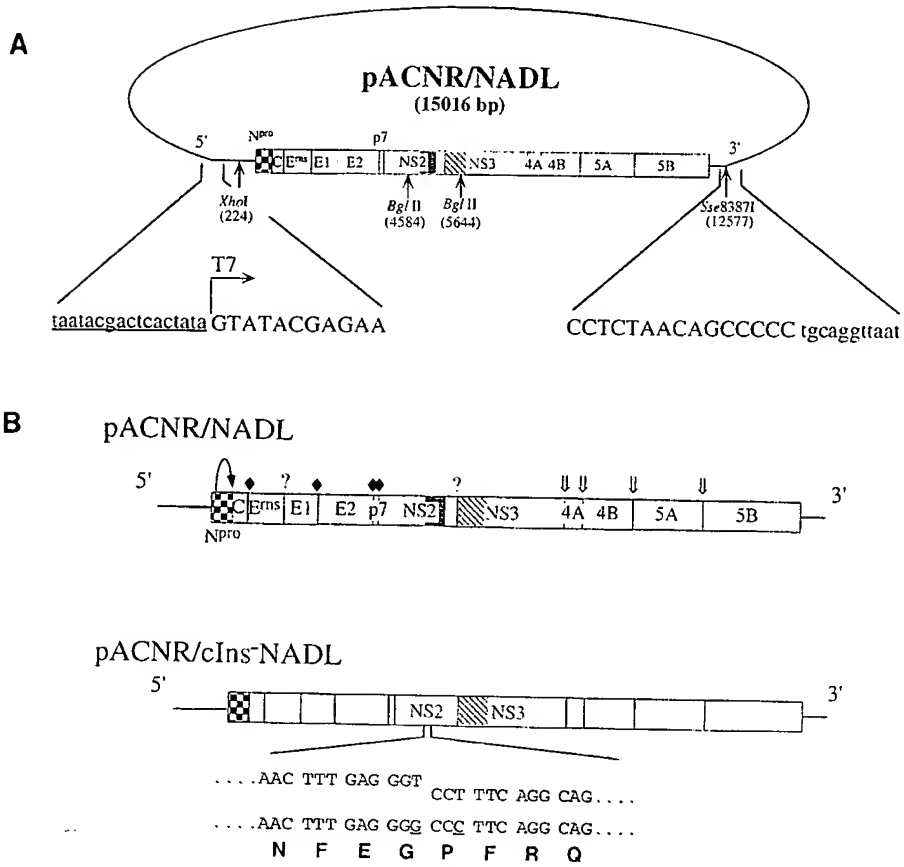

FIG. 1. Diagram of plasmid pACNR/NADL, sequences surrounding transcription initiation and runoff sites, and engineered pACNR/NADL derivatives. (A) pACNR/NADL (15,016 bp) with the BVDV cDNA insert and the positions of BVDV-encoded polyprotein cleavage products are indicated. The N^{pro} autoproteinase (checkered box), the cellular sequence insert (cIns; solid box), and serine proteinase domain (hatched box) are highlighted. Also shown are restriction sites used for subsequent constructions (positions are given in the NADL nucleotide sequence) and production of runoff RNA transcripts (*Sse*8387I). Sequences shown below include the T7 promoter (lowercase, underlined), the T7 transcription start site (arrow), the 5'- and 3'-terminal BVDV cDNA sequences (positive sense; uppercase), and the *Sse*8387I runoff site (shaded). (B) Structures of RNAs transcribed from pACNR/NADL (top) and pACNR/cIns⁻NADL (below). 5' and 3' NTRs are indicated by lines, and polyprotein cleavage products are represented by boxes. Processing sites for N^{pro} (curved arrow), signal peptidase (solid diamonds), the serine proteinase (double arrows), and unidentified proteinases (question marks) are also shown. For the cIns⁻ deletion mutant, the parental (upper staggered sequences) and mutant (below) nucleotide and amino acid sequences at the deletion breakpoints are shown. Silent nucleotide changes (underlined) were used to create a novel *Apa*I restriction site (shaded) to facilitate plasmid constructions and to serve as a convenient marker for distinguishing between each mutant and the parent.

Immunoprecipitates were washed three times with the same solution and then finally once with TNE lacking Triton X-100. Washed immunoprecipitates were resuspended in Laemmli sample buffer, heated to 85°C for 10 min, and centrifuged at 12,000 × *g* for 1 min. Immunoprecipitated proteins were separated by SDS-polyacrylamide gel electrophoresis (PAGE) on an 8% polyacrylamide gel and visualized by fluorography (15).

TABLE 1. Oligonucleotides used for construction of pACNR/NADL, pACNR/cIns⁻NADL, and RT-PCR analyses

Oligonucleotide	NADL nucleotide position	Sense
183[a]	1–27	
343	4509–4531	+
344	5810–5835	−
345	4980-4993/5264-5287[b]	+
346	4974-4993/5264-5276[b]	−
353	4754–4774	+

[a] Consists of a 5' *Xba*I restriction enzyme recognition sequence and the T7 promoter, followed by BVDV NADL nucleotides 1 to 27.
[b] Mutations relative to the BVDV NADL sequence are noted in Fig. 1B.

Analysis of the cIns genetic marker. Virus (culture media and freeze-thaw lysates) from ACNR/cIns-NADL- and control virus-infected MDBK cells was treated with 2 U of DNase I (RQI; Promega) and 1 μg of RNase A (catalog no. 1119915; Boehringer) for 30 min at 37°C and then used for infection of MDBK cells. Multiple sequential passages were conducted in duplicate, using these conditions. At each passage, RNA was obtained from the infected cells of one sample by using the RNAzol method as instructed by the manufacturer (Tel-Test, Inc.). RNA samples were used for RT-PCR with oligonucleotides 353 and 344 (Table 1). Amplified PCR products were extracted with phenol-chloroform and precipitated with ethanol before restriction enzyme digestion with *Apa*I or other enzymes. Passaged samples of wild-type (wt) BVDV/NADL and ACNR/NADL were used as controls for the absence of the *Apa*I site and presence of cIns.

Western blotting. SDS-solubilized MDBK cell lysates were separated by SDS-PAGE (10% gel) and transferred to Immobilon P nitrocellulose membranes by using the semidry Multiphor II Nova blot system (LKB). The membranes were then stained for 90 s with 0.25% (wt/vol) fast green FCF in 10% acetic acid and then destained for 10 min in 10% acetic acid. Nonspecific binding sites were blocked overnight at 4°C with 5% milk in 20 mM Tris-Cl–137 mM NaCl–0.1% Tween 20, pH 7.6 (TBS-T). All following serum dilutions and washing steps were carried out in TBS-T. The membranes were incubated for 1 h at room temperature with primary rabbit polyclonal antisera specific for BVDV NS3 (G40) and E2 (D31) (5, 7) diluted 1/400 each, ensuring antibody saturation (data not shown), followed by a secondary horseradish peroxidase-conjugated goat anti-rabbit serum. Extensive wash steps were performed before primary and second-

ary antibodies and prior to detection with SuperSignal chemiluminescent substrate (Pierce) and exposure to X-ray film.

Northern blotting. Total RNA was extracted from MDBK cells by using TRIZOL reagent (Gibco-BRL). Northern blotting and hybridization was performed essentially as described by Sambrook et al. (28). RNA from 10^6 cells was denatured with glyoxal for 1 h at 50°C, separated by sodium phosphate-buffered 1% agarose gel electrophoresis, and blotted overnight onto positively charged nylon membranes (Boehringer Mannheim), using the TurboBlotter system (Schleicher & Schuell) and alkaline transfer buffer (3 M NaCl, 8 mM NaOH). The membranes were then washed with 0.2 M sodium phosphate (pH 7.0), and the RNA was cross-linked by irradiation with a 254-nm light source (Stratalinker UV cross-linker; Stratagene). A ^{32}P-labeled antisense RNA probe hybridizing to nucleotides 5413 to 5648 of the NADL genome was transcribed in vitro from the *Bam*HI-linearized cDNA clone pGEM-3Zf(+)/NADLΔclns-Bgl, which was constructed by inserting the 790-bp *Bgl*II fragment of pNADL/clns$^-$NADL into the *Bam*HI site of pGEM-3Zf(+). One microgram of DNA was transcribed with SP6 polymerase in the presence of 0.5 mM each ATP, GTP, and CTP, 12.5 μM UTP, and 3.12 μM [α-^{32}P]UTP (800 Ci/mmol; Amersham). After treatment with DNase I, the RNA was purified from unincorporated ribonucleoside triphosphates using a Quick Spin G-50 Sephadex column (Boehringer Mannheim). The membrane was incubated in a Hybaid hybridization oven at 60°C for 5 h in prehybridization/hybridization solution (5× SSPE [1× SSPE is 0.18 M NaCl, 10 mM NaH_2PO_4, and 1 mM EDTA {pH 7.7}], 5× Denhardt's reagent, 0.5% SDS, 100 μg of denatured salmon sperm DNA per ml, 50 μg of yeast tRNA per ml, 50% formamide), followed by overnight incubation at 60°C in fresh hybridization solution supplemented with 2×10^7 cpm of labeled probe. The blot was then washed at 65°C three times for 30 min each with 1× SSPE–0.5% SDS and once for 30 min with 0.1× SSPE–0.5% SDS. Bands were visualized by X-ray autoradiography and quantified with a Molecular Imager (Bio-Rad Laboratories).

Metabolic labeling of viral RNA. For [^{32}P]orthophosphate incorporation, infected MDBK cells were cultured in phosphate-free DMEM supplemented with 2% heat-inactivated HS. Five hours postinfection, the cells were treated with dactinomycin (2 μg/ml) for 1 h prior to addition of [^{32}P]orthophosphate (200 μCi/ml; ICN Pharmaceuticals, Inc.). Total RNA was harvested at 12 and 18 h postinfection, using TRIZOL reagent. RNA from 7×10^4 cells was denatured with glyoxal and separated by agarose gel electrophoresis as described above. The gel was then fixed with methanol and dried, and RNA was visualized and quantified as described above.

RESULTS

Construction of a full-length functional clone of BVDV NADL in low-copy-number plasmid pACNR1180. Initial attempts to assemble stable full-length BVDV NADL cDNA clones in high- or medium-copy-plasmid vectors failed. Finally, low-copy-number vector pACNR1180, which had been used for stable propagation of full-length CSFV cDNA clones (27), was successfully employed. pACNR/NADL contains a T7 promoter, the full-length BVDV NADL cDNA reconstructed from previously sequenced overlapping cDNA clones (6) or RT-PCR products, and a unique 3′ *Sse*8387I site for production of runoff RNA transcripts (see Materials and Methods) (Fig. 1). T7 polymerase transcription of *Sse*8387I-linearized pACNR/NADL template DNA produced RNA transcripts infectious for MDBK cells, as shown in Table 2. Cap analog was not included in transcription reactions since pestivirus RNAs are believed to be uncapped (4, 19, 27); in fact, capping of in vitro-transcribed CSFV RNA actually reduced specific infectivity about 10-fold (27). Optimized electroporation conditions yielded $>10^5$ PFU/μg of RNA transcript. Template DNA alone was not infectious, but intact template was required during transcription since DNase treatment abolished infectivity. After transcription, treatment with DNase had no effect whereas RNase treatment abolished infectivity of transcribed RNAs. These results establish that infectivity was derived by transcription of RNA from the full-length BVDV cDNA template. Typical virus yields harvested from the culture supernatant and cells (by freeze-thaw cycles) at 36 h were 3×10^6 to 10^7 PFU/ml. The resulting virus was neutralized by BVDV-specific antiserum, as demonstrated by both plaque and CPE reduction (data not shown).

It should be noted that even in the pACNR1180 backbone, bacterial colonies harboring the full-length NADL cDNA were tiny, appearing on semisolid media only after 18 to 20 h at 37°C. The deleterious effects of long pestivirus cDNAs and full-length clones during propagation in *E. coli* have been noted previously (21, 27, 34). Since future genetic analyses depended on having a reliable NADL molecular clone for manipulation, we investigated the stability of pACNR/NADL in several bacterial hosts, including *E. coli* MC1061, ABLE-K, ABLE-C, XL1-Blue, and SURE cells. Plasmid DNA from our initial infectious clone was used to transform each of these strains. We monitored colony size, gross plasmid structure by restriction analysis, and the specific infectivity of transcribed RNAs. Among the host strains analyzed, MC1061, ABLE-K, and ABLE-C yielded heterogeneous mixtures of colony sizes. DNA from the larger colonies often showed evidence of deleted or rearranged sequences and no longer yielded infectious RNA transcripts. In contrast, transformation of XL1-Blue and SURE cells produced relatively uniform populations of small colonies, with no evidence of DNA rearrangement, and yielded transcribed RNAs with consistently high specific infectivities (data not shown). SURE cells proved slightly better (faster colony growth and higher specific infectivity RNA) and were used for all subsequent DNA manipulations.

TABLE 2. Specific infectivity of in vitro RNA transcripts generated from pACNR/NADL[a]

Material used to transfect MDBK cells	Expt 1, yield[b] (PFU)	Expt 2	
		Yield[b] (PFU)	Virus recovered[c] (PFU/ml)
DNA linearized with *Sse*8387I	0	0	0
Transcription reaction			
Complete	ND[d]	2.3×10^5	6.7×10^6
DNase during	0	0	0
DNase after	2.5×10^5	2.9×10^5	3.9×10^6
RNase after	0	0	0

[a] One microgram of pACNR/NADL linearized with *Sse*8387I was used for transcription either in the presence or in the absence of DNase I. Following synthesis, some transcription reactions were treated with DNase I or RNase A for 20 min at 37°C. After these treatments, samples were used to electroporate MDBK cells and infectious centers were determined as described in Materials and Methods.

[b] Data are expressed in PFU per microgram of RNA or input DNA.

[c] Viral titer harvested 36 h postelectroporation.

[d] ND, not determined.

Comparison of virus derived from pACNR/NADL to parental BVDV NADL. As shown in Fig. 2A, plaques on MDBK cells produced by transfection with RNA transcribed from pACNR/NADL were homogeneous and similar to the BVDV NADL parental virus originally used for cDNA cloning. Similar results were obtained in plaque assays using virus harvested from cells transfected with pACNR/NADL transcript RNA (called ACNR/NADL) or infected with the NADL parent (data not shown). Growth properties of ACNR/NADL and the parent were compared after infection of MDBK cells at both low (0.1 PFU/cell) and high (1.0 PFU/cell) multiplicity of infection (MOI). As is apparent from the experiment shown in Fig. 2B, the kinetics of replication and the yield of infectious virus were similar for ACNR/NADL and the parental virus at both MOIs. The patterns of viral proteins were also compared by metabolic labeling between 20 and 24 h postinfection and immunoprecipitation with a BVDV-specific polyclonal antiserum (Fig. 2C). Identical patterns of virus-specific proteins were observed for both ACNR/NADL and the parent. Proteins indicated in Fig. 2C were identified not only by size but also by immunoreactivity with a panel of region-specific antisera (reference 36

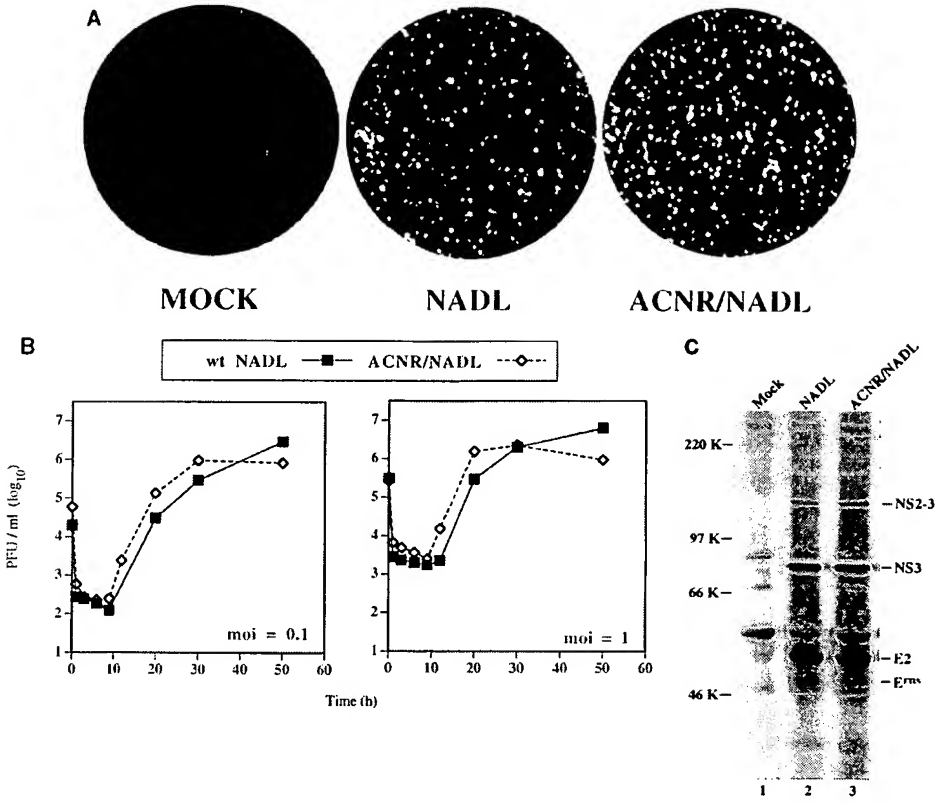

FIG. 2. Comparison of virus derived from pACNR/NADL and wt BVDV NADL. (A) Plaques were visualized by crystal violet staining at 3 days postinfection (NADL) or post-RNA transfection (ACNR/NADL) as described in Materials and Methods. The mock-transfected monolayer was treated the same as the transfected monolayer except that no RNA was present in the transfection mixture. (B) MDBK cells were infected with either wt NADL or ACNR/NADL at an MOI (as determined on MDBK monolayers) of either 0.1 or 1 PFU/cell, washed, and harvested at the indicated times postinfection. Titers were determined by plaque assay on MDBK monolayers as described in Materials and Methods. (C) MDBK cells were mock infected or infected with wt NADL or ACNR/NADL at an MOI of 1 PFU/cell. At 20 h postinfection, proteins were labeled for 4 h with Expre^{35}S^{35}S label (NEN) and lysed, and BVDV-specific proteins were immunoprecipitated with a polyclonal anti-BVDV serum (α49). Proteins were separated by SDS-PAGE (8% gel) and visualized by fluorography. Molecular mass markers are indicated at the left; BVDV-specific proteins, identified by size and, in some cases, by immunoreactivity with region-specific antisera (data not shown), are indicated at the right.

and data not shown). Of note was the uncleaved NS2-3 species migrating at 125 kDa and the prominent 80-kDa NS3 cleavage product, which are characteristic of CP BVDV strains. The similar plaque morphology, cytopathogenicity, growth properties, and polyprotein processing patterns of ACNR/NADL and the BVDV NADL parent validated the use of pACNR/NADL for future molecular genetic studies.

Deletion of cIns abrogates processing at the 2/3 site and NS3 production, and produces replication-competent, non-CP BVDV. Genome rearrangements and/or inserted sequences in CP isolates appear to be linked to processing at the 2/3 site, NS3 production, and cytopathogenicity. Although this hypothesis is supported by sequence comparisons of non-CP/CP pairs (17), it has been rigorously tested for only one CP isolate, CP7 (16, 30) (see Discussion). To address this for the NADL strain, we constructed pACNR/cIns$^-$NADL in which the 270-base cIns was deleted. At the deletion breakpoint, two silent nucleotide changes were introduced to create a novel *Apa*I restriction site, which was used as an additional genetic marker for the deletion mutant (Fig. 1; see also Materials and Methods).

Transfection of MDBK cells with RNA transcripts from linearized pACNR/cIns$^-$NADL template DNA did not induce CPE after 5 days at 37°C, and these cells looked similar to mock-transfected control monolayers. In contrast, RNA transcribed from pACNR/NADL induced CPE after 24 h (data not shown). We could, however, readily detect ACNR/cIns$^-$NADL replication by immunostaining of foci by using a polyclonal anti-BVDV antiserum (Fig. 3A). Using an infectious center assay for electroporated MDBK cells (see Materials and Methods) and this immunostaining protocol, we determined that RNA transcripts from pACNR/cIns$^-$NADL had a specific infectivity approaching that of pACNR/NADL (~8×10^4 focus-forming units [FFU] per μg of RNA). Low- and high-multiplicity infection comparisons of ACNR/cIns$^-$NADL and ACNR/NADL (Fig. 3B) revealed similar growth kinetics and virus yields, with the non-CP derivative showing slightly faster replication and higher cumulative virus titers, which approached 10^7 FFU/ml. As seen in Fig. 3C, ACNR/cIns$^-$NADL did not induce CPE in cultures even at 50 h postinfection, when peak titers were reached, in contrast to ACNR/NADL and wt BVDV NADL, which had caused dramatic CPE by this time.

To confirm the genomic structure of ACNR/cIns$^-$NADL, we serially passaged the virus in MDBK cells, each time incubating the resulting virus with RNase and DNase to avoid carryover of input transcript RNA and plasmid template DNA. Total cellular RNA, isolated at each passage, was used for amplification of a NS2-3 subregion that included the cIns locus, and the resulting fragments were analyzed by agarose gel electrophoresis, either with or without digestion with *Apa*I

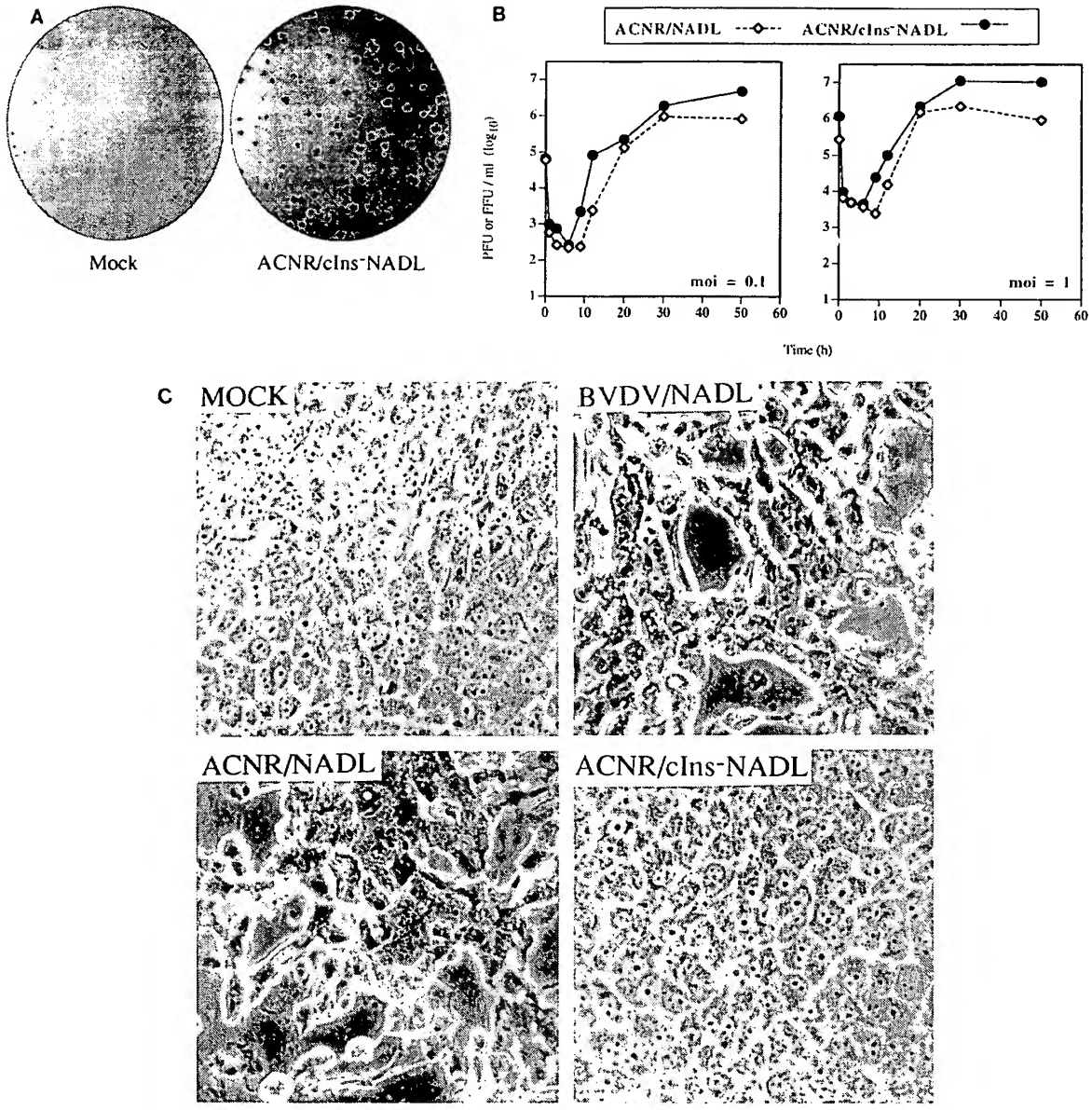

FIG. 3. Virus lacking cIns is non-CP. (A) MDBK cells were transfected with RNA transcribed from linearized pACNR/cIns⁻NADL template DNA (ACNR/cIns⁻NADL) or were mock transfected (Mock), and then dilutions of transfected cells were assayed for infectious centers as described in Materials and Methods. Foci were visualized after 3 days by immunostaining with polyclonal α49 serum as the primary antibody. (B) Viral growth analyses after low (0.1 PFU or FFU per cell)- or high (1 PFU or FFU per cell)-MOI infection were conducted as described for Fig. 2B. Titers were determined by a standard plaque assay for CP ACNR/NADL (PFU/milliliter) or a focus forming assay for non-CP ACNR/cIns⁻NADL (FFU/milliliter). The data shown represent one of three independent experiments yielding similar results. (C) Phase-contrast photomicrographs of MDBK cells either mock infected or infected with the indicated viruses (MOI of 0.1). Pictures were taken at 50 h postinfection and correspond to the same cultures used for the growth analyses shown in panel B.

(Fig. 4). As shown in Fig. 4, amplification of this region for the NADL parent and ACNR/NADL produced a fragment of 1,082 bp (Fig. 4A) that was resistant to digestion by *Apa*I (Fig. 4B, lanes 5 to 8). In contrast, amplification of both early (passage 1)- and late (passage 4)-passage RNA from ACNR/cIns⁻NADL yielded the expected smaller 812-bp fragment that was susceptible to digestion by *Apa*I (Fig. 4B, lanes 1 to 4).

To examine protein processing in the NS2-3 region, MDBK cells were infected with the NADL parent (ACNR/NADL) or ACNR/cIns⁻NADL and metabolically radiolabeled, and the NS3-related proteins were immunoprecipitated with an NS3-specific polyclonal rabbit antiserum. As shown in Fig. 5, both NS2-3 and NS3 were present in cells infected with NADL and ACNR/NADL (lanes 2 and 3), whereas only NS2-3 was found in ACNR/cIns⁻NADL-infected cells (lane 4). NS2-3 produced by ACNR/cIns⁻NADL migrated faster than that produced by NADL and ACNR/NADL, presumably because of the cIns deletion that shortens NS2-3 by 90 amino acids (~10 kDa).

Parallel comparison of RNA, protein, and virus accumula-

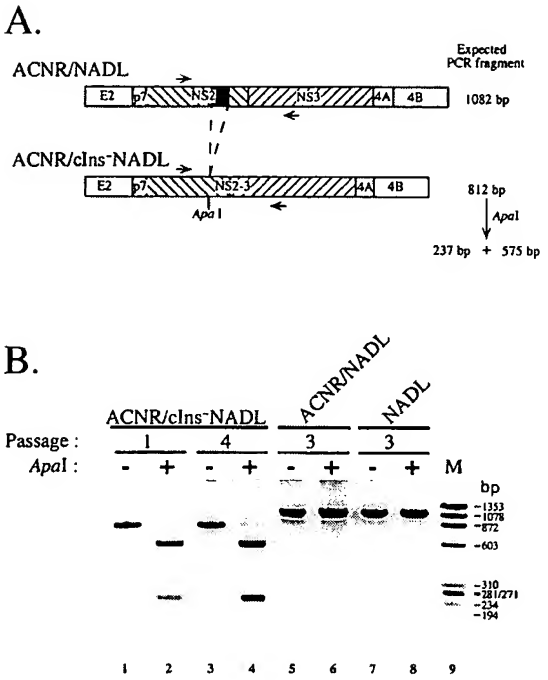

FIG. 4. Presence of the *Apa*I marker in virus derived from pACNR/cIns⁻NADL. (A) Diagram of the expected RT-PCR fragments of ACNR/NADL and ACNR/cIns⁻NADL. Indicated are the location of cIns (black box), the engineered *Apa*I site, the primers used for RT-PCR (arrows), and the NS2 and NS3 coding regions (hatched boxes). The expected sizes of the RT-PCR products are given, as are the sizes of the two *Apa*I digestion products for ACNR/cIns⁻NADL. (B) After infection (NADL) or transfection (ACNR/NADL and ACNR/cIns⁻NADL), virus was harvested at 20 to 26 h (when the CP derivatives caused demonstrable CPE) as described in Materials and Methods. At each passage, the resulting virus was treated with DNase I and RNase A for 30 min at 37°C before infection of new monolayers (0.3 ml of undiluted virus stock per 35-mm-diameter well). For the indicated passages, RNA from infected cells was used for RT-PCR and a portion of each amplification reaction was digested with *Apa*I. Products were separated by electrophoresis on a 1.5% agarose gel and visualized by staining with ethidium bromide. During this analysis, we consistently observed a small fraction of the RT-PCR product from ACNR/cIns⁻NADL which was resistant to digestion by *Apa*I (even in vast enzyme excess; lane 4). Control experiments demonstrated that this resistant fraction was generated not during virus propagation but rather during the T7 transcription or reverse transcription steps (data not shown).

tion over time for ACNR/NADL and ACNR/cIns⁻NADL revealed significantly higher levels of RNA for the CP virus than for its non-CP derivative (Fig. 6), whereas the analyzed proteins NS2-3 or NS3 and E2 (Fig. 7) as well as the virus titers (Fig. 6 and 7) accumulated to similar levels. The RNA, proteins, and virus titers shown in Fig. 6 and 7 were obtained in parallel from one single experiment and are representative of three identical experiments repeated independently. For viral RNA, Northern blotting and metabolic labeling yielded similar results (Fig. 6). As quantified by Molecular Imager analysis, the calculated ratio of ACNR/NADL to ACNR/cIns⁻NADL RNA was 3 (Fig. 6A and B) at 12 h postinfection and 5 (Fig. 6A) or 8 (Fig. 6B) at 18 h postinfection.

These results demonstrate that cIns modulates cleavage at the 2/3 site, NS3 production, and cytopathogenicity but does not have dramatic effects on synthesis of virus-specific proteins or virus yield. Remarkably, however, deletion of cIns resulted in significantly lower levels of viral RNA synthesis and accumulation.

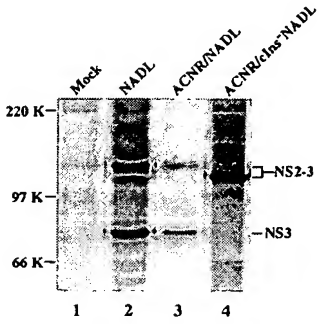

FIG. 5. Deletion of cIns abrogates NS3 production. MDBK cells were mock infected or infected with the indicated viruses at an MOI of 1 PFU/cell. At 20 h postinfection, monolayers were labeled for 4 h with Expre^{35}S^{35}S label (NEN) and lysed, and NS3-containing species were immunoprecipitated with a polyclonal anti-NS3 serum (G40 [5]). Proteins were separated by SDS-PAGE (8% gel) and visualized by fluorography. Molecular mass markers are indicated at the left; BVDV-specific proteins are indicated at the right.

DISCUSSION

In this work, we succeeded in constructing a functional BVDV NADL cDNA clone in a low-copy-number plasmid. Full-length RNAs transcribed by T7 polymerase from this cDNA template have the authentic viral 5′- and 3′-terminal sequences, are highly infectious for MDBK cells (>10^5 PFU/μg), and yield a virus that has properties similar to those of the BVDV NADL parent. This plasmid clone is stable when propagated in the SURE strain of *E. coli*. Recently, assembly of a full-length BVDV NADL clone in a high-copy-number plasmid was reported by another group (34). Although infectious RNA could be transcribed from this template, the authors noted problems with plasmid transformation efficiency and stability and the production of full-length RNA transcripts. Some of these difficulties mimic our earlier unsuccessful attempts to construct such clones in high- or medium-copy-number plasmids. These problems were alleviated when the pACYC177 backbone was used. This plasmid had been used successfully for several other full-length pestivirus cDNAs (16, 19, 27). The reason(s) for the observed toxic effects of pestiviral cDNAs in some *E. coli* strains remains to be determined, but similar problems have also been encountered for several members of the flavivirus genus (22, 25).

The creation of a functional BVDV NADL cDNA clone allowed us to directly test the role of cIns in NS3 production and cytopathogenicity. Deletion of the 270-base cIns element produced a viable non-CP virus, in which detectable cleavage at the 2/3 site and NS3 production were abolished. Similar results were recently reported for CP BVDV strain CP7, which contains a 27-base duplication of viral sequences in the NS2 region (30). Using a vaccinia virus transient expression assay, deletion of this 27-base sequence eliminated cleavage at the 2/3 site (30). Further studies demonstrated that an isogenic derivative lacking this insertion was non-CP (16).

The mechanism(s) by which cIns (NADL) or the 27-base (CP7) insertions in NS2 promote cleavage at the 2/3 site is unknown. Although the NS3 N terminus has yet to be precisely determined for these strains, based on the similar apparent molecular masses of pestivirus NS3 proteins (10, 11, 30) and the conserved Ub-NS3, N^{pro}-NS3, and Met-NS3 junctions observed for other CP isolates, Gly-1590 (SD-1 numbering [8, 9]) is the likely NS3 N-terminal residue. For NADL, this would imply that the 90-amino-acid cIns insertion, located 53 residues upstream of this Gly residue, somehow

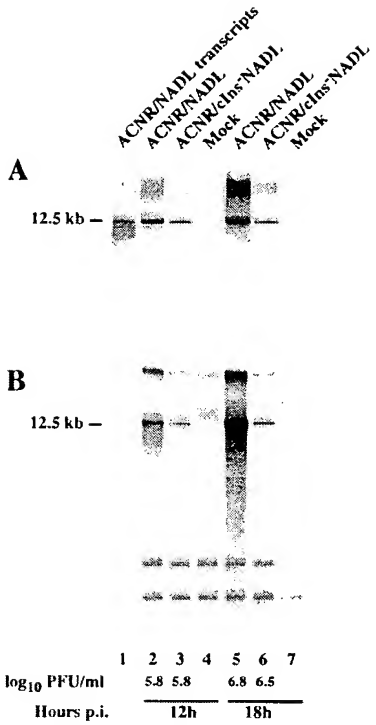

FIG. 6. Viral RNA accumulation in MDBK cells infected with ACNR/NADL and ACNR/cIns⁻NADL. MDBK cells were infected at an MOI of 2 with either ACNR/NADL (lanes 2 and 5) or ACNR/cIns⁻NADL (lanes 3 and 6) or were mock infected (lanes 4 and 7), and total RNA was harvested 12 h (lanes 2 to 4) and 18 h (lanes 5 to 7) postinfection (p.i.). (A) For each sample, RNA from 10^6 cells was analyzed by Northern blotting using a ^{32}P-labeled RNA probe hybridizing to positive-sense viral RNA in the NS3 gene. (B) For direct analysis of total viral RNA accumulation, infected cells were metabolically labeled with [^{32}P]orthophosphate between 6 and 18 h postinfection in the presence of dactinomycin. Glyoxal-denatured RNA from 7×10^4 cells harvested at 12 and 18 h postinfection was separated by agarose gel electrophoresis and visualized by X-ray autoradiography. Either unlabeled (A, lane 1) or ^{32}P-labeled (B, lane 1) transcripts of pACNR/NADL served as size markers for full-length viral RNA (12.5 kb). The virus titers at the time of RNA harvest in the same experiment are indicated.

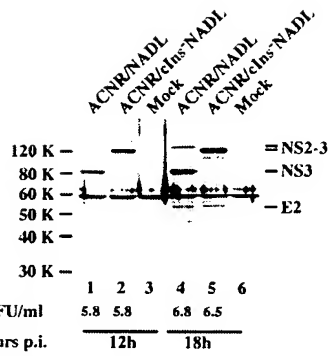

FIG. 7. Levels of NS2-3, NS3, and E2 in MDBK cells infected with ACNR/NADL or ACNR/cIns⁻NADL. MDBK cells were infected at an MOI of 2 with either ACNR/NADL (lanes 1 and 4) or ACNR/cIns⁻NADL (lanes 2 and 5) or were mock infected (lanes 3 and 6), using the same inocula and cell densities described for the experiment shown in Fig. 6. The cells were lysed at 12 h (lanes 1 to 3) and 18 h (lanes 4 to 6) postinfection (p.i.), and lysates from 3×10^4 cells were separated by SDS-PAGE (10% gel) and analyzed by Western blotting using a low-dilution mix of rabbit antisera G40 and D31, specific for BVDV NS3 and E2, respectively. Molecular mass markers are indicated at the left. BVDV-specific proteins are indicated at the right.

promotes cleavage at the 2/3 junction. In the case of CP7, the nine-residue insertion is located even further upstream of the putative 2/3 cleavage site. In addition to their different locations in NS2, there is no obvious sequence similarity between the NADL and CP7 inserts. Whether they activate a cryptic autoprotease present in the NS2-3 region or change the conformation of NS2-3 so as to render it susceptible to site-specific cleavage by a cellular enzyme remains to be determined (see references 29 and 36 for further discussion). Interestingly, in the absence of any inserted sequences or genome rearrangements, NS3 production occurs in cells infected with CSFV isolates (3, 33).

The strongest correlate of pestivirus cytopathogenicity is NS3 production, which is accomplished by myriad different strategies (17). Two groups have recently demonstrated that cell death induced by CP BVDV infection occurs via apoptosis (13, 37). It is possible that NS3 acts as a direct effector of apoptosis by somehow triggering cell death pathways. This is a plausible hypothesis given the obvious structural differences between NS2-3 and NS3, which could affect subcellular localization and interaction with host cell components, as previously discussed (35). Alternatively, cleavage at the 2/3 site (or NS3 production) could upregulate BVDV RNA replication to a level that is deleterious for host cells. In one model, viral RNA replication complexes might sequester cellular components present in limited quantities and required for maintaining homeostasis. In the case of BVDV NADL, increased numbers of replication complexes would then deplete such host factors to a level which triggers apoptosis. This model is consistent with our results, which demonstrate that RNA replication and accumulation are enhanced in ACNR/NADL-infected cells compared to ACNR/cIns⁻NADL-infected cells. It will be of interest to examine other isogenic non-CP/CP pairs to determine the generality of this observation and its possible correlation with cytopathogenicity.

In summary, genetic analyses of CP7 (16) and NADL (this report) have established that two distinct insertions in NS2 can regulate processing at the 2/3 site, NS3 production, and cytopathogenicity in cell culture. Such isogenic non-CP/CP pairs should be valuable for additional studies aimed at answering key questions in pestivirus biology. Examples include (i) defining the mechanism(s) of cleavage at the 2/3 site, including the responsible protease(s); (ii) establishing the pathway linking NS3 production to cytopathogenicity; and (iii) testing the hypothesis that CP strains with these insertions are sufficient to cause MD in animals persistently infected with the isogenic non-CP derivative.

ACKNOWLEDGMENTS

We thank Carol Read for expert technical assistance. We are also grateful to many colleagues for helpful discussions during the course of this work and to M. Scott McBride, Tina Myers, and Karen Reed for critical reading of the manuscript.

E.M. was supported by a fellowship from the Human Frontiers of Science Program Organization and by the Universidad Nacional Autónoma de México. N.R. was supported by fellowships from the Swiss National Science Foundation and from the Swiss Foundation for Biomedical Stipends (SSMBS).

REFERENCES

1. **Baker, J. C.** 1987. Bovine viral diarrhea virus: a review. J. Am. Vet. Med. Assoc. 190:1449–1458.
2. **Barnes, W. M.** 1994. PCR amplification of up to 35-kb DNA with high fidelity and high yield from λ bacteriophage templates. Proc. Natl. Acad. Sci. USA 91:2216–2220.

3. **Becher, P., A. D. Shannon, N. Tautz, and H.-J. Thiel.** 1994. Molecular characterization of border disease virus, a pestivirus from sheep. Virology **198**:542–551.
4. **Brock, K. V., R. Deng, and S. M. Riblet.** 1992. Nucleotide sequencing of 5′ and 3′ termini of bovine viral diarrhea virus by RNA ligation and PCR. J. Virol. Methods **38**:39–46.
5. **Collett, M. S., R. Larson, S. K. Belzer, and E. Retzel.** 1988. Proteins encoded by bovine viral diarrhea virus: the genomic organization of a pestivirus. Virology **165**:200–208.
6. **Collett, M. S., R. Larson, C. Gold, D. Strick, D. K. Anderson, and A. F. Purchio.** 1988. Molecular cloning and nucleotide sequence of the pestivirus bovine viral diarrhea virus. Virology **165**:191–199.
7. **Collett, M. S., M. A. Wiskerchen, E. Welniak, and S. K. Belzer.** 1991. Bovine viral diarrhea virus genomic organization. Arch. Virol. Suppl. **3**:19–27.
8. **Deng, R., and K. V. Brock.** 1992. Molecular cloning and nucleotide sequence of a pestivirus genome, noncytopathic bovine viral diarrhea virus strain SD-1. Virology **191**:867–869.
9. **Deng, R., and K. V. Brock.** 1993. 5′ and 3′ untranslated regions of pestivirus genomes: primary and secondary structure analyses. Nucleic Acids Res. **21**:1949–1957.
10. **Donis, R. O., and E. J. Dubovi.** 1987. Characterization of bovine viral diarrhoea-mucosal disease virus-specific proteins in bovine cells. J. Gen. Virol. **68**:1597–1605.
11. **Greiser-Wilke, I., K. E. Dittmar, B. Liess, and V. Moennig.** 1992. Heterogeneous expression of the non-structural protein p80/p125 in cells infected with different pestiviruses. J. Gen. Virol. **73**:47–52.
12. **Hertz, J. M., and H. V. Huang.** 1995. Evolution of the Sindbis virus subgenomic mRNA promoter in cultured cells. J. Virol. **69**:7768–7774.
13. **Hoff, H. S., and R. O. Donis.** 1997. Induction of apoptosis and cleavage of poly(ADP-ribose) polymerase by cytopathic bovine viral diarrhea virus infection. Virus Res. **49**:101–113.
14. **Kupfermann, H., H.-J. Thiel, E. J. Dubovi, and G. Meyers.** 1996. Bovine viral diarrhea virus: characterization of a cytopathogenic defective interfering particle with two internal deletions. J. Virol. **70**:8175–8181.
15. **Laskey, R. A., and A. D. Mills.** 1975. Quantitative film detection of ^{3}H and ^{14}C in polyacrylamide gels by fluorography. Eur. J. Biochem. **56**:335–341.
16. **Meyers, G., N. Tautz, P. Becher, H. J. Thiel, and B. M. Kümmerer.** 1996. Recovery of cytopathogenic and noncytopathogenic bovine viral diarrhea viruses from cDNA constructs. J. Virol. **70**:8606–8613.
17. **Meyers, G., and H.-J. Thiel.** 1996. Molecular characterization of pestiviruses. Adv. Virus Res. **47**:53–118.
18. **Meyers, G., and H. J. Thiel.** 1995. Cytopathogenicity of classical swine fever virus caused by defective interfering particles. J. Virol. **69**:3683–3689.
19. **Meyers, G., H. J. Thiel, and T. Rumenapf.** 1996. Classical swine fever virus: recovery of infectious viruses from cDNA constructs and generation of recombinant cytopathogenic defective interfering particles. J. Virol. **70**:1588–1595.
20. **Mittelholzer, C., C. Moser, J.-D. Tratschin, and M. A. Hoffman.** 1997. Generation of cytopathogenic subgenomic RNA of classical swine fever virus in persistently infected porcine cell culture. Virus Res. **51**:125–137.
21. **Moormann, R. J., H. G. van Gennip, G. K. Miedema, M. M. Hulst, and P. A. van Rijn.** 1996. Infectious RNA transcribed from an engineered full-length cDNA template of the genome of a pestivirus. J. Virol. **70**:763–770.
22. **Polo, S., G. Ketner, R. Levis, and B. Falgout.** 1997. Infectious RNA transcripts from full-length dengue virus type 2 cDNA clones made in yeast. J. Virol. **71**:5366–5374.
23. **Poole, T. L., C.-Y. Wang, R. A. Popp, L. N. D. Potgieter, A. Siddiqui, and M. S. Collett.** 1995. Pestivirus translation initiation occurs by internal ribosome entry. Virology **206**:750–754.
24. **Rice, C. M.** 1996. *Flaviviridae*: the viruses and their replication. p. 931–960. *In* B. N. Fields, D. M. Knipe, and P. M. Howley (ed.), Fields virology. Lippincott-Raven Publishers, Philadelphia, Pa.
25. **Rice, C. M., A. Grakoui, R. Galler, and T. J. Chambers.** 1989. Transcription of infectious yellow fever virus RNA from full-length cDNA templates produced by in vitro ligation. New Biol. **1**:285–296.
26. **Rijnbrand, R., T. van der Straaten, P. A. van Rijn, W. J. M. Spaan, and P. J. Bredenbeek.** 1997. Internal entry of ribosomes is directed by the 5′ noncoding region of classical swine fever virus and is dependent on the presence of an RNA pseudoknot upstream of the initiation codon. J. Virol. **71**:451–457.
27. **Ruggli, N., J. D. Tratschin, C. Mittelholzer, and M. A. Hofmann.** 1996. Nucleotide sequence of classical swine fever virus strain Alfort/187 and transcription of infectious RNA from stably cloned full-length cDNA. J. Virol. **70**:3478–3487.
28. **Sambrook, J., E. Fritsch, and T. Maniatis.** 1989. Molecular cloning: a laboratory manual. Cold Spring Harbor Laboratory, Cold Spring Harbor, N.Y.
29. **Tautz, N., K. Elbers, D. Stoll, G. Meyers, and H.-J. Thiel.** 1997. Serine protease of pestiviruses: determination of cleavage sites. J. Virol. **71**:5415–5422.
30. **Tautz, N., G. Meyers, R. Stark, E. J. Dubovi, and H. J. Thiel.** 1996. Cytopathogenicity of a pestivirus correlates with a 27-nucleotide insertion. J. Virol. **70**:7851–7858.
31. **Tautz, N., H. J. Thiel, E. J. Dubovi, and G. Meyers.** 1994. Pathogenesis of mucosal disease: a cytopathogenic pestivirus generated by an internal deletion. J. Virol. **68**:3289–3297.
32. **Thiel, H.-J., P. G. W. Plagemann, and V. Moennig.** 1996. Pestiviruses, p. 1059–1073. *In* B. N. Fields, D. M. Knipe, and P. M. Howley (ed.), Fields virology. Raven Press, New York, N.Y.
33. **Thiel, H.-J., R. Stark, E. Weiland, T. Rümenapf, and G. Meyers.** 1991. Hog cholera virus: molecular composition of virions from a pestivirus. J. Virol. **65**:4705–4712.
34. **Vassilev, V. B., M. S. Collett, and R. O. Donis.** 1997. Authentic and chimeric full-length genomic cDNA clones of bovine viral diarrhea virus that yield infectious transcripts. J. Virol. **71**:471–478.
35. **Wiskerchen, M., and M. S. Collett.** 1991. Pestivirus gene expression: protein p80 of bovine viral diarrhea virus is a proteinase involved in polyprotein processing. Virology **184**:341–350.
36. **Xu, J., E. Mendez, P. R. Caron, C. Lin, M. A. Murcko, M. S. Collett, and C. M. Rice.** 1997. Bovine viral diarrhea virus NS3 serine proteinase: polyprotein cleavage sites, cofactor requirements, and molecular model of an enzyme essential for pestivirus replication. J. Virol. **71**:5312–5322.
37. **Zhang, G., S. Aldridge, M. C. Clarke, and J. W. McCauley.** 1997. Cell death induced by cytopathic bovine viral diarrhea virus is mediated by apoptosis. J. Gen. Virol. **77**:1677–1681.

JOURNAL OF VIROLOGY, June 2003, p. 6450–6465 Vol. 77, No. 11
0022-538X/03/$08.00+0 DOI: 10.1128/JVI.77.11.6450–6465.2003

Development and Application of a Reverse Genetics System for Japanese Encephalitis Virus

Sang-Im Yun,[1] Seok-Yong Kim,[1] Charles M. Rice,[2] and Young-Min Lee[1]*

Department of Internal Medicine, Microbiology, College of Medicine and Medical Research Institute, Chungbuk National University, Cheongju, Korea,[1] and *Center for the Study of Hepatitis C, Laboratory for Virology and Infectious Disease, The Rockefeller University, New York, New York 10021-6399*[2]

Received 26 September 2002/Accepted 6 March 2003

Japanese encephalitis virus (JEV) is a common agent of viral encephalitis that causes high mortality and morbidity among children. Molecular genetic studies of JEV are hampered by the lack of a genetically stable full-length infectious JEV cDNA clone. We describe here the development of such a clone. A JEV isolate was fully sequenced, and then its full-length cDNA was cloned into a bacterial artificial chromosome. This was then further engineered so that transcription of the cDNA in vitro would generate synthetic RNAs with authentic 5′ and 3′ ends. The synthetic RNAs thus produced were highly infectious in susceptible cells (>10^6 PFU/μg), and these cells rapidly generated a high titer of synthetic viruses (>5 × 10^6 PFU/ml). The recovered viruses were indistinguishable from the parental virus in terms of plaque morphology, growth kinetics, RNA accumulation, protein expression, and cytopathogenicity. Significantly, the structural and functional integrity of the cDNA was maintained even after 180 generations of growth in *Escherichia coli*. A single point mutation acting as a genetic marker was introduced into the cDNA and was found in the genome of the recovered virus, indicating that the cDNA can be manipulated. Furthermore, we showed that JEV is an attractive vector for the expression of heterologous genes in a wide variety of cell types. This novel reverse genetics system for JEV will greatly facilitate research into JEV biology. It will also be useful as a heterologous gene expression vector and will aid the development of a vaccine against JEV.

Research investigating positive-sense RNA viruses has been considerably advanced by the development of the reverse genetics system. Here, infectious cDNA clones of the viral genome in question are constructed and become the templates for infectious RNA synthesis that generates synthetic viruses. In the classical RNA-launched approach, cells are transfected with RNA transcripts made from the infectious cDNA clones, and the synthetic viruses are then recovered from these cells (18, 29, 30, 32, 43). However, an alternative DNA-launched approach also exists. This approach was first reported for poliovirus (27) and has been adapted for alphaviruses (34). Here, synthetic viruses are generated by directly transfecting infectious cDNA clones into susceptible cells. Both of these approaches have been used to construct infectious cDNA clones for many positive-sense RNA virus families, including coronaviruses, which have the largest RNA genomes (2). These clones have been invaluable in addressing many questions regarding the positive-sense RNA viruses. However, the construction of a full-length infectious cDNA clone for Japanese encephalitis virus (JEV) has been hampered, largely because of the genetic instability of the cloned cDNA. Despite extensive efforts (23, 38, 39, 51), a genetically stable full-length infectious cDNA molecular clone for JEV does not exist.

JEV is a member of the *Flaviviridae* family and is transmitted by mosquitoes. It is an important human pathogen that causes permanent neuropsychiatric sequelae and even fatal disease, especially in children (37, 40, 41). Transmission of the virus has recently been observed in the southern hemisphere, indicating that this virus could become a worldwide public health threat (12, 13, 20). From its genome structure, which is similar to that of other flaviviruses, JEV is a small-enveloped virus with a single-stranded, positive-sense RNA genome approximately 11 kb in length. The genome contains a single long open reading frame (ORF) flanked by 5′ and 3′ nontranslated regions (NTRs) that are important *cis*-acting elements for viral replication. The RNA genome has a type I cap structure at its 5′ terminus but lacks a poly(A) tail at its 3′ terminus. The ORF is translated into a large polyprotein that is co- or posttranslationally processed into three structural and seven nonstructural proteins whose genes are arranged in the genome as follows: C-prM-E-NS1-NS2A-NS2B-NS3-NS4A-NS4B-NS5 (7, 19, 45). Further information, for example, on the function of the majority of the JEV gene products and the molecular mechanisms involved in JEV replication, neurovirulence, and pathogenesis, is limited largely because of the lack of a reliable reverse genetics system.

Here we report the JEV reverse genetics system that we have developed. We showed that in vitro transcription of the full-length cDNA produces synthetic RNAs that, when transfected into susceptible BHK-21 cells, have a specific infectivity exceeding 10^6 PFU/μg. Synthetic JEVs recovered from the culture supernatant of the transfected cells 24 h posttransfection exceeded 5 × 10^6 PFU/ml. The recovered viruses were similar to the parent in terms of plaque morphology, growth kinetics, RNA accumulation, protein expression, and cytopathogenicity. A genetic marker, a single point mutation that

* Corresponding author. Mailing address: Department of Internal Medicine, Microbiology, College of Medicine and Medical Research Institute, Chungbuk National University, 48 Gaeshin-Dong Heungduk-Ku, Cheongju, Korea. Phone: 82 43 261 2863. Fax: 82 43 272 1603. E-mail: ymlee@med.chungbuk.ac.kr.

Exhibit B

TABLE 1. Oligonucleotides used for ligation, cDNA synthesis, and PCR amplification

Oligonucleotide	Sequence[a]	Position[b]	Polarity
J1	5′-GATCCTGTGTTCTTCCTCACC	10947–10967	Antisense
J2	5′-AGAAGATCTCCCAGTCTATTCCCA	10870–10893	Antisense
J3	5′-GATTTAATTAACACCTCCTCTACAGCTTCG	10795–10813	Antisense
J4	5′-AGGACGCGTAGTGTGCGTTGT	8150–8170	Antisense
J6	5′-GCCCCTAGGACCAGAACCACG	3845–3865	Antisense
J7	5′-AGCGCTAAGACTGGCATG	3986–4003	Antisense
J8	5′-GATCGGACCGAGAAGTTTATCTGTGTGA	1–18	Sense
J12	5′-GATCGGACCGAATTCCACCACAGCCAC	7565–7582	Sense
J20	5′-AAACCAGGGACCTTGGGA	3266–3283	Sense
J31	5′-GGCTGTGGGCCCACTTGT	8821–8838	Sense
J35	5′-AGCAACCTGGGCTGAGAA	10259–10276	Sense
J39	5′-CCCACTAGTGGGAATACG	164–181	Antisense
J40	5′-AAACGTACTGGTCCTCTG	215–232	Antisense
J41	5′-TCCGTGGAATGAACAATG	17911–17928	Sense
J42	5′-GAGAAGTTTATCTGTGTG	1–17	Sense
J43	5′-ACAGATAAACTTCTCTATAGTGTCCCCTAA	1–14	Antisense
J45	5′-AGTACTAGTCGGTCCGCGGCCGCTCGAGATCCTGTGTTCTT	10954–10968	Antisense
J46	5′-AGTACTAGTCGGTCCGCGGCCGCTCTAGAGATCCTGTGTTCTT	10954–10968	Antisense
J47	5′-CCAAAGCTTCAAACTCAAGATACC	9127–9150	Antisense
J48	5′-ACTGAGCTCACGCGTCCTCGAGATGAC	8162–8179	Sense
J72	5′-GAAGGTACCCCATTGTATGG		
J73	5′-TTCTCCTTTACCCATGGTTGTGGCAAGCTT		
J74	5′-ATGGGTAAAGGAGAAGAA		
J75	5′-AAGATGCATTCATTAACCGTCGACTGCAGA		
J76	5′-TTTGGCGTCTTCCATGGTTGTGGCAAGCTT		
J77	5′-ATGGAAGACGCCAAAAAC		
J78	5′-CTTAAGATGCATTCATTACACGGCGATCTT		
J80	5′-ACAGATAAACTTCTCTATAGTGAGTCGTAT	1–14	Antisense
J81	5′-TCTTGCCCGCCTGATGAA		
J82	5′-GCCCATGGTAAGCTTAGG	636–653	Antisense
J89	5′-TGCTTTGGCCTTCTTGGCCAC	2417–2437	Sense
J90	5′-TTGAGGCCCCCACGGCCCAA	10687–10706	Sense
J91	5′-ACCCGCATATTCTGTGATCCGTGGTTCCAG	5566–5575, 5659–5678	Antisense
J92	5′-ACAGAATATGCGGGTAAA	5664–5681	Sense
J93	5′-AGCTAACGGCCGATCTCTTTC	6457–6477	Antisense
T	5′-CCAGTGTTGTGGCCTGCAGGGCGAATT		
TR	5′-GATGAATTCGCCCTGCAGGCCACAACA		

[a] JEV-specific sequences are shown in boldface type. Restriction enzyme recognition sites used for cDNA cloning are underlined.
[b] Nucleotide position refers to the complete nucleotide sequence of pBAC^{SP6}/JVFLx/*Xba*I.

had been introduced into the infectious cDNA, was observed in the genome of the recovered virus. Most significantly, the infectious bacterial artificial chromosome (BAC) remained genetically stable even after 180 generations of serial growth in *Escherichia coli*. Furthermore, foreign genes engineered into the JEV cDNA were expressed as genomic RNA transcripts, indicating that JEV could be exploited as a eukaryotic expression vector. Thus, we have established a reverse genetics system for JEV that will be a useful tool for many areas of biological research.

MATERIALS AND METHODS

Cell lines and viruses. BHK-21 cells were maintained in alpha minimal essential medium (MEM) supplemented with 10% fetal bovine serum, 2 mM L-glutamine, vitamins, and antibiotics. All reagents used in cell culture were purchased from Gibco-BRL Life Technologies, Inc., Gaithersburg, Md. The Korean JEV strain K87P39 (8) was obtained from the Korean National Institute of Health. This isolate was isolated from wild mosquitoes in Korea in 1987 and underwent five passages in suckling mouse brains. The YF17D yellow fever virus strain was generated from the infectious cDNA pACNR/YF17D by SP6 polymerase runoff transcription as described below.

Isolation of viruses by plaque purification. Cells infected with the JEV K87P39 strain were overlaid with MEM containing 10% fetal bovine serum and 0.5% SeaKem LE agarose (FMC BioProducts, Rockland, Maine) and incubated for 3 to 4 days. Individual plaques were picked with sterile Pasteur pipettes and resuspended in 1 ml of medium. Viruses were eluted from the agarose at 4°C for 2 h. The eluate was amplified only once in BHK-21 cells and stored at −80°C until use.

Complete nucleotide sequence analysis of JEV genomic RNA. Viral genomic RNA was extracted from 100 μl of virus-containing culture fluid with 300 μl of Trizol LS reagent as recommended by the manufacturer (Gibco-BRL) and then resuspended in 20 μl of RNase-free water. To analyze the complete nucleotide sequence of the viral genomic RNA, three overlapping cDNAs (JVF, JVM, and JVR) representing the entire viral RNA genome apart from the 3′-terminal sequences were amplified by long reverse transcription (RT)-PCR as illustrated in Fig. 2. Oligonucleotides used for cDNA synthesis and amplification were designed according to the consensus sequence of all 16 fully sequenced JEV RNA genomes available from the GenBank database [CH2195LA, CH2195SA, FU, GP78, HVI, JaOArI01, JaGArS982, K94P05, Vellore P20778, p3, SA(A), SA(V), SA14, SA14-14-2, TC, and TL strains] (Table 1).

For JVF amplicons (nucleotides [nt] 1 to 3865), primer J7, complementary to nt 3986 to 4003 of the JEV genome, was used for cDNA synthesis. The primers for PCR amplification were primer J8, complementary to nt 1 to 18, and primer J6, complementary to nt 3845 to 3865. For JVM amplicons (nt 3266 to 8170), primer J4, complementary to nt 8150 to 8170, was used for cDNA synthesis. The primers for PCR amplification were primer J20, complementary to nt 3266 to 3283, and primer J4. For JVR amplicons (nt 7565 to 10893), primer J1, complementary to nt 10947 to 10967, was used for cDNA synthesis. The primers for PCR amplification were primer J12, complementary to nt 7565 to 7582, and primer J2, complementary to nt 10870 to 10893.

The standard RT reaction was conducted in a 20-μl reaction mixture contain-

ing 10 μl of extracted viral RNA, 5 pmol of the appropriate primer, 100 U of Superscript II RT (Gibco-BRL), 40 U of RNaseOUT (Gibco-BRL), 0.1 mM dithiothreitol (DTT), 10 mM deoxynucleoside triphosphate mix, and the RT buffer supplied by the manufacturer (Gibco-BRL). The reaction mixture was incubated at 37°C for 1 h and then heated at 70°C for 15 min. A 5-μl aliquot of the RT mixture was subsequently used for PCR amplification with Pyrobest DNA polymerase (Takara Bio Inc., Shiga, Japan) and the appropriate primer pair. The PCRs were performed with 30 cycles of denaturation at 94°C for 30 s, annealing at 60°C for 30 s, and extension at 72°C for 5 min, followed by a final extension step at 72°C for 10 min.

To sequence the 3′-terminal sequences, a synthetic oligodeoxyribonucleotide T was ligated to the 3′ end of the viral genomic RNA to provide a primer-binding site for cDNA synthesis and PCR amplification as previously described (17). The 3′ end of oligonucleotide T was first modified by incorporating ddATP with terminal deoxynucleotidyltransferase (Takara), which blocks the intramolecular and intermolecular ligation of oligonucleotide T. The 5′ end of oligonucleotide T was also phosphorylated with T4 polynucleotide kinase (Takara). Thereafter, the modified oligonucleotide T was ligated to the 3′ end of the viral genomic RNA by T4 RNA ligase (New England Biolabs, Inc., Beverly, Mass.). The ligation reaction mixture (20 μl) contained 10 U of T4 RNA ligase, 40 U of RNaseOUT, 10 pmol of oligonucleotide T, viral genomic RNA, and the buffer supplied by the manufacturer (NEB). After incubation at 16°C for 12 h, the ligated viral RNA was phenol extracted, precipitated with ethanol, and resuspended with 20 μl of RNase-free water.

Subsequently, half of the oligonucleotide-ligated viral RNA was used for cDNA synthesis with oligonucleotide TR, which is complementary to oligonucleotide T, as previously described. First-strand cDNA was amplified with primer J35, complementary to nt 10259 to 10276, and primer TR. For PCR, one quarter of the RT reaction mix was amplified with Pyrobest DNA polymerase and 30 cycles of 30 s at 94°C, 30 s at 60°C, and 1 min at 72°C, followed by a final extension of 10 min at 72°C. The PCR mixtures were as described above. cDNA amplicons were cloned into the pRS2 vector with *Hin*dIII and *Eco*RI sites incorporated in the positive-sense and negative-sense primers, respectively.

The 5′-terminal sequence was determined by self-ligation of viral RNA (5). The cap structure of viral genomic RNA was first cleaved off with tobacco acid pyrophosphatase. The cleavage reaction mixture (20 μl) contained 10 U of tobacco acid pyrophosphatase (Epicentre Technology Co., Madison, Wis.), 10 μl of viral RNA, and the buffer supplied by the manufacturer (Epicentre Technology Co.). After incubation at 37°C for 1 h, the tobacco acid pyrophosphatase-treated viral RNA was subjected to phenol extraction and ethanol precipitation and resuspended with 20 μl of RNase-free water. Half of the decapped viral RNA was self-ligated in a 20-μl reaction mixture with T4 RNA ligase as described above. A quarter of the self-ligated viral RNA was used for cDNA synthesis with primer J40, complementary to nt 215 to 232. First-strand cDNA was PCR amplified with primer J39, which is complementary to nt 164 to 181, and primer J35. cDNA amplicons were digested with *Apo*I and *Spe*I and ligated into the pRS2 vector which had been digested with *Apo*I and *Xba*I, leading to construct pRS2/JV3′5′.

Complete nucleotide sequence analysis was carried out by directly sequencing the cDNA amplicons representing the entire viral genome of JEV and the individual clones inserted into pRS2 vectors with an automatic 3700 DNA sequencer.

Construction of full-length infectious cDNAs for JEV. Recombinant DNA techniques were used according to standard procedures (31). Three overlapping cDNA amplicons (JVF, JVM, and JVR) originally used for complete nucleotide sequence analysis were first subcloned into pBAC/SV, a derivative of the pBeloBAC11 plasmid (S.-I. Yun and Y.-M. Lee, unpublished data). The pBAC/SV plasmid contains the 491-bp *Not*I-*Aat*II (T4 DNA polymerase-treated) fragment of pACNR/NADL (21), the 9,215-bp *Sac*I (T4 DNA polymerase-treated)-*Ssp*I (T4 DNA polymerase-treated) fragment of pSINrep 19 (10), and the 6,875-bp *Sfi*I (T4 DNA polymerase-treated)-*Not*I fragment of pBeloBAC11. Thus, the 3,863-bp *Rsr*II-*Avr*II fragment of the JVF amplicons, the 4,717-bp *Bsp*EI-*Mlu*I fragment of the JVM amplicons, and the 3,326-bp *Rsr*II-*Bgl*II fragment of the JVR amplicons were inserted into the pBAC/SV plasmid which had been digested with the same enzymes. This led to the pBAC/JVF, pBAC/JVM, and pBAC/JVR subclone constructs, respectively. These BAC plasmids were grown in *E. coli* DH10B cells and sequenced. The nucleotide sequences of the cloned cDNAs were identical to that of CNU/LP2 with the exception of a point mutation, $T^{8906}\rightarrow$ C (silent), within the NS5 gene in pBAC/JVR. The $T^{8906}\rightarrow$ C substitution was corrected by recloning a 315-bp *Apa*I-*Hin*dIII fragment corresponding to nt 8827 to 9142, leading to the construct pBAC/JVRR.

To facilitate the precise adjoining of the bacteriophage SP6 promoter transcription start to the 5′ end of the full-length JEV cDNA, pBAC/JVF was modified. Two fragments were first isolated by PCR of pBAC/SV with primer J41 and primer J43, which incorporates the negative-sense sequence of the SP6 promoter and PCR of pBAC/JVF with primers J42 and J40. These two fragments were fused by a second round of PCR with primers J41 and J40. The resulting amplicons were digested with *Pac*I and *Pme*I and ligated with pBAC/JVF which had been digested with the same two enzymes. This produced $pBAC^{SP6}$/JVF.

To generate an authentic or nearly authentic 3′ terminus during runoff transcription of plasmid linearized at the 3′ end of the viral genome, we modified pBAC/JVRR so that the nucleotide sequence of the authentic 3′ terminus was followed by a unique restriction endonuclease recognition site, either *Xho*I or *Xba*I. To create the pBAC/JVRR/*Xho*I subclone containing a unique *Xho*I site at the end of the viral genome, fragment I was synthesized by PCR amplification of pRS2/JV3′5′ with primer J90 and primer J45, which incorporates an *Xho*I site (Table 1; underlined). The 298-bp *Sfi*I-*Spe*I portion of fragment I amplicons was ligated with pBAC/JVRR which had been digested with *Sfi*I and *Nhe*I. To create pBAC/JVRRx/*Xba*I, which has an *Xba*I site at the end of the viral genome, the existing *Xba*I site at nt 9131 to 9136 within the NS5 gene was first inactivated by introducing a silent point mutation ($A^{9134}\rightarrow$ T) by PCR. Here, pBAC/JVRR was amplified with primer J31 and primer J47, which incorporated the $A^{9134}\rightarrow$ T substitution. The 315-bp *Apa*I-*Hin*dIII portion of the cDNA amplicons, corresponding to nt 8828 to 9143, was cloned into pBAC/JVRR, leading to the construct pBAC/JVRRx. Subsequently, pBAC/JVRRx/*Xba*I was constructed in the same manner as described for pBAC/JVRR/*Xho*I. Thus, fragment II was obtained by PCR amplification of pRS2/JV3′5′ with primer J90 and primer J46, which incorporated an *Xba*I site (Table 1; underlined). The 298-bp *Sfi*I-*Spe*I portion of the fragment II amplicons was then ligated into pBAC/JVRRx which had been digested with *Sfi*I and *Nhe*I. To create pBAC/JVRRx/*Xho*I containing a unique *Xho*I site and the $A^{9134}\rightarrow$ T substitution, the 298-bp *Sfi*I-*Spe*I portion of fragment I amplicons was ligated into pBAC/JVRRx which had been digested with *Sfi*I and *Nhe*I.

Thus, we constructed five plasmids, $pBAC^{SP6}$/JVF, pBAC/JVM, pBAC/JVRR/*Xho*I, pBAC/JVRRx/*Xba*I, and pBAC/JVRRx/*Xho*I. These contained contiguous regions of the JEV genome and could now be used to assemble three different full-length JEV cDNAs, as illustrated in Fig. 3. First, the $pBAC^{SP6}$/JVFM subclone was constructed by ligating together the 4,717-bp *Bsp*EI-*Mlu*I fragment of pBAC/JVM, the 8,970-bp *Bsp*EI-*Xba*I fragment of $pBAC^{SP6}$/JVF, and the 3,670-bp *Xba*I-*Mlu*I fragment of pBAC/SV. Subsequently, two fragments of $pBAC^{SP6}$/JVFM (the 8,142-bp *Pac*I-*Sap*I fragment and the 4,801-bp *Pac*I-*Bsr*GI fragment) were ligated with either (i) the 5,620-bp *Sap*I-*Bsr*GI fragment of pBAC/JVRR/*Xho*I to generate $pBAC^{SP6}$/JVFL/*Xho*I, (ii) the 5,622-bp *Sap*I-*Bsr*GI fragment of pBAC/JVRRx/*Xba*I to generate $pBAC^{SP6}$/JVFLx/*Xba*I, or (iii) the 5,620-bp *Sap*I-*Bsr*GI fragment of pBAC/JVRRx/*Xho*I to generate $pBAC^{SP6}$/JVFLx/*Xho*I.

In addition to the SP6-driven JEV cDNAs, we also constructed a set of three T7-driven full-length cDNAs. A fragment from pBAC/NADLcIns$^-$/PAC (Y.-M. Lee and C. M. Rice, unpublished data) was first synthesized by PCR with the primers J81 and J80. A fragment from $pBAC^{SP6}$/JVFLx/*Xba*I was also synthesized with the primers J42 and J82. These two fragments were fused by a second round of PCR with the primers J81 and J82. The 793-bp *Eco*RI-*Spe*I fragment of the resulting amplicons was inserted into the pRS2 vector digested with *Eco*RI and *Xba*I, leading to the construct $pRS2^{T7}$/5′JV. The 675-bp *Pvu*I-*Pme*I fragment of $pRS2^{T7}$/5′JV was ligated with either (i) the 18,364-bp *Pac*I-*Pme*I fragment of $pBAC^{SP6}$/JVFL/*Xho*I to create $pBAC^{T7}$/JVFL/*Xho*I, (ii) the 18,364-bp *Pac*I-*Pme*I fragment of $pBAC^{SP6}$/JVFLx/*Xho*I to create $pBAC^{T7}$/JVFLx/*Xho*I, or (iii) the 18,366-bp *Pac*I-*Pme*I fragment of $pBAC^{SP6}$/JVFLx/*Xba*I to create $pBAC^{T7}$/JVFLx/*Xba*I.

Mutagenesis of full-length infectious JEV cDNA and insertion of foreign genes. The point mutation $A^{8171}\rightarrow$ C (silent) was placed inside the NS5 gene in $pBAC^{SP6}$/JVFLx/*Xba*I by PCR-based site-directed mutagenesis to generate $pBAC^{SP6}$/JVFLx/gm/*Xba*I (see Fig. 6A). The point mutation resulted in the acquisition of a unique *Xho*I restriction endonuclease recognition site. A fragment from $pBAC^{SP6}$/JVFLx/*Xba*I was first generated by PCR with primer J48, in which the *Xho*I site (Table 1; underlined) was created by the $A^{8171}\rightarrow$ C substitution (Table 1; bold), and primer J3. The 665-bp *Mlu*I-*Apa*I fragment of the resulting amplicons was then ligated with the 4,802-bp *Apa*I-*Bsr*GI and the 5,874-bp *Bsr*GI-*Mlu*I fragments of $pBAC^{SP6}$/JVFLx/*Xba*I, resulting in the $pBAC^{SP6}$/JVFLx/gm/*Xba*I construct.

To generate the $pBAC^{SP6}$/JVFLx/LUC/*Xba*I construct (Fig. 8A), a fragment of $pBAC^{SP6}$/JVFLx/*Xba*I was amplified with primers J72 and J76. A fragment was also amplified from pACNR/NADLcIn$^-$/luciferase (Y.-M. Lee and C. M. Rice, unpublished data) with primers J77 and J78. These two fragments were then fused by a second round of PCR with primers J72 and J78. The 1,801-bp *Kpn*I-*Nsi*I fragment of the resulting amplicons was then ligated with the 8,011-bp

*Nsi*I-*Pac*I and 11,021-bp *Pac*I-*Kpn*I fragments of pBAC^{SP6}/JVFLx/*Xba*I, leading to pBAC^{SP6}/JVFLx/LUC/*Xba*I.

To create the pBAC^{SP6}/JVFLx/GFP/*Xba*I construct (see Fig. 8A), a fragment from pBAC^{SP6}/JVFLx/LUC/*Xba*I was amplified by PCR with the primers J72 and J73. A fragment was also amplified from pRSGFP-C1 with the primers J74 and J75. These two fragments were fused by a second round of PCR with the primers J72 and J75. The 913-bp *Kpn*I-*Nsi*I fragment of the resulting amplicons was then ligated with the 8,011-bp *Nsi*I-*Pac*I and 11,021-bp *Pac*I-*Kpn*I fragments of pBAC^{SP6}/JVFLx/LUC/*Xba*I, resulting in the pBAC^{SP6}/JVFLx/GFP/*Xba*I construct.

To generate pBAC^{SP6}/JVFLx/LUC^{REP-}/*Xba*I (see Fig. 8A), which contains an 83-nucleotide deletion (nt 5581 to 5663) in the middle of the NS3 gene that results in premature termination of viral translation at nt 5596, a fragment of pBAC^{SP6}/JVFLx/LUC/*Xba*I was amplified with primers J89 and J91. A fragment was also amplified from pBAC^{SP6}/JVFLx/LUC/*Xba*I with primers J92 and J93. These two fragments were then fused by a second round of PCR with primers J89 and J93. The 3,960-bp *Sfi*I-*Eag*I fragment of the resulting amplicons was then ligated with the 6,493-bp *Eag*I-*Sfi*I and 10,297-bp *Sfi*I-*Sfi*I fragments of pBAC^{SP6}/JVFLx/LUC/*Xba*I, leading to pBAC^{SP6}/JVFLx/LUC^{REP-}/*Xba*I.

Transcriptions and transfections. RNA transcripts were synthesized by in vitro transcription. Here, 100 to 200 ng of the template DNA linearized with *Xho*I or *Xba*I digestion and in some cases modified with mung bean nuclease was added to a 25-μl reaction mixture consisting of the buffer supplied by the manufacturer (Gibco-BRL) plus 0.6 mM cap analog [m^{7}G(5′)ppp(5′)A or m^{7}G(5′)ppp(5′)G; NEB Inc.], 0.5 μM [^{3}H]UTP (1.0 mCi/ml, 50 Ci/mmol; New England Nuclear Corp., Boston, Mass.), 10 mM DTT, 1 mM each UTP, GTP, CTP, and ATP, 40 U of RNaseOUT, and 15 U of SP6 RNA polymerase (Gibco-BRL). The reaction mixtures were incubated at 37°C for 1 h. RNAs were quantified on the basis of [^{3}H]UTP incorporation as measured by RNA adsorption to DE-81 (Whatman, Maidstone, United Kingdom) filter paper (31). A 1- to 1.5-μl aliquot of reaction mixture was examined by agarose gel electrophoresis, and aliquots were stored at −80°C until use.

For RNA transfection, cells were electroporated with synthetic RNAs with a model ECM 830 electroporator (BTX Inc., San Diego, Calif.) as recommended by the manufacturer. Briefly, subconfluent cells were trypsinized, washed three times with ice-cold RNase-free phosphate-buffered saline (PBS), and resuspended at a density of 2×10^7 cells/ml in PBS. A 400-μl aliquot of the suspension was mixed with 2 μg of synthetic RNA, and the cells were immediately electroporated under the conditions determined previously to be optimal (980 V, 99-μs pulse length, and five pulses). The electroporated mixture was then transferred to 10 ml of fresh medium.

An infectious center assay was used to quantify the specific infectivity of the synthetic RNA. The electroporated cells were serially diluted 10-fold and plated on monolayers of untransfected cells (5×10^5) in a six-well plate. Cells were allowed to attach to the plate for 6 h, after which they were overlaid with 0.5% SeaKem LE agarose-containing MEM as described above. The plates were incubated for 3 to 4 days at 37°C with 5% CO_2, and infectious plaque centers were visualized by crystal violet staining.

Western blot analysis. Cells (3×10^5) were lysed with 200 μl of sample loading buffer [80 mM Tri-HCl (pH 6.8), 2.0% sodium dodecyl sulfate (SDS), 10% glycerol, 0.1 M DTT, 0.2% bromophenol blue], and one-tenth of the lysate was boiled for 5 min and fractionated on an SDS-polyacrylamide gel. Proteins were transferred electrophoretically onto a methanol-activated polyvinylidene difluoride membrane with a Trans-Blot SD electrophoretic transfer cell machine (Bio-Rad Laboratories Inc., Hercules, Calif.), and the membrane was blocked at room temperature for 1 h with 5% nonfat dried milk in washing solution (0.2% Tween 20 in PBS). After three washes with washing solution, membranes were incubated at room temperature for 2 h with either a monoclonal antiactin antibody (A4700) that recognizes the epitope conserved in the C terminus of all actin isoforms (Sigma, St. Louis, Mo.) or mouse hyperimmune ascites fluid specific for JEV (ATCC VR-1259AF; American Type Culture Collection). The membranes were then washed three times with washing solution and incubated at room temperature for 2 h with alkaline phosphatase-conjugated goat anti-mouse immunoglobulin G (Jackson ImmunoResearch Labs Inc., West Grove, Pa.). The membranes were washed three times with washing solution and once with PBS. Actin and JEV protein bands were visualized by incubation with the substrates 5-bromo-4-chloro-3-indolylphosphate and nitroblue tetrazolium.

Northern blot analysis. Total RNA was extracted from infected BHK-21 cells (3×10^5) with 1 ml of Trizol reagent (Gibco-BRL). One-third of the RNA was analyzed for JEV-specific RNA by Northern blot analysis as described elsewhere (31). Briefly, the RNA was electrophoresed in denaturing 2.2 M formaldehyde–1% agarose gels and transferred onto nylon membranes (Amersham Biosciences Inc., Piscataway, N.J.). The RNA on the membranes was cross-linked by irradiation with a 254-nm light source (Stratalinker UV cross-linker; Stratagene, La Jolla, Calif.), and the JEV-specific RNAs were detected by hybridization with a [^{32}P]CTP-labeled antisense riboprobe that binds to nt 9143 to 9351 of the JEV genome. [This probe had been synthesized by in vitro transcription from the *Bam*HI-linearized cDNA clone pGEM3Zf(+)/JV9143, which was constructed by ligating the 209-bp *Hin*dIII-*Sac*I fragment of pBAC^{SP6}/JVFLx/*Xba*I with pGEM3Zf(+) digested with the same enzymes. This clone was transcribed with the T7-MEGAscript kit (Ambion, Austin, Tex.) as recommended by the manufacturer with a 20-μl reaction mixture containing 3.12 μM [α-^{32}P]CTP (800 Ci/mmol; Amersham). After being treated with DNase I, the reaction mixture was spun in a Quick Spin G-50 Sephadex column (Boehringer Mannheim) to remove unincorporated ribonucleoside triphosphates.

The membrane was prehybridized at 55°C for 6 h in hybridization solution [5× SSPE (0.9 M NaCl, 50 mM NaH_2PO_4, and 5 mM EDTA, pH 7.7), 5× Denhardt's reagent, 0.5% SDS, 100 μg of denatured salmon sperm DNA per ml, 50% formamide] and then incubated at 55°C overnight in the hybridization solution containing 10^7 cpm of the labeled riboprobe. The membrane was washed three times at 55°C for 10 min with 1× SSPE–0.5% SDS and once for 10 min with 0.1× SSPE–0.5% SDS. Viral RNA bands were visualized by autoradiography and quantified with a Molecular Imager (Bio-Rad).

Direct immunofluorescence. To examine JEV expression in infected BHK-21 cells by confocal microscopy, cells (2×10^5) were seeded in a four-well chamber slide, incubated for 12 h, and then mock-infected or infected at a multiplicity of infection of 1 for 18 h with either the original JEV K87P39 strain, the JEV CNU/LP2 isolate, or the YF17D strain. Immunostaining for JEV viral proteins was accomplished by first fixing the cells by incubation in PBS containing 0.37% (vol/vol) formaldehyde for 30 min at 25°C. The cells were then washed three times with PBS and permeabilized for 10 min at 37°C with PBS containing 0.2% (vol/vol) Triton X-100. Thereafter, the cells were washed four times with PBS, rehydrated in PBS for 15 min, and blocked for 1 h at 37°C with PBS containing 5% (wt/vol) bovine serum albumin. The cells were then incubated for 2 h at 25°C with 1:500-diluted mouse hyperimmune ascites fluid specific for JEV, washed three times with PBS, incubated for 2 h at 25°C with 1:500-diluted fluorescein isothiocyanate-conjugated goat anti-mouse immunoglobulin G (Jackson ImmunoResearch Labs Inc.), and washed again three times with PBS. Thereafter, the cells were incubated for 30 min at 37°C in PBS containing 5 μg of propidium iodide and 5 μg of RNase A per ml to localize the nuclei and mounted with 0.2 ml of 80% glycerol. Images were acquired on a Zeiss Axioskop confocal microscope equipped with a 63× objective with a Bio-Rad MRC 1024 and LaserSharp software.

To examine green fluorescent protein (GFP) expression, BHK-21 cells were mock-transfected or transfected with 2 μg of JVFLx/GFP/*Xba*IMBN RNA. Transfected cells (10^5) were incubated for 30 h in a four-well chamber slide. Cells were washed twice with PBS, fixed by incubation for 30 min at 25°C in PBS containing 0.37% (vol/vol) formaldehyde, and mounted with 0.2 ml of 80% glycerol. Cells were viewed by confocal microscopy and analyzed as described above.

Luciferase assay. For the luciferase assay, BHK-21 cells (8×10^6) were mock-transfected or transfected with 2 μg of JVFLx/LUC/*Xba*IMBN RNA or JVFLx/LUC^{REP-}/*Xba*IMBN RNA. Cells were seeded at a concentration of 6×10^5 cells/well in a six-well plate and cultivated. At the given time points, the cells were washed with Ca^{2+}- and Mg^{2+}-free PBS solution and then lysed by adding 0.2 ml of lysis buffer [25 mM Tris-phosphate (pH 7.8), 2 mM DTT, 2 mM 1,2-diaminocyclohexane-*N*,*N*,*N*′,*N*′-tetraacetic acid, 10% glycerol, 1% Triton X-100 (vol/vol)] to each well. Cell lysates were incubated for 10 min at room temperature, and cellular debris was then removed by centrifugation. The supernatants were quickly placed at −80°C for storage until use. To determine the luciferase activity, 20 μl of the cell lysates was placed in a luminometer tube containing 100 μl of luciferase assay reagent [20 mM Tricine, 1.07 mM $(MgCO_3)_4Mg(OH)_2 \cdot 5H_2O$, 2.67 mM $MgSO_4$, 0.1 mM EDTA, 33.3 mM DTT, 270 μM coenzyme A, 470 μM luciferin (Promega), 530 μM ATP]. The activity was usually measured for 10 s. Each data point represents the results of three independent experiments.

Cloned full-length cDNA stability. The genetic structure and functional integrity of the infectious JEV cDNAs were analyzed as follows. *E. coli* strain DH10B was transformed with pBAC^{SP6}/JVFLx/*Xba*I, and two independently derived clones were grown at 37°C overnight in 10 ml of 2xYT containing 12.5 μg of chloramphenicol per ml. Cells from these primary cultures were maintained for 9 days by diluting them 10^6-fold every day. After the third, sixth, and ninth passages, large-scale preparation of the infectious cDNA plasmid was made by the SDS-alkaline method and purified further by cesium chloride density gradient centrifugation (31). The genetic structure of the plasmid DNA was monitored by its restriction endonuclease pattern, and its functional integrity was

assessed by measuring the specific infectivities of the synthetic RNAs transcribed from the cDNA template, which was linearized by *Xba*I digestion and mung bean nuclease treatment.

RESULTS

Isolation and complete nucleotide sequence analysis of JEV isolate CNU/LP2. JEV strain K87P39, which was isolated from a wild mosquito in Korea and underwent five passages in suckling mouse brains, was obtained from the Korean National Institute of Health (8). The viral plaque sizes of susceptible BHK-21 cells infected with K87P39 and grown as a monolayer varied, indicating that the viral population is heterogeneous (Fig. 1A, K87P39-infected). Consequently, we employed the plaque purification assay with BHK-21 cells to isolate homogeneous populations of three large-plaque-forming variants that we named CNU/LP1, -2, and -3 (data not shown). Of these three variants, CNU/LP2 consistently maintained its large-plaque phenotype on BHK-21 cells (Fig. 1A, CNU/LP2-infected) or Vero cells (data not shown).

Confocal microscopy with anti-JEV hyperimmune ascites revealed that CNU/LP2-infected BHK-21 cells expressed JEV viral proteins around the perinuclear membranes (Fig. 1B, CNU/LP2-infected), similar to K87P39-infected cells (Fig. 1B, K87P39-infected). This fluorescence staining was not observed in mock-infected BHK-21 cells (Fig. 1B, mock-infected). As a negative control, BHK-21 cells infected with yellow fever virus 17D, a flavivirus closely related to JEV, did not stain with anti-JEV hyperimmune ascites, as expected (Fig. 1B, YF17D-infected). CNU/LP2 infection of a variety of animal cell lines, including the neuronal SHSY-5Y (human) and B103 (mouse) cell lines and the nonneuronal Vero (monkey) and MDCK (dog) cell lines, resulted in high virus titers (10^6 to 10^7 PFU/ml) in the culture supernatants (data not shown). We thus decided to use CNU/LP2 as the parental strain for developing a reverse genetics system for JEV.

Prior to establishing the JEV reverse genetics system, we first had to determine the complete nucleotide sequence of CNU/LP2. Long RT-PCR was used to amplify the entire viral RNA genome apart from the 5′ and 3′ termini (Fig. 2A) and yielded three overlapping cDNA products denoted JVF (nt 1 to 3865), JVM (nt 3266 to 8170), and JVR (nt 7565 to 10893) (about 3.9, 4.9, and 3.3 kb in length, respectively). To ensure faithful cDNA synthesis and amplification, we used the RNase H-negative RT together with the low-error-rate *Pfu* DNA polymerase. To avoid the selection bias that can occur due to cloning, the uncloned materials of the amplified products were directly sequenced in both directions in all cases. Sequencing analysis with two independently isolated preparations of viral RNA resulted in identical sequences.

The 3′-terminal sequence of CNU/LP2 viral RNA was analyzed after synthetic oligonucleotide T was ligated to it. Oligonucleotide T serves as a specific priming site for cDNA synthesis and PCR amplification (Fig. 2B) and has been used successfully to identify the highly conserved 3′ terminus of the hepatitis C virus RNA genome (17). Thus, synthetic oligonucleotide T that had been modified by adding ddATP at its 3′ end to prevent intramolecular and intermolecular ligation was ligated to the 3′ end of the viral RNA, and RT-PCR was then performed with a negative-sense primer complementary to oligonucleotide T and a positive-sense primer corresponding to a sequence near the 3′ end of the viral genome (nt 10259 to 10276) (Fig. 2B). Agarose gel electrophoresis revealed that the amplified products migrated as two bands, a larger band of approximately 700 bp and a smaller band of about 450 bp (Fig. 2C). Both bands were purified and cloned, and 20 and 10 randomly picked clones containing the larger and the smaller bands, respectively, were sequenced. As has been documented for most of the fully sequenced JEV isolates, we found that all the clones with the larger insert terminated the viral genome with GGA TCT^{10968}. In contrast, all the clones with the smaller insert showed the viral genome truncated at nt 10684, resulting in a band 284 bp shorter. During assembly of the full-length JEV cDNA, we used the nucleotide sequences of the larger insert because the smaller insert did not contain 284 nucleotides at the 3′ end of the viral genome.

The 5′-terminal sequence of CNU/LP2 viral RNA was examined after the cap structure at its 5′ end had been removed by incubation with tobacco acid pyrophosphatase (5). The resulting viral RNA was then self-ligated, and the 3′-5′ junction was subjected to cDNA synthesis and PCR amplification with a positive-sense primer for RT-PCR complementary to a sequence near the viral 3′ end (nt 10259 to nt 10276) and a negative-sense primer corresponding to a sequence near the viral 5′ end (nt 164 to nt 181) (Fig. 2D). Agarose gel electrophoresis revealed the amplified products as a single band of about 850 bp (Fig. 2E). The amplicons were cloned, and 12 randomly picked clones were sequenced. In all 12 clones, the GGA TCT^{10968} of the viral 3′-terminal sequence (see Fig. 2B and C) was followed by the 5′-terminal sequence^{1}AGA AGT. Identical results were also obtained by direct cycle sequencing of uncloned material.

Thus, we have determined the complete nucleotide sequence of the CNU/LP2 isolate. The nucleotide sequence of CNU/LP2 was identical to that of the consensus primers used with the exception of a substitution, T^{3851}→ C (Table 1, oligonucleotide J6). This sequence information will soon be available in the GenBank database.

Construction of cDNA encoding the JEV RNA genome as a bacterial artificial chromosome. During our initial attempts to clone the cDNA of the CNU/LP2 RNA genome, it became apparent that a particular region of the viral genome was not compatible with cloning in high-copy-number plasmids in *E. coli* because the cloned DNA underwent genetic rearrangements (data not shown). Attempts to clone this region into a low-copy-number bacterial plasmid were also unsuccessful due to genetic instability together with a low DNA yield (data not shown). These difficulties have also been reported for other flaviviruses (5, 11, 26, 29, 38, 39). We finally succeeded in cloning this cDNA by employing the bacterial artificial chromosome (BAC) plasmid pBeloBAC11 (22, 36, 46). This vector also later proved itself suitable for housing the full-length JEV cDNA.

Each of the three overlapping amplicons JVF, JVM, and JVR that were originally obtained for sequence analysis was subcloned into the pBeloBAC11 plasmid. The nucleotide sequences of the cloned cDNA in all three subclones were identical to that of the parental virus with the exception of a base substitution (T^{8906}→C) in the NS5 gene contained within JVR. This substitution was translationally silent and must have

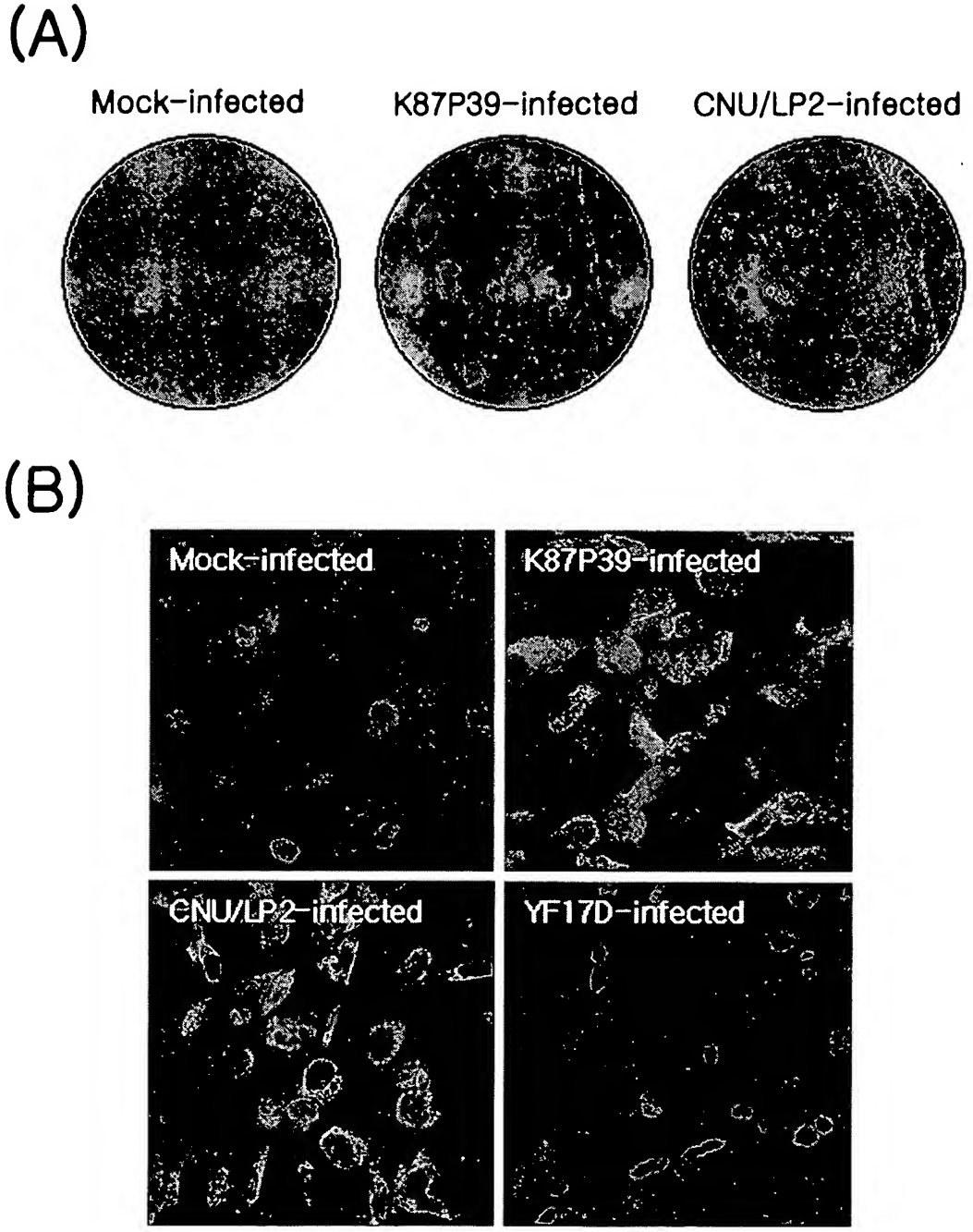

FIG. 1. Comparison of large-plaque-forming JEV isolate CNU/LP2 and original K87P39 strain. (A) Plaque morphology. BHK-21 cells were mock infected or infected with the original JEV K87P39 strain, which formed a heterogeneous mixture of viral plaque sizes. The CNU/LP2 isolate purified in this study formed a homogeneous population of large plaques (CNU/LP2-infected). (B) Levels and patterns of JEV protein expression. Naïve BHK-21 cells were mock infected or infected with K87P39, CNU/LP2, or the yellow fever virus strain YF17D; 18 h later they were fixed and stained with JEV-specific mouse hyperimmune ascites followed by fluorescein isothiocyanate-conjugated goat anti-mouse immunoglobulin G (green fluorescence) and confocal microscopy. Nuclei were visualized by staining with propidium iodide (red fluorescence) in the presence of RNase A.

arisen during the cloning because sequencing of eight randomly picked individual clones revealed a T residue at nt 8906. Although the T^{8906}→C substitution does not alter the corresponding amino acid, it is possible that this change could affect viral replication (43), and thus we corrected this substitution back to a T residue. During their manipulation and propagation in the *E. coli* strain DH10B, all three subcloned cDNAs remained genetically stable (data not shown).

By sequentially linking the overlapping JEV cDNA fragments at natural restriction sites (see Materials and Methods),

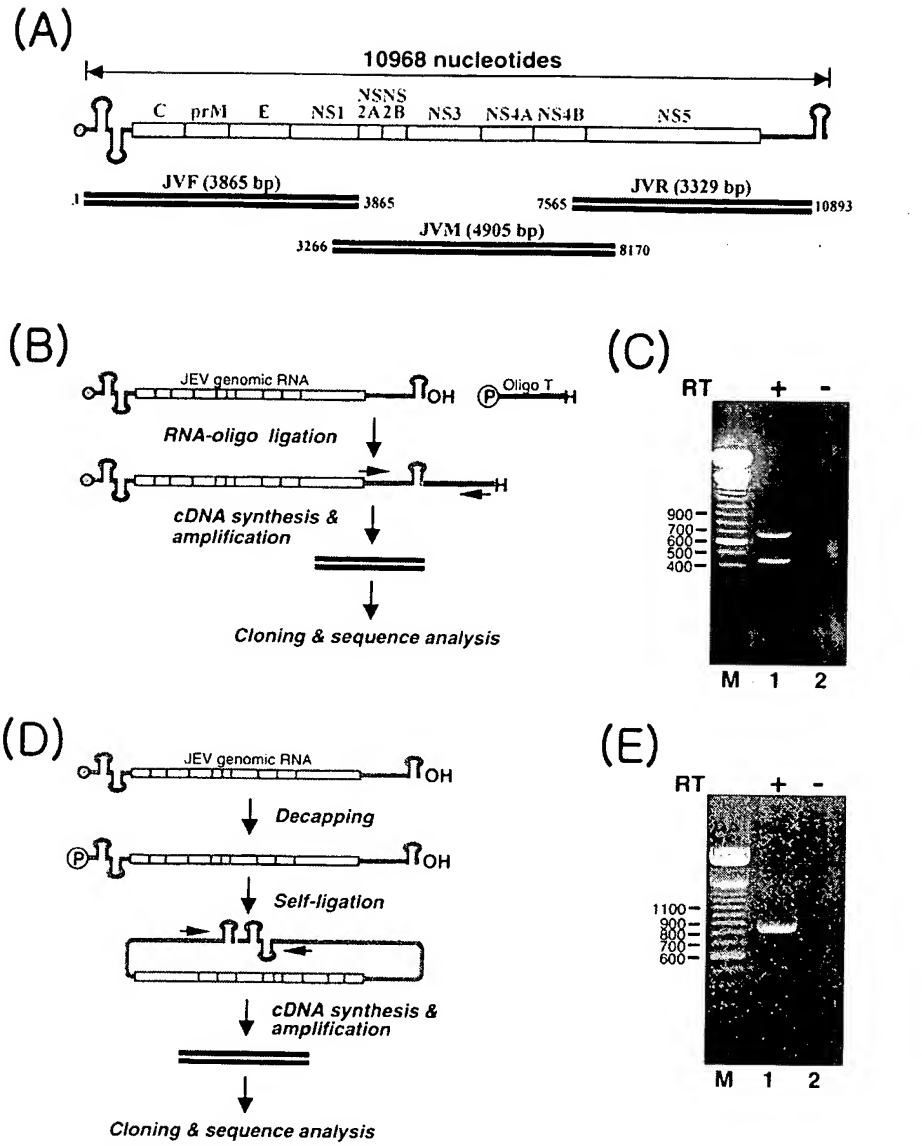

FIG. 2. Strategies used to sequence genomic RNA of CNU/LP2. (A) Scheme for RT-PCR amplification of three overlapping cDNA amplicons representing the entire JEV genomic RNA apart from the 5′ and 3′ termini. RNA is indicated in gray, and cDNA is indicated by solid parallel lines. The top panel schematically depicts the CNU/LP2 JEV genomic RNA (10,968 bp in length). The bottom panels portray the three overlapping cDNAs, JVF (nt 1 to 3865), JVM (nt 3266 to 8170), and JVR (nt 7565 to 10893). (B) Scheme used to sequence the 3′ end of CNU/LP2 genomic RNA. The 5′-phosphorylated and 3′-blocked oligonucleotide T (Oligo T) was ligated to the 3′ end of JEV genomic RNA by T4 RNA ligase, and the resulting RNA was then used for cDNA synthesis and amplification with the primers indicated by an arrow. The resulting products were cloned and sequenced. (C) JEV-specific amplicons synthesized from the oligonucleotide T-ligated JEV genomic RNA described in B. First-strand cDNA was synthesized with oligonucleotide TR, complementary to oligonucleotide T, and the RT reaction was carried out in the presence (lane 1) or absence (lane 2) of Superscript II RT. The cDNA was amplified with oligonucleotide TR and primer J35, which is complementary to nt 10259 to 10276. The expected size of the PCR product is 727 bp. The products were separated on a 1.2% agarose gel and visualized by staining with ethidium bromide. (D) Scheme used to sequence the 5′ end of CNU/LP2 genomic RNA. The cap structure of viral genomic RNA was removed with tobacco acid pyrophosphatase, and the decapped viral RNA was then self-ligated with T4 RNA ligase and used for cDNA synthesis and amplification. The resulting amplified products were cloned and sequenced. (E) JEV-specific amplicons synthesized from the self-ligated JEV genomic RNA described in D. First-strand cDNA synthesis was carried out with primer J40, which is complementary to nt 215 to 232. The RT reaction was performed in the presence (lane 1) or absence (lane 2) of Superscript II RT. The cDNA was amplified with primer J35 and primer J39, which is complementary to nt 164 to 181. The expected size of the PCR product is 890 bp. The products were analyzed on a 1.2% agarose gel as described above. Lane M, 100-bp DNA size ladder (in base pairs).

we assembled six full-length cDNA clones of CNU/LP2 (Fig. 3). Three were designated pBAC^{SP6}/JVFL/*Xho*I, pBAC^{SP6}/JVFLx/*Xho*I, and pBAC^{SP6}/JVFLx/*Xba*I (Fig. 3B). These cDNA clones all had the SP6 promoter transcription start at the beginning of the viral genome so that synthetic RNA transcripts with an authentic 5′ end would be generated. To ensure that the 3′ end of the viral genome after runoff transcription would be close to authentic, we placed a unique restriction

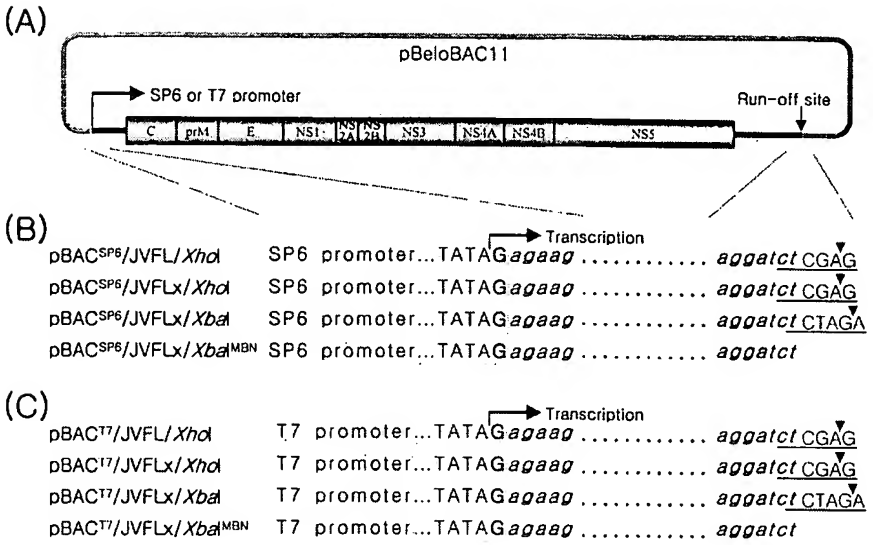

FIG. 3. Construction of full-length JEV cDNA clones in bacterial artificial chromosome pBeloBAC11. (A) Schematic diagram of the full-length JEV cDNAs constructed in this study. Viral proteins are shown with thick solid lines at both termini representing the 5′ and 3′ NTRs of the viral genome. The SP6 and T7 promoter transcription start sites and the unique restriction endonuclease recognition site ensuring runoff transcription are shown at the 5′ and 3′ ends, respectively. (B and C) 5′ and 3′ termini of full-length JEV cDNA clones. Nucleotide sequences of JEV genomic RNA are shown as bold italic lowercase letters. Illustrated are the 5′ termini of four SP6-driven (B) and four T7-driven (C) full-length JEV cDNA templates. To produce SP6 and T7 RNA polymerase runoff products, the 3′ termini of two SP6-driven (B, pBAC^{SP6}/JVFL/*Xho*I and pBAC^{SP6}/JVFLx/*Xho*I) and two T7-driven (C, pBAC^{T7}/JVFL/*Xho*I and pBAC^{T7}/JVFLx/*Xho*I) JEV cDNA templates were linearized by *Xho*I digestion, resulting in three nucleotides (CGA) of virus-unrelated sequence at the 3′ ends. Similarly, the cutting of the 3′ termini of an SP6-driven (B, pBAC^{SP6}/JVFLx/*Xba*I) and a T7-driven (C, pBAC^{T7}/JVFLx/*Xba*I) JEV cDNA template with *Xba*I resulted in four nucleotides (CTAG) of virus-unrelated sequence at the 3′ ends. In contrast, the authentic 3′ end of JEV genomic RNA was present when SP6-driven (B, pBAC^{SP6}/JVFLx/*Xba*IMBN) and T7-driven (C, pBAC^{T7}/JVFLx/*Xba*IMBN) JEV cDNA templates were linearized by *Xba*I digestion and then treated with mung bean nuclease to remove the unrelated single-stranded sequences. Underlined is the restriction endonuclease recognition site introduced at the 3′ end of the viral genome. An arrowhead indicates a cleavage site.

endonuclease site, either *Xho*I or *Xba*I, at the end of the viral genome (Fig. 3B, underlined). Thus, pBAC^{SP6}/JVFL/*Xho*I bears an *Xho*I site at the end of the viral genome. For the construct with an *Xba*I site immediately at the end of viral genome, as the viral genome already contains an *Xba*I site in the NS5 gene, this site had to be destroyed by introducing a silent point mutation ($A^{9134}\rightarrow T$). This construct was designated pBAC^{SP6}/JVFLx/*Xba*I, where the x denotes the presence of the silent point mutation that destroyed the original *Xba*I site. The third clone, pBAC^{SP6}/JVFLx/*Xho*I, contains both the *Xho*I site at the end of viral genome and the $A^{9134}\rightarrow T$ substitution. Three other full-length cDNA clones under the control of the T7 RNA promoter were assembled in a similar manner and led to the constructs designated pBAC^{T7}/JVFL/*Xho*I, pBAC^{T7}/JVFLx/*Xho*I, and pBAC^{T7}/JVFLx/*Xba*I (Fig. 3C). At every cloning step during the assembly process, the structural integrity of the cloned cDNAs was assessed by extensive restriction and nucleotide sequence analyses. Structural instability of the inserts leading to deletions or rearrangements was never observed (data not shown).

In vitro generation of highly infectious synthetic JEV RNAs transcribed from BAC constructs. We first examined the specific infectivity of the synthetic RNAs transcribed from the three SP6-driven constructs. For runoff transcription, the constructs were linearized by digestion with *Xho*I or *Xba*I (Fig. 3). SP6 polymerase runoff transcription of the two *Xho*I-linearized plasmids in the presence of the $m^7G(5')ppp(5')A$ cap structure analog yielded capped synthetic RNAs containing three nucleotides (CGA) of virus-unrelated sequence at their 3′ ends. This is the result of copying the 5′ overhang left by the *Xho*I digestion (Fig. 3B). Similarly, SP6 polymerase runoff transcription of the *Xba*I-linearized pBAC^{SP6}/JVFLx/*Xba*I plasmid produced capped synthetic RNAs with four nucleotides (CTAG) of virus-unrelated sequence at their 3′ ends (Fig. 3B). When susceptible BHK-21 cells were transfected with the synthetic RNAs from these constructs, all were highly infectious (Table 2). That is, the synthetic RNAs obtained from pBAC^{SP6}/JVFL/*Xho*I, pBAC^{SP6}/JVFLx/*Xho*I, and pBAC^{SP6}/JVFLx/*Xba*I transfected under optimal electroporation conditions had specific infectivities of 3.5×10^5, 4.3×10^5, and 3.4×10^5 PFU/μg, respectively (Table 2, infectivity). Similar results were also obtained with synthetic RNAs transcribed from the T7-driven cDNA constructs by T7 polymerase runoff transcription (Table 2, infectivity).

It has been reported that for some flaviviruses, the presence of unrelated sequences at the 3′ end of synthetic RNAs transcribed from infectious cDNA diminishes or abrogates their specific infectivity (48). This motivated us to generate synthetic RNAs lacking the unrelated sequences by treating the *Xba*I-linearized pBAC^{SP6}/JVFLx/*Xba*I plasmid with mung bean nuclease (MBN) prior to the transcription reaction, which removed the four excess nucleotides of CTAG. To verify mung bean nuclease activity, *Xba*I-linearized and mung bean nuclease-treated pBAC^{SP6}/JVFLx/*Xba*I plasmid was self-ligated,

TABLE 2. Specific infectivity of in vitro RNA transcripts generated from full-length JEV cDNAs and virus titer

Template used for transcription[a]	Infectivity[b] (PFU/μg of RNA)	Virus titer[c] (PFU/ml)	
		24 h	48 h
pBAC^{SP6}/JVFL/*Xho*I	3.5×10^5	4.4×10^5	3.6×10^6
pBAC^{T7}/JVFL/*Xho*I	2.9×10^5	2.0×10^5	2.3×10^6
pBAC^{SP6}/JVFLx/*Xho*I	4.3×10^5	2.1×10^5	5.2×10^6
pBAC^{T7}/JVFLx/*Xho*I	3.8×10^5	3.3×10^5	4.1×10^6
pBAC^{SP6}/JVFLx/*Xba*I	3.4×10^5	3.5×10^5	3.2×10^6
pBAC^{T7}/JVFLx/*Xba*I	3.0×10^5	2.4×10^5	2.7×10^6
pBAC^{SP6}/JVFLx/*Xba*IMBN	3.1×10^6	6.2×10^6	1.4×10^6
pBAC^{T7}/JVFLx/*Xba*IMBN	2.7×10^6	5.6×10^6	2.4×10^6

[a] All full-length JEV cDNAs were linearized with an appropriate restriction endonuclease (*Xho*I or *Xba*I) for runoff transcription as indicated in the names of the cDNAs. For pBAC^{SP6}/JVFLx/*Xba*IMBN and pBAC^{T7}/JVFLx/*Xba*IMBN, these cDNA templates were prepared by linearization with *Xba*I digestion, which was followed by treatment with MBN.

[b] After in vitro transcription with SP6 or T7 RNA polymerase, as indicated, samples were used to electroporate BHK-21 cells, and infectious plaque centers were determined as described in Materials and Methods.

[c] Virus titers at 24 and 48 h postelectroporation.

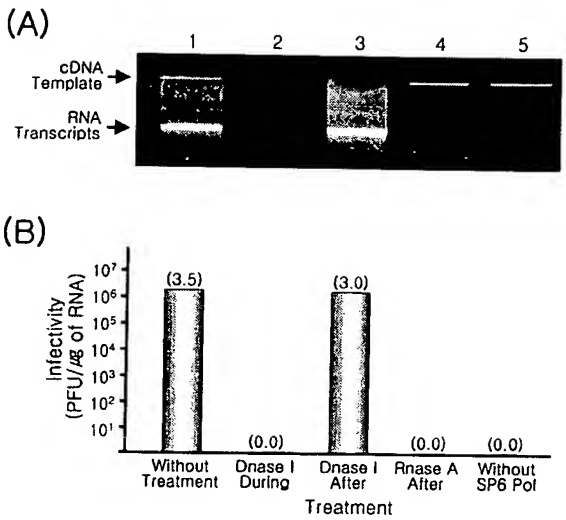

FIG. 4. Full-length JEV cDNA template alone is not infectious but is required for generation of infectious synthetic RNAs during in vitro transcription. pBAC^{SP6}/JVFLx/*Xba*I (100 to 200 ng) linearized with *Xba*I and treated with mung bean nuclease was used for SP6 polymerase transcription in the absence (A, lane 1; B, without treatment) or presence (A, lane 2; B, DNase I during) of DNase I. After synthesis, the transcription reaction mix was treated for 30 min at 37°C with DNase I (A, lane 3; B, Dnase I after) or RNase A (A, lane 4; B, RNase A after). As a control, the reaction was carried out in the absence of SP6 RNA polymerase (A, lane 5; B, without SP6 Pol). (A) Following treatment, 5% of the reaction mixture was separated on a 0.6% agarose gel, and the cDNA template and RNA transcripts were visualized by staining with ethidium bromide. (B) The reaction mixtures were used to transfect BHK-21 cells, and infectious centers of plaques were estimated.

and its viral 3′ end was sequenced, demonstrating removal of the four excess nucleotides of CTAG (data not shown). RNA transcripts from *Xba*I-linearized and mung bean nuclease-treated pBAC^{SP6}/JVFLx/*Xba*I and pBAC^{T7}/JVFLx/*Xba*I (Fig. 3B, pBAC^{SP6}/JVFLx/*Xba*IMBN, and Fig. 3C, pBAC^{T7}/JVFLx/*Xba*IMBN) both had increased specific infectivities compared to the untreated transcripts (Table 2, infectivity). That is, the infectivity of RNAs transcribed from pBAC^{SP6}/JVFLx/*Xba*IMBN was estimated to be 3.1×10^6 PFU/μg, approximately 10-fold higher than the infectivity (3.4×10^5 PFU/μg) of the unmodified template (Table 2, infectivity). The RNAs derived from pBAC^{T7}/JVFLx/*Xba*I (3.0×10^5 PFU/μg) also had increased infectivity after mung bean nuclease modification (2.7×10^6 PFU/μg) (Table 2, infectivity). Thus, the authentic 3′ end of the JEV genome should be present to ensure highly infectious synthetic JEV RNA transcripts are generated.

The altered specific infectivity of the RNA transcripts due to the presence of three or four virus-unrelated nucleotides at the 3′ end also influences the virus titers harvested from culture supernatants of the transfected BHK-21 cells. Virus titers released from BHK-21 cells transfected with RNA transcripts from mung bean nuclease-untreated pBAC^{SP6}/JVFL/*Xho*I, pBAC^{SP6}/JVFLx/*Xho*I, and pBAC^{SP6}/JVFLx/*Xba*I ranged from 2.1×10^5 to 4.4×10^5 PFU/ml at 24 h posttransfection (Table 2, virus titer 24 h), at which time half of the transfected cells were still attached to culture dishes showing virus-induced strong cytopathic effect. These titers increased about 10-fold to the range of 3.2×10^6 to 5.2×10^6 PFU/ml at 48 h posttransfection (Table 2, virus titer 48 h), at which point most of the cells had died and detached from the bottom of the culture dishes. In contrast, the virus titer released from BHK-21 cells transfected with RNA transcripts from mung bean nuclease-treated pBAC^{SP6}/JVFLx/*Xba*IMBN had already reached 6.2×10^6 PFU/ml at 24 h posttransfection, at which time the majority of the transfected cells had died (Table 2, virus titer 24 h). This titer decreased slightly to 1.4×10^6 PFU/ml at 48 h posttransfection (Table 2, virus titer 48 h). Similar patterns of virus production were seen with the T7 polymerase-driven RNA transcripts (Table 2).

We confirmed that specific infectivity requires the transcription of RNA from the full-length JEV cDNA template by using the full-length cDNA clone pBAC^{SP6}/JVFLx/*Xba*IMBN (Fig. 4). The cDNA template alone was not infectious (Fig. 4A, lane 5, and B, without SP6 Pol), but the intact cDNA template was needed during the transcription reaction because DNase I treatment abolished infectivity (Fig. 4A, lane 2, and B, DNaseI during). Addition of DNase I after the transcription reaction had no effect (Fig. 4A, lane 3, and B, DNaseI after) relative to the intact reaction mixture (Fig. 4A, lane 1, and B, without treatment), but RNase A treatment abolished the infectivity of the transcribed synthetic RNAs (Fig. 4A, lane 4, and B, RNase A after).

Synthetic JEVs recovered from full-length infectious cDNAs are indistinguishable from the CNU/LP2 parental virus. We compared the synthetic JEVs recovered from full-length infectious cDNAs with the parental virus CNU/LP2 originally used for cDNA construction. As shown in Fig. 5A, BHK-21 cells infected with synthetic viruses recovered from pBAC^{SP6}/JVFL/*Xho*I (dish 1), pBAC^{SP6}/JVFLx/*Xho*I (dish 2), pBAC^{SP6}/JVFLx/*Xba*I (dish 3), and pBAC^{SP6}/JVFLx/*Xba*IMBN (dish 4) formed homogeneous large plaques, similar to the cells infected with CNU/LP2 (dish 5). The growth properties were also similar. Here, BHK-21 cells were infected with low (0.01

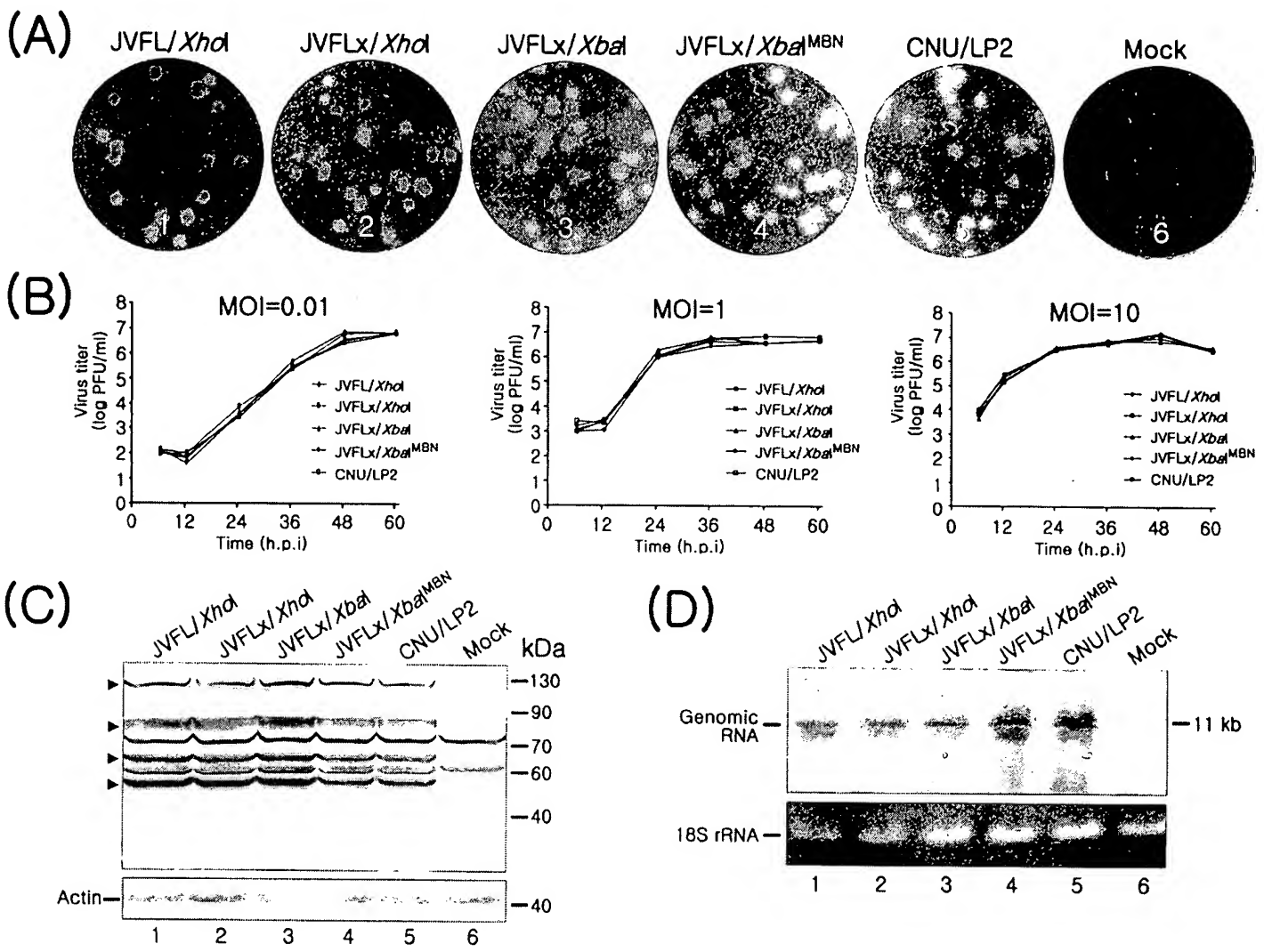

FIG. 5. Comparison of synthetic JEVs with parental virus CNU/LP2. (A) Representative plaque assays of synthetic JEVs and parent CNU/LP2. BHK-21 cells were infected with parent or synthetic viruses, overlaid with agarose, and stained 3 days later with crystal violet. (B) Growth kinetics in BHK-21 cells of synthetic JEVs and parent CNU/LP2 infected at multiplicities of infection of 0.01, 1, and 10. Viruses were harvested at the hour postinfection (h.p.i.) indicated, and titers were determined by plaque assays. The data shown represent one of two independent experiments yielding similar results. (C and D) Viral protein and RNA levels were analyzed by immunoblotting (C) and Northern blotting (D), respectively. BHK-21 cells were infected at a multiplicity of infection of 1 with synthetic JEVs (lanes 1 to 4) or CNU/LP2 (lane 5) or mock-infected (lane 6) and cultured for 18 h. (C) Protein extracts were prepared from approximately 3×10^4 cells and separated on 10% SDS–polyacrylamide gels. Viral proteins were visualized by immunoblotting with JEV-specific mouse hyperimmune ascites (top panel). In parallel, actin protein was detected as a loading and transfer control (bottom panel). The positions of viral protein-related cleavage intermediates and actin are indicated with arrowheads on the left. Molecular mass markers (in kilodaltons) are indicated on the right. (D) Total RNA from approximately 10^5 cells was extracted and analyzed by Northern blotting with a ^{32}P-labeled antisense riboprobe hybridizing to the sequence in the NS5 gene encompassing nt 9143 to 9351 (top panel). Ethidium bromide-stained 18S rRNA bands are shown as a loading control (bottom panel). The positions of full-length genomic viral RNA (11 kb) and 18S rRNA are indicated on the left.

PFU/cell), medium (1 PFU/cell), and high (10 PFU/cell) multiplicities of infection, after which the cell culture fluids were harvested periodically and used to determine the kinetics of infectious virus release over time. As shown in Fig. 5B, the multiplicity of infection-dependent virus titers accumulating over time were similar for the four recovered viruses and the parental virus.

The viral protein and RNA levels in BHK-21 cells infected with the four recovered viruses and the parental virus were also assessed. Anti-JEV hyperimmune ascites used in immunoblotting revealed that the synthetic and parental viruses produced similar amounts and identical patterns of virus-specific proteins (Fig. 5C, top panel). Actin protein was measured as an internal sample loading control and revealed equivalent levels of actin protein in mock-infected and infected cells (Fig. 5C, bottom panel). Viral RNA levels were also similar, as determined by Northern blotting (Fig. 5D). Quantification of these blots by image analysis revealed that the ratios of viral genomic RNA (Fig. 5D, top panel) to 18S rRNA (Fig. 5D, bottom panel) did not differ significantly, demonstrating that all viral genomic RNAs were produced at similar levels.

Thus, all the synthetic viruses were indistinguishable from the parental virus in terms of plaque morphology, cytopathogenicity, growth kinetics, protein expression, and RNA production. Furthermore, analyses of the 3′ end sequence did not reveal an extra three (CGA) or four (CTAG) nucleotides of virus-unrelated sequence at the 3′ end of the viral RNA genomes derived from any of the synthetic viruses (data not shown). These results validate the use of infectious JEV cDNA clones developed in this study for future molecular genetics.

Genetic marker introduced into JEV cDNA observed in the genome of recovered virus. While the above results strongly suggest that the JEV cDNA clones can produce highly infectious RNA transcripts after SP6 or T7 polymerase transcription, the possibility that the transfected cultures were contaminated with the parental virus CNU/LP2 was not formally excluded. To assess this remote possibility, we used PCR-based site-directed mutagenesis to introduce a genetic marker (gm) into the pBAC^{SP6}/JVFLx/*Xba*I construct. This marker is a silent substitution (A^{8171}→C) that results in the gain of a unique *Xho*I site in the NS5 gene (Fig. 6A). The mutagenized construct was designated pBAC^{SP6}/JVFLx/gm/*Xba*I. BHK-21 cells transfected with RNA transcripts from *Xba*I-linearized mung bean nuclease-treated pBAC^{SP6}/JVFLx/gm/*Xba*IMBN produced infectious virus containing the genetic marker (denoted JVFLx/gm/*Xba*IMBN) (Fig. 6A). The phenotypic characteristics of JVFLx/gm/*Xba*IMBN did not differ from those of the original virus JVFLx/*Xba*IMBN, indicating that the A^{8171}→C substitution did not affect viral replication (data not shown).

To verify that the JVFLx/gm/*Xba*IMBN virus had been recovered from the cDNA template of pBAC^{SP6}/JVFLx/gm/*Xba*IMBN, we serially passaged the recovered virus in BHK-21 cells at an multiplicity of infection of 0.1. The viruses resulting from each passage were incubated with RNase A and DNase I to avoid the carryover of the input transcript RNA and template plasmid cDNA (21). Viral RNAs extracted from the JVFLx/gm/*Xba*IMBN and JVFLx/*Xba*IMBN viruses released at passages 1 and 3 were used in RT-PCR to amplify a 2,580-bp product that encompassed the A^{8171}→C substitution (Fig. 6B, lanes 1, 3, and 5). Digestion of the amplified product from JVFLx/gm/*Xba*IMBN with *Xho*I resulted in two fragments of 1,506 and 1,074 bp (Fig. 6B, lanes 2 and 4). The JVFLx/*Xba*IMBN-derived RT-PCR product did not digest with *Xho*I (Fig. 6B, compared lane 5 with lane 6), demonstrating that the A^{8171}→C substitution was indeed present in the JVFLx/gm/*Xba*IMBN virus. Thus, the recovered virus JVFLx/gm/*Xba*IMBN originated from the full-length infectious cDNA pBAC^{SP6}/JVFLx/gm/*Xba*IMBN.

Full-length infectious JEV cDNA as a BAC is maintained with a high degree of genetic stability in *E. coli*. A previous study has shown that constructs containing full-length JEV cDNA frequently acquired stabilizing nonsense mutations in the regions encoding the structural proteins prM and E (38). Since studies into the molecular genetics of JEV will indispensably require a reliable infectious JEV molecular clone for manipulation, we manipulated pBAC^{SP6}/pJVFLx/*Xba*I in several ways and extensively investigated its genetic structure and functional integrity. We first assessed the clones of *E. coli* DH10B bacteria transformed with pBAC^{SP6}/pJVFLx/*Xba*I and grown on semisolid medium at 37°C. Small but homogeneous bacterial colonies appeared after 15 to 20 h, and extensive restriction analysis with 10 randomly picked clones showed no evidence of deletions or rearrangements. That is, the restriction endonuclease patterns of all 10 clones were identical when digested with *Nco*I (nine sites), *Bgl*I (nine sites), *Pst*I (seven sites), *Hin*dIII (seven sites), *Ssp*I (six sites), *Bgl*II (six sites), and *Sac*I (six sites) (data not shown). SP6 polymerase transcription with each of these 10 clones as the template consistently yielded synthetic RNAs with high specific infectivities ranging from 2.7×10^6 to 3.1×10^6 PFU/μg (Table 2 and data not shown).

We also assessed the construct stability of two independent pBAC^{SP6}/JVFLx/*Xba*I-containing *E. coli* clones propagated for 9 days. The cells were grown in liquid medium overnight and subsequently propagated by diluting them 10^6-fold daily as described previously (2). In our experimental conditions, each passage represented approximately 20 generations, which is consistent with observations made previously (2). The plasmids extracted from the two cultures at passages 0, 3, 6, and 9 were examined by restriction enzyme analysis. The restriction enzyme patterns at passages 3, 6, and 9 did not differ visibly from those at passage 0 (data not shown). Thus, within the resolution of agarose gel electrophoresis analysis, the two infectious BAC clones appeared to be structurally stable. Furthermore, the infectivity of the RNA transcripts made from the two cDNA clones did not differ between passage 0 and passage 9 (Fig. 7), confirming that the infectious JEV cDNA remained functionally stable during serial growth in *E. coli*.

Infectious JEV cDNA as a vector for foreign gene expression. As previously described (3), we found that JEV was able to replicate in a wide variety of eukaryotic cells originating from a number of species, including humans, mice, monkeys, swine, dogs, cats, and hamsters (data not shown). This suggests that JEV could be useful as a vector for the expression of heterologous genes in a variety of different cells. To test this, two commonly used reporter genes, the *Aequorea victoria* green fluorescent protein (GFP) and the *Photinus pyralis* luciferase (LUC), were inserted at the beginning of the viral 3′NTR of pBAC^{SP6}/JVFLx/*Xba*I as expression cassettes driven by the internal ribosome entry site of encephalomyocarditis virus

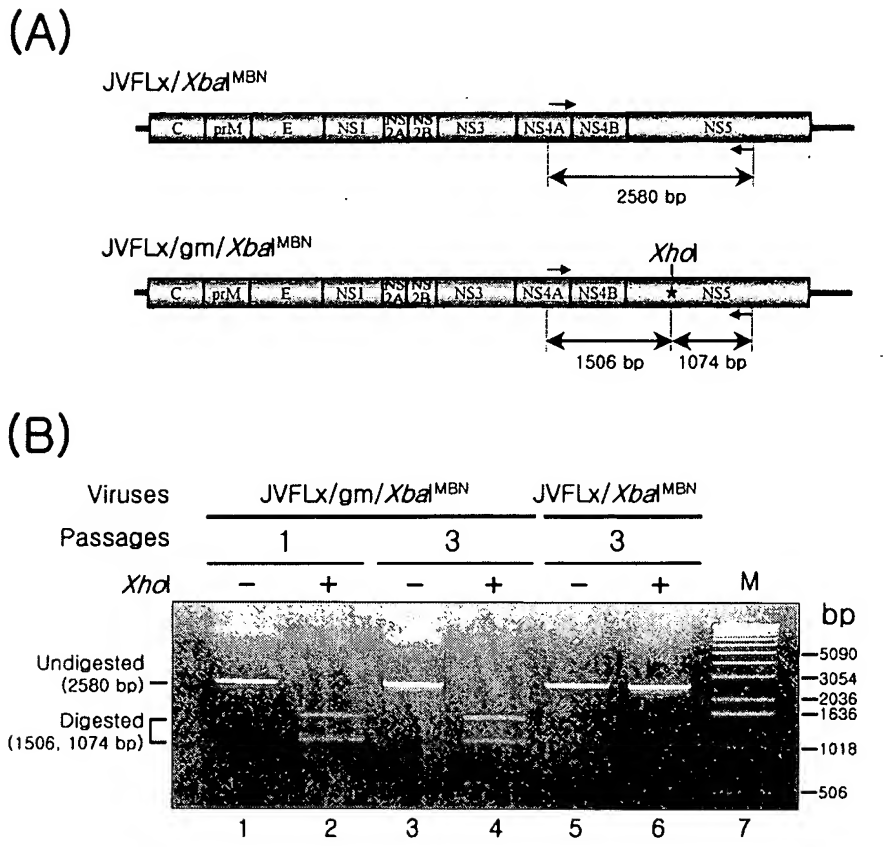

FIG. 6. Presence of *Xho*I genetic marker in recombinant JEVs derived from pBAC^{SP6}/JVFLx/gm/*Xba*I. (A) Schematic diagram of the RT-PCR fragments of JVFLx/*Xba*IMBN and JVFLx/gm/*Xba*IMBN expected after *Xho*I digestion. Indicated are the primers used for RT-PCR (arrows), the introduced *Xho*I site (asterisk), and the sizes of the RT-PCT products (2,580 bp) and the two *Xho*I digestion products (1,506 bp and 1,074 bp) expected after digestion of JVFLx/gm/*Xba*IMBN with *Xho*I. (B) BHK-21 cells were transfected with synthetic RNAs transcribed from either pBAC^{SP6}/JVFLx/*Xba*IMBN or pBAC^{SP6}/JVFLx/gm/*Xba*IMBN. Viruses were recovered 24 h later and serially passaged in BHK-21 cells at a multiplicity of infection of 0.1. At each passage prior to the next round of infection, viruses were incubated with DNase I and RNase A (21). At passages 1 and 3, viral RNA was extracted from the culture supernatant containing the released viruses and used for RT-PCR. The PCR products were incubated in the presence (+) or absence (−) of *Xho*I, separated on a 1% agarose gel, and stained with ethidium bromide. The expected sizes of the undigested and digested PCR products are shown on the left. Lane M, 1-kb DNA ladder.

(Fig. 8A). A deletion of 11 to 25 nucleotides exists at the beginning of the viral 3′NTR in CNP/LP2 and three other fully sequenced JEV strains (14, 25, 47), suggesting that this may be a good site to insert the foreign genes. In both cases, the insertion did not alter the infectivity of the synthetic RNA transcripts, although the level of viral replication was slightly decreased (data not shown).

To examine GFP expression, naive BHK-21 cells were transfected with infectious synthetic RNA transcribed from the pBAC^{SP6}/JVFLx/GFP/*Xba*IMBN template and examined by confocal microscopy. Cells expressing GFP displayed green fluorescence in both the nucleus and the cytoplasm (Fig. 8B, JVFLx/GFP/*Xba*IMBN) because GFP is small enough (≈30 kDa) to permit diffusion between the nucleus and the cytoplasm. As expected, this fluorescence was not observed in mock-transfected cells (Fig. 8B, mock) or in cells transfected with RNA transcripts from pBAC^{SP6}/JVFLx/*Xba*IMBN (data not shown).

To monitor the induction of luciferase over time in a quantitative manner, we produced not only replication-competent RNA transcripts from pBAC^{SP6}/JVFLx/LUC/*Xba*IMBN but

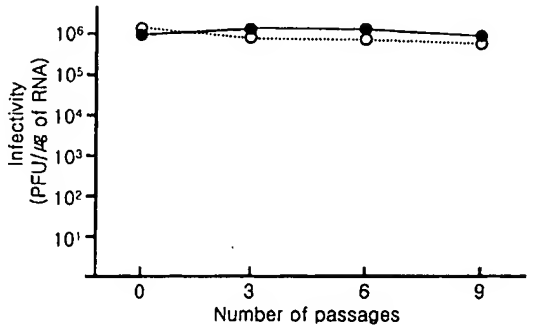

FIG. 7. Specific infectivity of synthetic RNAs transcribed from infectious JEV cDNA clones propagated for 180 generations. Two independent clones carrying pBAC^{SP6}/JVFLx/*Xba*I (solid and open circles) were cultivated at 37°C overnight in 2xYT with chloramphenicol. The primary cultures were propagated every day for 9 days by 10^6-fold dilution and adding fresh broth for overnight growth. Each passage was estimated to be about 20 generations (2). At the indicated passages, the DNA plasmids were purified, linearized by *Xba*I digestion, treated with mung bean nuclease, and used as templates for runoff transcription with SP6 RNA polymerase. The transcripts were then used to transfect BHK-21 cells to determine specific infectivity.

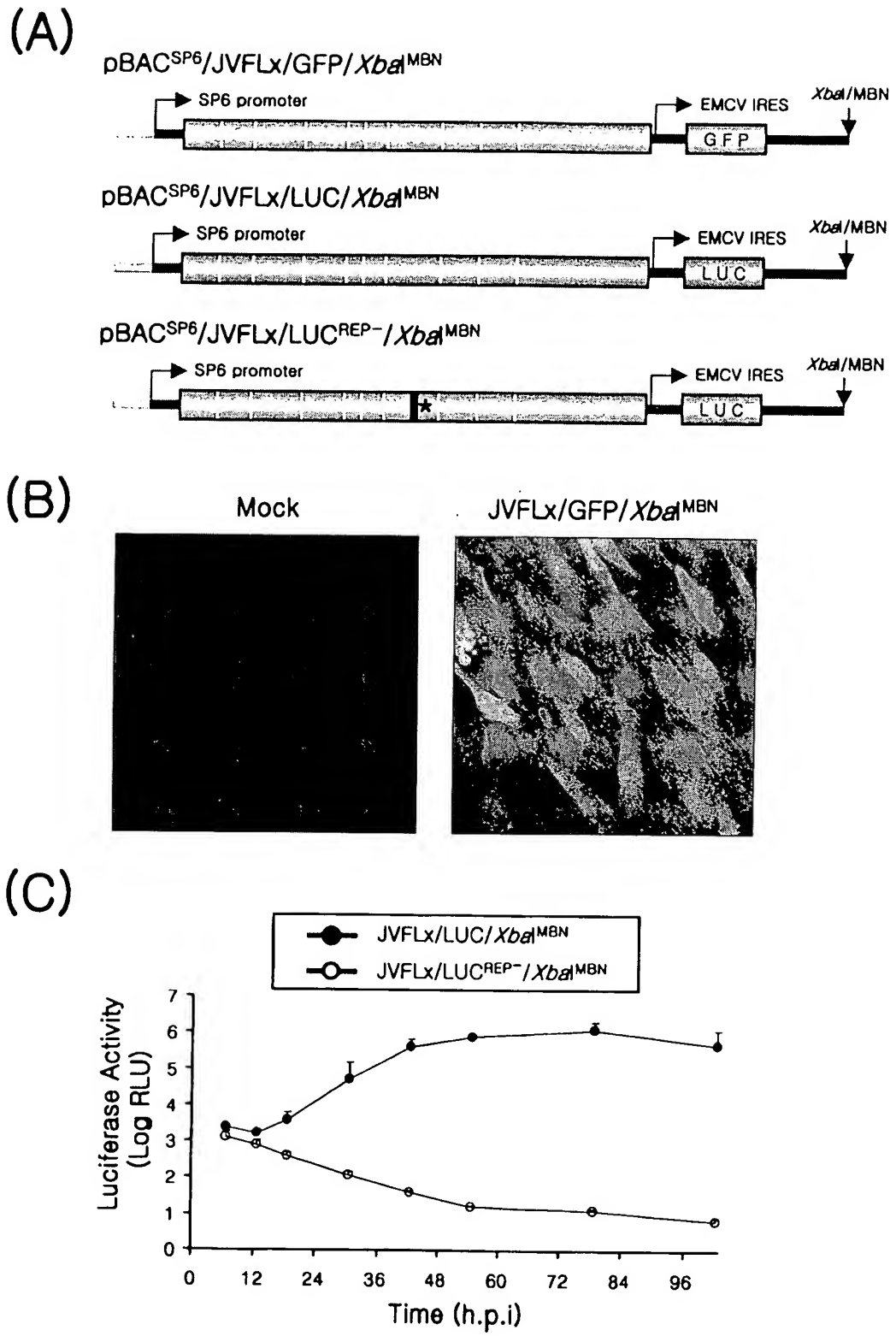

FIG. 8. Expression of foreign genes with JEV cDNA as the vector. (A) Schematic diagram of the pBAC^{SP6}/JVFLx/GFP/*Xba*IMBN, pBAC^{SP6}/JVFLx/LUC/*Xba*IMBN, and pBAC^{SP6}/JVFLx/LUC^{REP-}/*Xba*IMBN cDNA templates used for runoff transcription with SP6 RNA polymerase. Indicated are the encephalomyocarditis virus (EMCV) internal ribosome entry site (IRES)-driven GFP and luciferase genes that were inserted at the beginning of the 3′NTR of the viral genome, the SP6 promoter transcription start, and the runoff site generated by *Xba*I digestion and mung bean nuclease treatment (*Xba*I/MBN). In pBAC^{SP6}/JVFLx/LUC^{REP-}/*Xba*IMBN, a solid vertical bar indicates an 83-nucleotide deletion (nt 5581 to 5663) in the middle of the NS3 gene that determines viral translation at nt 5596 (asterisk). (B) Expression of GFP protein. BHK-21 cells were mock transfected or transfected with 2 μg of synthetic RNAs transcribed from the pBAC^{SP6}/JVFLx/GFP/*Xba*IMBN template (JVFLx/GFP/

also replication-incompetent RNA transcripts from pBAC^{SP6}/JVFLx/LUC^{REP-}/*Xba*IMBN (Fig. 8A). The pBAC^{SP6}/JVFLx/LUC^{REP-}/*Xba*IMBN template contains an 83-nucleotide deletion (nt 5581 to nt 5663) in the middle of the NS3 gene that prematurely terminates viral translation at nt 5596 (see asterisk in Fig. 8A, pBAC^{SP6}/JVFLx/LUC^{REP-}/*Xba*IMBN). In BHK-21 cells transfected with the replication-competent JVFLx/LUC/*Xba*IMBN RNA (Fig. 8C, solid circles), the initial luciferase activity 6 h posttransfection was $2.4 \times 10^3 \pm 0.2 \times 10^3$ relative light units (RLU). This activity was dramatically increased to $5.3 \times 10^4 \pm 0.1 \times 10^4$ RLU 30 h posttransfection and reached $7.8 \times 10^5 \pm 0.6 \times 10^5$ RLU 54 h posttransfection, at which point >50% of the cells were dying. In contrast, in BHK-21 cells transfected with the replication-incompetent JVFLx/LUC^{REP-}/*Xba*IMBN RNA, the initial luciferase activity 6 h posttransfection was $1.9 \times 10^3 \pm 0.4 \times 10^3$ RLU (Fig. 8C, open circles), like the JVFLx/LUC/*Xba*IMBN-transfected cells (Fig. 8C, solid circles), but this activity gradually decreased over time to 16 ± 1.2 RLU at 54 h posttransfection, which is at the level of background luminescence of naïve cells (Fig. 8C, open circles). Thus, the level of luciferase activity expressed over time varied depending on the presence or absence of viral replication.

We recovered the recombinant JVFLx/GFP/*Xba*IMBN and JVFLx/LUC/*Xba*IMBN viruses and infected a variety of commonly used animal cell lines, including nonneuronal and neuronal cells. The GFP or luciferase gene was expressed in all cell types tested (data not shown). Thus, recombinant JEV RNAs and viruses are useful as vectors for foreign gene expression in eukaryotic cells.

DISCUSSION

Here we report the development of a convenient and reliable reverse genetics system for JEV that can be used to generate synthetic viruses from genetically stable full-length infectious JEV cDNAs. Previous attempts to develop such a system (23, 38, 39, 51), including our own, were thwarted by the instability of the cloned JEV cDNA. The system described in this paper will greatly facilitate the study of the molecular mechanisms of replication, virulence, and pathogenesis employed by the virus. Furthermore, we showed that this system can be used as a JEV RNA vector that will rapidly express heterologous genes in a wide variety of eukaryotic cells.

We were able to overcome the instability of JEV cDNA by employing bacterial artificial chromosomes (BACs), which could even stably accommodate the full-length infectious JEV cDNA. These could be used as templates for runoff transcription that generated highly infectious synthetic RNAs with a specific infectivity of 10^5 to 10^6 PFU/μg. The transfected cells also released synthetic virus progeny with a virus titer of 10^6 to 10^7 PFU/ml. The recovered viruses were phenotypically indistinguishable from the parental virus. We also used a standard mutagenesis procedure to introduce a point mutation that acted as a genetic marker into the BAC construct. This allowed us to confirm that the recovered viruses were derived from the infectious cDNA. It also indicated that virus mutants can be generated by genetically manipulating the infectious cDNA in *E. coli*. Thus, our system will facilitate the genetic analysis of the replicative mechanisms of the JEV genome.

It is important to produce full-length infectious JEV cDNA that, in in vitro transcription, would generate RNA transcripts with authentic 5′ and 3′ ends because several studies have shown that both the 5′- and 3′-terminal regions are needed for the initiation of flavivirus RNA replication in vitro (49, 50) and in vivo (16). To achieve this objective, we adapted approaches used previously for other flaviviruses (29, 42). The cap structure in JEV genomic RNA is followed by the dinucleotide AG, an absolutely conserved feature of the flaviviruses (28). The authenticity of the 5′ end was ensured by placing either the SP6 or the T7 promoter transcription start at the beginning of the viral genome. Incorporating the m^{7}G(5′)ppp(5′)A cap structure analog in the SP6 and T7 polymerase-driven transcription reactions (9) then allowed us to synthesize capped RNA transcripts with authentic 5′ ends that were highly infectious upon transfection into susceptible cells. In addition, incorporating the m^{7}G(5′)ppp(5′)G cap structure analog in the SP6 and T7 polymerase-driven transcription reactions (9) places an unrelated extra G nucleotide upstream of the dinucleotide AG. As reported earlier (29), we did find that the extra nucleotide was lost from the genomic RNA of the recovered JEV progeny (data not shown). Furthermore, we did not observe that the infectivity or the replication of synthetic RNAs transcribed from infectious cDNA templates was altered if we added the extra nucleotide (data not shown).

The dinucleotide CU located at the 3′ end of JEV RNA is absolutely conserved among the flaviviruses except for the cell fusing agent (4, 28). This suggests that these nucleotides are important in viral replication and that transcripts from infectious cDNAs must have authentic 3′ ends. We thus designed our reverse genetics system for JEV so that the synthetic RNA would be terminated with the authentic 3′ end. We showed indeed that RNA transcripts with authentic 3′ ends were 10-fold more infectious than transcripts with three or four virus-unrelated nucleotides hanging on their 3′ ends. This is consistent with a previous study showing that unrelated sequences at the 3′ end of synthetic RNAs of the West Nile virus delayed the establishment of a productive infection (48).

A variety of vector systems were used previously in attempts to assemble a full-length JEV cDNA (23, 38, 39, 51), including a cosmid vector in *E. coli* (51). In all cases, the cloned cDNA became genetically unstable during its propagation in a host. Similarly, our attempts to clone stable full-length JEV CNU/LP2 cDNA in all high-copy-number pUC-derived, medium-copy-number pBR322-derived, and low-copy-number pACYC184-derived vectors tested were unsuccessful. One study attempted to

*Xba*IMBN), incubated for 30 h, and then fixed and examined by confocal microscopy. (C) Induction of luciferase protein. BHK-21 cells (8×10^6) were mock transfected or transfected with 2 μg of synthetic RNAs transcribed from the pBAC^{SP6}/JVFLx/LUC/*Xba*IMBN (solid circles) and pBAC^{SP6}/JVFLx/LUC^{REP-}/*Xba*IMBN (open circles) templates and seeded in a six-well plate at a density of 6×10^5 cells per well. Cells were lysed at the indicated time points, and luciferase activity was determined. The standard deviations obtained from three independent experiments are indicated by error bars.

overcome this problem by designing a system in which the template would be generated by in vitro ligation of two overlapping JEV cDNAs (38). This template was then used to synthesize infectious RNA transcripts in vitro. However, the specific infectivity of these transcripts was about 100 PFU/μg, which was too low to make this system useful for molecular and genetic analyses of virus biology (38).

In this report, we were able to overcome the genetic instability of JEV cDNA by cloning it into a BAC plasmid that is maintained at one or two copies in *E. coli*. The genetic structure and functional integrity of the infectious cDNA plasmid remained stable for at least 180 generations during its propagation in *E. coli*. It should be noted that the genetic stability of this system is not simply due to use of the BAC plasmid as a cloning vector, as an attempt to clone full-length cDNA of the avian infectious bronchitis virus into the same BAC plasmid was unsuccessful (6). Further studies elucidating the reason for the genetic stability of the full-length JEV cDNA in the BAC plasmid may be useful for the construction of other infectious flavivirus cDNAs.

Alphaviruses, which are also RNA viruses, can replicate in a variety of commonly used animal cells and thus have been successfully exploited as eukaryotic expression vectors in cell culture and in vivo (1, 10, 33). We and others (3) have found that JEV, like the alphaviruses, is also able to replicate in a wide variety of primary and continuous cell cultures from humans, mice, monkeys, cows, pigs, dogs, cats, and hamsters (data not shown). This makes JEV attractive as a eukaryotic expression vector. Supporting this are our studies showing that when two representative reporter genes, GFP and luciferase, were inserted into JEV genomic RNA and placed in BHK-21 cells, they were expressed. Thus, the infectious JEV cDNA can act as an expression vector for the rapid expression of a number of heterologous genes in a wide variety of eukaryotic cells.

In this regard, previous studies have shown that replicons of other flaviviruses are employed for efficient expression of heterologous genes, including GFP and luciferase (15, 24, 35, 44). In addition to a transient gene expression system, development of a noncytopathic JEV RNA replicon vector for generation of stable cell lines continuously expressing heterologous genes is desirable, if possible. When a particular type of cell is to be targeted, however, gene expression systems derived from flaviviruses might be disadvantageous due to their broad host range. The JEV cDNA clones described here would be useful in defining the minimal and optimal viral genetic elements needed to use JEV as an expression vector and to develop a packaging system for RNA vectors.

The reverse genetics system for JEV described here will greatly aid several basic and applied research areas. First, this system will help us to investigate the molecular mechanisms of JEV replication, transcription, and translation as well as to identify the JEV genetic elements involved in neurovirulence and pathogenesis. Second, the JEV RNA vector could be an invaluable genetic tool for heterologous gene expression in a wide variety of eukaryotic cells for many applications in biological research. Third, in connection with the ongoing JEV epidemic in Asia and the recent expansion of the virus to Australia, the ability to generate recombinant JEV by targeted manipulation of the infectious JEV cDNA opens up new approaches to the design of genetically modified anti-JEV vaccines.

ACKNOWLEDGMENTS

We are very grateful to Cheong-Sun Chen for excellent technical assistance with the confocal microscopy experiments. We also thank Chan-Hee Lee for plasmid pRSGFP-C1.

This study was supported by grants from the Korea Ministry of Health and Welfare, Republic of Korea (02-PJ1-PG3-20203-0014 and 01-PJ1-PG3-20200-0060).

REFERENCES

1. **Agapov, E. V., I. Frolov, B. D. Linderbach, B. M. Pragai, S. Schlesinger, and C. M. Rice.** 1998. Noncytopathic Sindbis virus RNA replicons for heterologous gene expression. Proc. Natl. Acad. Sci. USA **95**:12989–12994.
2. **Almazan, F., J. M. Gonzalez, Z. Penzes, A. Izeta, E. Calvo, J. Plana-Duran, and L. Enjuanes.** 2000. Engeneering the largest RNA virus genome as an infectious bacterial artificial chromosome. Proc. Natl. Acad. Sci. USA **97**: 55–5521.
3. **Burke, D. S., and T. P. Monath.** 2001. Flaviviruses. p. 1043–1125. *In* D. M. Knipe, P. M. Howley, D. E. Griffin, R. A. Lamb, M. A. Martin, B. Roizman, and S. E. Straus (ed.), Fields virology, 4th ed. Lippincott Williams & Wilkins Publishers, Philadelphia, Pa.
4. **Cammisa-Parks, H., L. A. Cisar, A. Kane, and V. Stollar.** 1992. The complete nucleotide sequence of cell fusing agent (CFA): homology between the nonstructural proteins encoded by CFA and the nonstructural proteins encoded by arthropod-borne flaviviruses. Virology **189**:511–524.
5. **Campbell, M. S., and A. G. Pletnev.** 2000. Infectious cDNA clones of Langat tick-borne flavivirus that differ from their parent in peripheral neurovirulence. Virology **269**:225–237.
6. **Casais, R., V. Thiel, S. G. Siddell, D. Cavanagh, and P. Britton.** 2001. Reverse genetics system for the avian coronavirus infectious bronchitis virus. J. Virol. **75**:12359–12369.
7. **Chambers, T. J., C. S. Halm, R. Galler, and C. M. Rice.** 1990. Flavivirus genome organization, expression, and replication. Annu. Rev. Microbiol. **44**:649–688.
8. **Chung, Y.-J., J.-H. Nam, S.-J. Ban, and H.-W. Cho.** 1996. Antigenic and genetic analysis of Japanese encephalitis virus isolated from Korea. Am. J. Trop. Med. Hyg. **55**:91–97.
9. **Contreras, R., H. Cheroutre, W. Degrave, and W. Fiers.** 1982. Simple, efficient in vitro synthesis of capped RNA useful for direct expression of cloned eukaryotic genes. Nucleic Acids Res. **10**:6353–6362.
10. **Frolov, I., T. A. Hoffman, B. M. Pragai, S. A. Dryga, H. V. Huang, S. Schlesinger, and C. M. Rice.** 1996. Alphavirus-based expression vectors: strategies and applications. Proc. Natl. Acad. Sci. USA **93**:11371–11377.
11. **Gritsun, T. S., and E. A. Gould.** 1995. Infectious transcripts of tick-borne encephalitis virus, generated in days by RT-PCR. Virology **214**:611–618.
12. **Hanna, J. N., S. A. Ritchie, D. A. Phillips, J. Shield, M. C. Bailey, J. S. Mackenzie, M. Poidinger, B. J. McCall, and P. J. Mills.** 1996. An outbreak of Japanese encephalitis in the Torres Strait, Australia, 1995. Med. J. Aust. **165**:256–260.
13. **Hanna, J. N., S. A. Ritchie, D. A. Phillips, J. M. Lee, S. L. Hills, A. F. van den Hurk, A. T. Pyke, C. A. Johansen, and J. S. Mackenzie.** 1999. Japanese encephalitis in north Queensland, Australia, 1998. Med. J. Aust. **170**:533–536.
14. **Jan, L. R., K. L. Chen, C. F. Lu, Y. C. Wu, and C. B. Horng.** 1996. Complete nucleotide sequence of the genome of Japanese encephalitis virus ling strain: the presence of a 25-nucleotide deletion in the 3′-nontranslated region. Am. J. Trop. Med. Hyg. **55**:603–609.
15. **Khromykh, A. A., and E. G. Westaway.** 1997. Subgenomic replicons of the flavivirus Kunjin: construction and applications. J. Virol. **71**:1497–1505.
16. **Khromykh, A. A., H. Meka, K. J. Guyatt, and E. G. Westaway.** 2001. Essential role of cyclization sequences in flavivirus RNA replication. J. Virol. **75**:6719–6728.
17. **Kolykhalov, A. A., S. M. Feinstone, and C. M. Rice.** 1996. Identification of a highly conserved sequence element at the 3′ terminus of hepatitis C virus genome RNA. J. Virol. **70**:3363–3371.
18. **Liljestrom, P., and H. Garoff.** 1991. A new generation of animal cell expression vectors based on the Semliki Forest virus replicon. Bio/Technology **9**:1356–1361.
19. **Lindenbach, B. D., and C. M. Rice.** 2001. *Flaviviridae*: The viruses and their replication, p. 991–1041. *In* D. M. Knipe, P. M. Howley, D. E. Griffin, R. A. Lamb, M. A. Martin, B. Roizman, and S. E. Straus (ed.), Fields virology, 4th ed. Lippincott Williams & Wilkins Publishers, Philadelphia, Pa.
20. **Mackenzie, J. S., M. D. Lindsay, R. J. Coelen, A. K. Broom, R. A. Hall, and D. W. Smith.** 1994. Arboviruses causing human disease in the Australian zoogeographic region. Arch. Virol. **136**:447–467.
21. **Mendez, E., N. Ruggli, M. S. Collett, and C. M. Rice.** 1998. Infectious bovine viral diarrhea virus (strain NADL) RNA from stable cDNA clones: a cellular

insert determines NS3 production and viral cytopathogenicity. J. Virol. **72:** 4737–4745.

22. **Messerle, M., I. Crnkovic, W. Hammerschmidt, H. Ziegler, and U. H. Koszinowski.** 1997. Cloning and mutagenesis of a herpesvirus genome as an infectious bacterial artificial chromosome. Proc. Natl. Acad. Sci. USA **94:** 14759–14763.
23. **Mishin, V. P., F. Cominelli, and V. F. Yamshchikov.** 2001. A 'minimal' approach in design of flavivirus infectious DNA. Virus Res. **81:**113–123.
24. **Molenkamp, R., E. A. Kooi, M. A. Lucassen, S. Greve, J. C. Thijssen, W. J. Spaan, and P. J. Bredenbeek.** 2003. Yellow fever virus replicons as an expression system for hepatitis C virus structural proteins. J. Virol. **77:**1644–1648.
25. **Nam, J.-H., S.-L. Chae, S.-Y. Won, E.-J. Kim, K.-S. Yoon, B.-I. Kim, Y.-S. Jeong, and H.-W. Cho.** 2001. Short report: genetic heterogeneity of Japanese encephalitis virus assessed via analysis of the full-length genome sequence of a Korean isolate. Am. J. Trop. Med. Hyg. **65:**388–392.
26. **Polo, S., G. Ketner, R. Levis, and B. Falgout.** 1997. Infectious RNA transcripts from full-length dengue virus type 2 cDNA clones made in yeast. J. Virol. **71:**5366–5374.
27. **Racaniello, V. R., and D. Baltimore.** 1981. Cloned poliovirus complementary DNA is infectious in mammalian cells. Science **214:**916–919.
28. **Rice, C. M.** 1996. *Flaviviridae*: the viruses and their replication, p. 931–960. *In* B. N. Fields, D. M. Knipe, and P. M. Howley (ed.), Fields virology, 3rd ed. Lippincott-Raven, Philadelphia, Pa.
29. **Rice, C. M., A. Grakoui, R. Galler, and T. J. Chambers.** 1989. Transcription of infectious yellow fever virus RNA from full-length cDNA templates produced by in vitro ligation. New Biol. **1:**285–296.
30. **Rice, C. M., R. Levis, J. H. Strauss, and H. V. Huang.** 1987. Production of infectious RNA transcripts from Sindbis virus cDNA clones: mapping of lethal mutations, rescue of a temperature-sensitive marker, and in vitro mutagenesis to generate defined mutants. J. Virol. **61:**3809–3819.
31. **Sambrook, J., E. F. Fritsch, and T. Maniatis.** 1989. Molecular cloning: a laboratory manual, 2nd ed. Cold Spring Harbor Laboratory, Cold Spring Harbor, N.Y.
32. **Satyanarayana, T., S. Gowda, V. P. Boyko, M. R. Albiach-Marti, M. Mawassi, J. Navas-Castillo, A. V. Karasev, V. Dolja, M. E. Hilf, D. J. Lewandowski, P. Moreno, M. Bar-Joseph, S. M. Garnsey, and W. O. Dawson.** 1999. An engineered closterovirus RNA replicon and analysis of heterologous terminal sequences for replication. Proc. Natl. Acad. Sci. USA **96:**7433–7438.
33. **Schlesinger, S.** 1993. Alphaviruses-vectors for the expression of heterologous genes. Trends Biotechnol. **11:**18–22.
34. **Schlesinger, S., and T. W. Dubensky.** 1999. Alphaviruses vectors for gene expression and vaccines. Curr. Opin. Biotechnol. **10:**434–439.
35. **Shi, P. Y., M. Tilgner, and M. K. Lo.** 2002. Construction and characterization of subgenomic replicons of New York strain of West Nile virus. Virology **296:**219–233.
36. **Shizuya, H., B. Birren, U. J. Kim, V. Mancino, T. Slepak, Y. Tachiiri, and M. Simon.** 1992. Cloning and stable maintenance of 300-kilobase-pair fragments of human DNA in *Escherichia coli* with an F-factor-based vector. Proc. Natl. Acad. Sci. USA **89:**8794–8797.
37. **Solomon, T.** 1997. Viral encephalitis in Southeast Asia. Neurol. Infect. Epidemiol. **2:**191–199.
38. **Sumiyoshi, H., C. H. Hoke, and D. W. Trent.** 1992. Infectious Japanese encephalitis virus RNA can be synthesized from in vitro-ligated cDNA templates. J. Virol. **66:**5425–5431.
39. **Sumiyoshi, H., G. H. Tignor, and R. E. Shope.** 1995. Characterization of a highly attenuated Japanese encephalitis virus generated from molecularly cloned cDNA. J. Infect. Dis. **171:**1144–1151.
40. **Tsai, T. F.** 2000. New initiatives for the control of Japanese encephalitis by vaccination: minutes of a W. H. O./CVI meeting, Bangkok, Thailand, 13–15 October 1998. Vaccine **18:**1–25.
41. **Umenai, T., O. Krzysko, T. A. Bektimirov, and F. Assaad.** 1985. Japanese encephalitis: current worldwide status. Bull. W. H. O. **63:**625–631.
42. **van der Werf, S., J. Bradley, E. Wimmer, F. W. Studier, and J. J. Dunn.** 1986. Synthesis of infectious poliovirus RNA by purified T7 RNA polymerase. Proc. Natl. Acad. Sci. USA **83:**2330–2334.
43. **van Dinten, L. C., J. A. den Boon, A. L. Wassenaar, W. J. Spaan, and E. J. Snijder.** 1997. An infectious arterivirus cDNA clone: identification of a replicase point mutation that abolishes discontinuous mRNA transcription. Proc. Natl. Acad. Sci. USA **94:**991–996.
44. **Varnavski, A. N., and A. A. Khromykh.** 1999. Noncytopathic flavivirus replicon RNA-based system for expression and delivery of heterologous genes. Virology **255:**366–375.
45. **Venugopal, K., and E. A. Gould.** 1994. Towards a new generation of flavivirus vaccines. Vaccine **12:**966–975.
46. **Wang, K., C. Boysen, H. Schizuya, M. I. Simon, and L. Hood.** 1997. Complete nucleotide sequence of two generations of a bacterial artificial chromosome cloning vector. BioTechniques **23:**992–994.
47. **Williams, D. T., L. F. Wang, P. W. Daniels, and J. S. Mackenzie.** 2000. Molecular characterization of the first Australian isolate of Japanese encephalitis virus, the FU strain. J. Gen. Virol. **81:**2471–2480.
48. **Yamshchikov, V. F., G. Wengler, A. A. Perelygin, M. A. Brinton, and R. W. Compans.** 2001. An infectious clone of the West Nile flavivirus. Virology **281:**294–304.
49. **You, S., and R. Padmanabhan.** 1999. A novel in vitro replication system for Dengue virus. Initiation of RNA synthesis at the 3′ end of exogeneous viral RNA templates requires 5′- and 3′-terminal complementary sequence motifs of the viral RNA. J. Biol. Chem. **274:**33714–33722.
50. **You, S., B. Falgout, L. Markoff, and R. Padmanabhan.** 2001. In vitro RNA synthesis from exogenous dengue viral RNA templates requires long range interactions between 5′- and 3′-terminal regions that influence RNA structure. J. Biol. Chem. **276:**15581–15591.
51. **Zhang, F., Q. Huang, W. Ma, S. Jiang, Y. Fan, and H. Zhang.** 2001. Amplification and cloning of the full-length genome of Japanese encephalitis virus by a novel long RT-PCR protocol in a cosmid vector. J. Virol. Methods **96:**171–182.

JOURNAL OF VIROLOGY, Dec. 1987, p. 3809–3819
0022-538X/87/123809-11$02.00/0

Vol. 61, No. 12

Production of Infectious RNA Transcripts from Sindbis Virus cDNA Clones: Mapping of Lethal Mutations, Rescue of a Temperature-Sensitive Marker, and In Vitro Mutagenesis To Generate Defined Mutants

CHARLES M. RICE,[1] ROBIN LEVIS,[1] JAMES H. STRAUSS,[2] AND HENRY V. HUANG[1]*

Department of Microbiology and Immunology, Washington University School of Medicine, St. Louis, Missouri 63110-1093,[1] and Division of Biology, California Institute of Technology, Pasadena, California 91125[2]

Received 3 June 1987/Accepted 25 August 1987

We constructed full-length cDNA clones of Sindbis virus that can be transcribed in vitro by SP6 RNA polymerase to produce infectious genome-length transcripts. Viruses produced from in vitro transcripts are identical to Sindbis virus and show strain-specific phenotypes reflecting the source of RNA used for cDNA synthesis. The cDNA clones were used to confirm the mapping of the causal mutation of *ts2* to the capsid protein. A general strategy for mapping Sindbis virus mutations is described and was used to identify two lethal mutations in an original full-length construct which did not produce infectious transcripts. An *Xba*I linker was inserted in the cDNA clone near the transcriptional start of the subgenomic mRNA; the resulting virus retains the *Xba*I recognition sequence, thus providing formal evidence that viruses are derived from in vitro transcripts of cDNA clones. The potential applications of the cDNA clones are discussed.

Sindbis virus is the type species of the *Alphavirus* genus. It is among the least pathogenic of the alphaviruses, a group that includes such important pathogens as Venezuelan, Western, and Eastern equine encephalitis viruses (25). In nature, Sindbis virus is transmitted by mosquitos, and its alternate vertebrate host is usually a bird or a mammal (80). In vitro, Sindbis virus infects a variety of avian, mammalian, reptilian (12), and amphibian cells (40). It also infects many species of mosquitos, a tick (80), and *Drosophila melanogaster* (6). Infection of vertebrate cells in culture is usually characterized by a dramatic cytopathic effect and rapid cell death, whereas growth in mosquito cells often leads to the establishment of chronic or persistent infections.

Since its isolation in 1952 (80), Sindbis virus and the closely related Semliki Forest virus have been widely studied (for a review, see reference 69). The genome of Sindbis virus consists of a single molecule of single-stranded RNA, 11,703 nucleotides (nt) in length (74, 76). The genomic RNA is infectious, is capped at the 5′ terminus and polyadenylated at the 3′ terminus, and serves as mRNA and is therefore by convention of plus polarity. During infection of vertebrate cells, the virus attaches to the cell surface and is endocytosed. Acidification of the endocytic vesicle activates the viral envelope proteins to mediate fusion of the viral envelope with the vesicle wall, thus depositing the genome in the cytoplasm (31). The 5′ two-thirds of the genomic 49S RNA is translated during early infection to produce two polyproteins that are processed by cotranslational or posttranslational cleavage into four nonstructural proteins (called nsP1 through nsP4, numbered in order as they appear in the genome sequence; 74) presumably required for RNA replication. A full-length minus strand complementary to the genomic RNA is first synthesized; this minus strand then serves as a template for the synthesis of new 49S genomic RNA molecules. The three structural proteins are encoded in the 3′ one-third of the genome. They are expressed by transcription of the minus strand at an internal site to produce a 26S subgenomic mRNA that is 4,106 nt long and colinear with the 3′-terminal one-third of the 49S genome. The subgenomic mRNA is capped and polyadenylated. It does not serve as a template for minus-strand synthesis, nor is it packaged into mature virions. Translation of the 26S mRNA produces a polyprotein that is cleaved cotranslationally by a combination of viral and presumably host-encoded proteases to give the capsid protein (C) and the two envelope glycoproteins (E1 and PE2, the precursors of the virion E2). The translation, proteolytic cleavage, glycosylation, fatty acid attachment, and transport of these proteins have been extensively studied both in vivo and in vitro as models for membrane protein biogenesis (for a review, see reference 68). The capsid protein complexes with the 49S genomic RNA to form intracellular icosahedral nucleocapsids, which interact with the cytoplasmic domains of the transmembrane envelope proteins at the cell surface, resulting in the budding of virus from the plasma membrane (23). The virus thus acquires a lipid envelope derived from the host cell. The proteins and RNA in mature virions are exclusively virus encoded.

Genetic analysis of Sindbis virus has been facilitated by the isolation of *ts* mutants defective in RNA replication (RNA^- mutants) and in the production of the structural proteins (RNA^+ mutants). These mutants have been grouped by complementation into three RNA^+ and four RNA^- groups (8–10, 65, 67, 73, 75). Representative mutant-revertant pairs from RNA^+ groups C, D, and E have been analyzed by sequence analysis, and there is excellent correlation between specific sequence changes and phenotypes (2, 27, 44). None of the RNA^- defects has been rigorously assigned to specific nonstructural proteins or RNA sequences.

* Corresponding author.

Exhibit C

Over the past several years, recombinant DNA technology has profoundly advanced the study of RNA viruses. Sequence analysis of cDNA clones of RNA viruses contributed to the identification of potential translation products and, by sequence comparison, of conserved, potentially *cis*-acting sequences implicated in replication and gene expression. However, rigorous tests of these conclusions require the manipulation and expression of functional viral genomes. This has led to the construction of cDNA copies of the bacteriophage Qβ (79) and poliovirus (55, 60, 70) which, after transfection of the appropriate host cells, produce infectious transcripts in vivo. Subsequently, a number of laboratories have succeeded in producing infectious transcripts synthesized in vitro from cDNA clones for several plant viruses (1, 13, 14, 18, 24, 50, 71, 77, 82) and animal viruses (16, 30, 52, 81). Using the same approach, we previously reported the deletion mapping of the *cis*-acting sequences required for the replication and encapsidation of defective-interfering genomes of Sindbis virus (43). We describe here the construction of cDNA clones of Sindbis virus capable of producing infectious transcripts in vitro. We also demonstrate the use of these clones for mapping the causal lesions for mutants with interesting phenotypes and for site-directed mutagenesis to construct novel mutants of Sindbis virus.

MATERIALS AND METHODS

Virus stocks, growth, and purification. Sindbis virus stocks derived from the cDNA clones described below, as well as the HR small plaque strain (HRsp, stock no. 80-5724; 74); temperature-sensitive (*ts*) mutants *ts*2, *ts*6, *ts*11, *ts*18, and *ts*24; and an HR large plaque strain (HR; S. Schlesinger laboratory strain; 8, 9) were grown on monolayers of primary or secondary chicken embryo fibroblasts (CEF) and titers were determined as previously described (73). The *ts* mutants were plaque purified for use in complementation analyses. The virus was purified by polyethylene glycol precipitation from the culture media, followed by successive velocity sedimentation and equilibrium density centrifugations (58). The isolation of intracellular (43, 57, 84) and virion RNA (4, 58, 62) was as described.

General recombinant DNA techniques. Restriction endonucleases and DNA modifying enzymes were purchased from commercial sources and used essentially as recommended by the manufacturer. Plasmids were grown, purified, and analyzed by standard methods with minor modifications (47).

cDNA synthesis, purification, and primer extension. cDNA synthesis and cloning of Sindbis virion RNA from purified virus have been described (62, 74). Double-stranded cDNA restriction fragments used to construct derivatives of Toto5 (see below) were purified by extraction from preparative low-melting-temperature agarose gels (83). For sequence analysis of RNA prepared from Toto1000- and Toto1002-infected CEF cells, a 5'-end-labeled oligonucleotide (complementary to nt 7644 through nt 7662 of the Sindbis virus genome; 74) was annealed to total cytoplasmic RNA and extended with avian myeloblastosis virus reverse transcriptase (15). Discrete extension products corresponding to the 5' end of 26S RNA were isolated from a preparative sequencing gel and sequenced by the chemical method (48).

Construction of full-length Sindbis cDNA clones. An original full-length cDNA clone of Sindbis virus HRsp, called Toto1 (Fig. 1), was reconstructed from the four *Hin*dIII subclones of the Sindbis virus genome used for determination of the sequence (74). The *Hin*dIII cDNA fragments were subcloned into Proteus1. Proteus1 consists of the replicon and the beta-lactamase gene of pBR322, from the *Tha*I (position 2522) to *Eco*RI (position 1) sites, with the *Tha*I end fused to the filled-in *Bgl*II end of a *Bgl*II-*Cla*I fragment from SP6 phage containing a SP6 RNA polymerase promoter (E. Butler and P. Little, unpublished data.) The same promoter was subsequently used to construct pSP64 (49). A polylinker sequence (5'-AAGCTTCTAGAGATCTGCAGGTCGAC GGATCCCCGGGAATTCCGCGGAATT-3') was positioned between the *Cla*I site from SP6 phage and the filled-in *Eco*RI site from pBR322.

The 5' terminus of Sindbis virus cDNA was fused to the *Sma*I site in the polylinker of Proteus1 (74). The GC tail at the 5' terminus regenerated the *Sma*I site. The site was converted to a *Cla*I site by cutting with *Sma*I and ligating in *Cla*I linkers (pCATCGATG), and it was used to fuse the Sindbis virus 5' terminus to the *Cla*I site downstream of the SP6 promoter. This 5' clone included the *Hin*dIII site at position 125 of Sindbis virus. The 3' terminus of Sindbis virus cDNA was cloned as a *Hin*dIII (position 6267) to the poly(A)-poly(T) fragment between the *Hin*dIII and *Sma*I sites of Proteus1 (74). The 5' and 3' clones were combined by ligating at the respective *Hin*dIII sites. (The *Sst*II site in the polylinker was converted to a *Sst*I site, by using *Sst*I linkers, for subsequent runoff transcription). The two internal *Hin*dIII fragments (nt 125 to 1302 and 1302 to 6267) were then inserted, in the correct order and orientation, in the *Hin*dIII site of the 5'-3' clone to produce Toto1. Toto1 has 198 nt between the SP6 transcription start and the 5' nucleotide of the Sindbis virus genome, including 9 G residues, derived during cDNA cloning, immediately 5' to the Sindbis virus sequences. The 3'-terminal poly(A) tract consists of ca. 35 residues followed by the sequence 5'-G GGAATTCGAGCTC-3', the last six nucleotides of which comprise the *Sst*I site used for runoff transcription.

Toto2 was derived from Toto1 by inserting a *Cla*I linker (pCATCGATG) into a *Hae*III site in SP6-derived sequences, cutting with *Cla*I, and ligating to the SP6-derived *Cla*I site downstream of the SP6 promoter (see above). This left 48 nt between the SP6 transcription start and the Sindbis virus 5' nucleotide. Toto3 was derived from Toto2 by deleting all SP6-derived sequences preceding the Sindbis virus sequences. We took advantage of an *Hph*I recognition sequence in the SP6 promoter that directs *Hph*I cutting after the A 1 nt 3' from the G that corresponds to the major transcriptional initiation site for SP6 RNA polymerase (unpublished observations; 29). We fused the *Hph*I cut site (T4 DNA polymerase treated to remove the 3' protruding A) to a *Sfa*NI site (filled in by treatment with the large fragment of DNA polymerase I) created by the *Hae*III-*Cla*I linker fusion in Toto2. Toto3 has eight extra G's preceding the Sindbis virus sequences. Toto5, derived from Toto3, had all but one extra G removed. The fragment from Toto3 containing the SP6 promoter and the 5'-terminal 125 nt of Sindbis virus (to a *Hin*dIII site at position 125) was first subcloned into πAN8 (W. C. Hollifield et al., unpublished data). This clone, called πK1, has an unique *Rsa*I site 14 nt downstream from the Sindbis virus 5' terminus and an unique *Hph*I recognition sequence in the SP6 promoter (see above). A pair of complementary synthetic oligonucleotides, corresponding to the Sindbis virus 5' terminus through nt 14, was ligated to *Rsa*I- and *Hph*I-digested and T4 DNA polymerase-treated πK1. The resulting clone, πK2, was verified by sequence analysis, and the SP6 promoter-Sindbis virus 5'-terminal sequences were recloned into Toto3 to give Toto5.

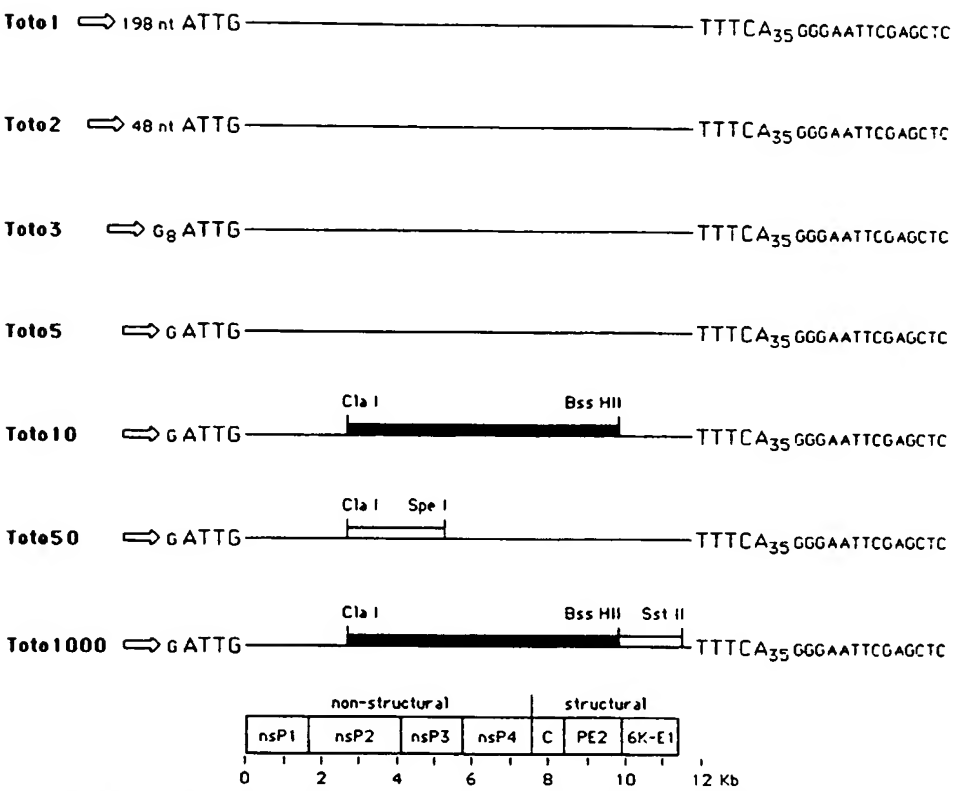

FIG. 1. Structure of full-length cDNA clones of Sindbis virus. The open arrow denotes the SP6 RNA polymerase promoter. Extraneous sequences preceding the Sindbis virus sequences are indicated. The first and last four nucleotides of Sindbis are shown. All clones have a 3' poly(A) tract ca. 35 nt long. The sequence between the poly(A) tract and the *Sst*I site used for runoff transcription is shown. All clones consisted of HRsp cDNA except the HR-derived sequences in Toto10 and Toto1000, indicated by filled-in bars extending from *Cla*I 2713 to *Bss*HII 9804. Toto1000 contains an additional substitution from *Bss*HII 9804 to *Sst*II 11484 of HRsp cDNA (open bar). The open bar in Toto50 indicates HRsp-derived sequences, from *Cla*I 2713 to *Spe*I 5262, from an independent HRsp cDNA clone. The coding regions of the viral proteins are outlined at the bottom of the figure (nucleotide positions are indicated in kilobases). The plasmid beta-lactamase gene and replicon are not shown.

A derivative of Toto5 was made by substituting the *Cla*I (nt 2713) to *Spe*I (nt 5262) region of Toto5 with that from an independent subclone (of the *Hin*dIII [nt 1302] to *Hin*dIII [nt 6267] region) of cDNA from Sindbis virus HRsp to produce Toto50. Similarly, the *Cla*I to *Spe*I fragment from Sindbis virus HR cDNA was used to replace the corresponding region of Toto5 to give Toto5CS. The same *Cla*I to *Spe*I fragment of Sindbis virus HRsp cDNA was used to replace the corresponding region of Toto3 to give Toto30. The *Cla*I (nt 2713) to *Avr*II (nt 4280) region of Toto5 was replaced with Sindbis virus HR cDNA from Toto1101 (see below) to give Toto5CA. Subclones of Toto5 were made for smaller substitutions between the *Cla*I and *Avr*II sites. Two fragments of Toto5, from *Hin*dIII (nt 1302) to *Bam*HI (nt 4633) and from *Bgl*II (nt 2288) to *Bam*HI (nt 4633), were cloned in πAN7 (46). Various regions of the two subclones were replaced with corresponding regions from the *Hin*dIII subclone of HRsp cDNA (see above). The *Cla*I (nt 2713) or *Bgl*II (nt 2288) to *Avr*II (nt 4280) fragment from the resulting clones was then used to replace the corresponding region of Toto5 to produce the clones Toto5CP, Toto5CN, Toto5BN, Toto5NT, Toto5PT, Toto5Bs, and Toto5TA (see Results and Table 2).

The *Cla*I (nt 2713) to *Bss*HII (nt 9804) interval of Toto5 was also replaced with the corresponding Sindbis virus HR cDNA, transformants were screened for clones that produced infectious transcripts, and one such clone was called Toto10. The *Bss*HII (nt 9804) to *Sst*II (nt 11484) interval of Toto10 was further replaced with Sindbis virus HRsp cDNA, and transformants were screened for clones that gave infectious transcripts, one of which was called Toto1000. Toto10 and Toto1000 are therefore hybrids of Sindbis virus HRsp and HR (Fig. 1).

A plasmid clone, called πnsP4C1, consisting of the *Acc*I (nt 7492) to *Nco*I (nt 8038) region of Toto1000 cloned in πAN7, was digested with *Rsa*I (nt 7611) and ligated in the presence of 43 mM *Xba*I linker (pTCTAGA). After transformation, clones that contain the *Xba*I linker were selected by digestion with *Xba*I, isolation of linear DNA, ligation, and retransformation. A representative clone, πC1R, with a single *Xba*I linker inserted at *Rsa*I (nt 7611) was then extended in the 5' direction by cloning in the *Hin*dIII (nt 6267) to *Acc*I (nt 7492) interval from Toto1000. The resulting clone, πnsP4CR, contains unique *Hpa*I (nt 6919) and *Aat*II (nt 7999) sites, which were used to excise the *Xba*I linker-containing fragment for replacement into Toto1000 to give Toto1002.

λToto1101, a lambda phage clone of a full-length copy of the Sindbis virus genome downstream from the SP6 promoter, was constructed from λgt*WES*-λB (41) by replacing the *Sst*I-*Xho*I region (λ positions 25881 to 33498) with the *Sst*I to *Xho*I fragment of Toto1101 containing the SP6

promoter and the Sindbis virus genome (Toto1101 is derived from Toto1000 by replacing the 3′ *Sst*I site used for runoff transcription with a *Xho*I site).

Toto *ts*2.1 was constructed by replacing the *Nar*I (nt 7870) to *Mst*II (nt 8892) region of Toto1000 with the corresponding region from a cDNA clone of *ts*2 designated *ts*2A (this clone was produced as described in reference 44 and contains the *ts*2 RNA sequence from the *Hin*dIII site at nt 6267 to the poly(A) tail, and it was generously provided by C. S. Hahn). The presence of the putative *ts*2 mutation (27) in the resulting clone was verified by chemical sequence analysis.

In vitro transcription and capping. RNA transcripts were synthesized in vitro by SP6 RNA polymerase with either supercoiled plasmid templates or plasmid DNAs digested with appropriate restriction endonucleases for production of runoff transcripts. Reactions containing 40 mM Tris chloride (pH 7.6); 6 mM $MgCl_2$; 2 mM spermidine; 1 mM each ATP, CTP, UTP, and GTP; 100 μg of nuclease-free bovine serum albumin per ml; 5 mM dithiothreitol; 500 U of human placental RNase inhibitor per ml; 400 U of SP6 RNA polymerase per ml; and 10 to 100 μg of template DNA per ml were incubated at 38°C for 1 h (11, 36, 49). 5′-capped transcripts were produced by inclusion of 1 mM $m^7G(5')ppp(5')G$ or $m^7G(5')ppp(5')A$ cap analogs in the transcription reaction (34). Trace quantities of ^{3}H-UTP or [α-^{32}P]CTP included in the transcription reactions allowed quantitation and gel analysis of the RNA transcripts. Incorporation was measured either by trichloracetic acid precipitation or by adsorption to DE 81 filter paper (Whatman, Inc., Clifton, N.J.) (47). Template DNAs did not need to be purified by banding on CsCl gradients, and several protocols for rapid plasmid and phage DNA preparation were satisfactory, provided that the template DNA was RNase-free and salt-free (11). Transcripts made from supercoiled plasmid DNA from minipreps were infectious. However, their specific infectivities were variable, typically about 10-fold lower than the transcripts produced by runoff transcription. RNA products which comigrated with full-length runoff transcripts were found when either uncut lambda or supercoiled plasmid templates were used, and such products may result from the falloff of the SP6 polymerase in the poly(A) tract or shortly thereafter. For rapid assay of transcript infectivity or for production of virus stocks, the transcription mix was used directly for transfection (see below). For purified transcripts, the template DNA was removed by digestion with DNase I, followed by extraction with phenol-chloroform and ethanol precipitation.

RNA transfection. Typically, confluent monolayers of secondary CEF in 35-mm tissue culture plates (about 10^6 cells) were used for transfection. After washing once with Eagle minimal essential medium with Earle salts (MEM) without serum, the cells were incubated with 1.5 ml of MEM containing 50 mM Tris chloride (pH 7.3) (at 25°C) and 200 μg of DEAE dextran per ml (average molecular weight, 500 kilodaltons [kDa]; Sigma Chemical Co., St. Louis, Mo.) for 15 to 60 min at 37°C. This medium was removed and 200 μl of RNA or transcription mix (diluted in phosphate-buffered saline) was added to the cells and incubated at room temperature for 15 to 60 min with occasional rocking. PFU were quantitated by overlaying the monolayers with 2 ml of 1.2% agarose (SeaKem; FMC Corp., Marine Colloids Div., Rockland, Maine) in MEM and 2% fetal calf serum followed by incubation at 37°C for wild-type stocks or at 30 and 40°C for *ts* mutants. Plaques were visualized by staining with neutral red or crystal violet after 24 to 48 h (37 or 40°C incubation) or 48 to 72 h (30°C incubation). For production of virus stocks, the transfection mix was removed and the cells were incubated with 2 ml of MEM containing 2% fetal calf serum for 24 (37°C) or 48 h (30°C).

RNA gel analysis. Monolayers of secondary CEF cells were infected with Sindbis virus stocks at a multiplicity of infection of 20 PFU per cell. Virus-specific RNA was labeled in the presence of MEM containing 1 μg of actinomycin D per ml and 20 μCi of [^{3}H]uridine per ml from 3 to 6 h postinfection. Cytoplasmic RNA was isolated, denatured with glyoxal and dimethylsulfoxide, and analyzed by electrophoresis in 1% agarose gels (47).

Analysis of 5′ and 3′ termini of transcripts and virion RNAs. For 5′-end analysis, in vitro transcripts were labeled by transcription in the presence of [α-^{32}P]ATP. Virion RNAs were labeled in vivo with $^{32}PO_4$. Cells were infected with Sindbis virus HRsp or virus derived from Toto50 and incubated with phosphate-free MEM and 3% chicken serum. At 5 h postinfection, 100 μCi of $^{32}PO_4$ per ml was added, and the infection was allowed to proceed for an additional 9 h. The virus was purified, and the virion RNA was extracted (see above). For 3′-end labeling, [5′-^{32}P]pCp was first synthesized with 3′ CMP and crude [γ-^{32}P]ATP (7,000 Ci/mmol, 200 μCi/μl; ICN Pharmaceuticals Inc., Irvine, Calif.). The reaction contained 3 μl of crude [γ-^{32}P]ATP, 4.5 nmol of 3′ CMP, and 5 U of T4 kinase in a final volume of 5 μl and was incubated for 6 h at 37°C, after which it was judged to be essentially complete by ascending chromatography on polyethyleneimine cellulose (developed in 2M sodium formate, pH 3.5). Approximately 0.5 pmol of either virion RNA or in vitro transcripts was 3′-end labeled with the crude [5′-^{32}P]pCp and T4 RNA ligase (21). The reactions contained 25 mM Tris chloride (pH 8.3), 7 mM $MgCl_2$, 20 mM dithiothreitol, 1 mM ATP, 15% dimethyl sulfoxide, 70 mCi of [5′-^{32}P]pCp per ml, 1,000 U of T4 RNA ligase (Bethesda Research Laboratories, Inc., Gaithersburg, Md.) per ml, and 200 μg of RNA per ml and were incubated at 4°C for 20 h. The end-labeled RNAs were recovered by ethanol precipitation after extraction with phenol and chloroform. The labeled RNAs were further purified by two selections with oligo(dT) cellulose (Pharmacia, Inc., Piscataway, N.J.) by following the directions of the supplier. RNA samples containing 10 μg of carrier tRNA were digested with 1 U of RNase T2 at 50°C for 1 h in 50 mM NH_4OAc (pH 5.3). The digestion products were spotted onto cellulose plates and separated by two-dimensional thin-layer chromatography (34).

Protein analysis. For comparison of structural and nonstructural proteins of parental virus strains and stocks derived from infectious transcripts, secondary CEF cells were infected at a multiplicity of infection of 20 to 50 PFU/cell. At 3 h postinfection, cells were labeled in methionine-free media containing 20 μCi of L-[^{35}S]methionine per ml (ICN translabel) for 1 h. Proteins in *ts*2-infected cells or in cells infected with virus derived from Toto*ts*2.1 were labeled from 7 to 8 h (30°C) or 6 to 7 h (40°C) postinfection. Cell extracts were prepared by washing the monolayers twice with ice-cold phosphate-buffered saline and by lysis of the monolayer with 0.5% sodium dodecyl sulfate containing 40 μg of phenylmethylsulfonyl fluoride per ml. Samples were electrophoresed on 10% discontinuous sodium dodecyl sulfate-polyacrylamide gels (37), treated for fluorography (39), and exposed to X-ray film. Sindbis virus-specific structural and nonstructural protein standards were prepared by immunoprecipitation (63) with monospecific polyclonal rabbit antisera to each of the proteins (63); antisera to nsP1, nsP2, nsP3, and nsP4 were generously provided by W. Reef Hardy, California Institute of Technology, Pasadena.

RESULTS

Infectious in vitro transcripts of Sindbis virus cDNA clones. We constructed full-length cDNA copies of the Sindbis virus RNA genome, positioned downstream from the SP6 RNA polymerase promoter, such that transcripts have either 198 nt (Toto1), 48 nt (Toto2), 8 G's (Toto3, Toto30), or a single G (Toto5, Toto10, Toto50, Toto1000) preceding the Sindbis virus-derived sequences (Fig. 1; Materials and Methods). The clones may be linearized at a *Sst*I site 3' of the poly(A) sequences of Sindbis virus for runoff transcription in vitro.

Although a substantial proportion of the in vitro transcripts derived from Toto1, Toto2, Toto3, and Toto5 template DNAs appeared to be full-length (e.g., Fig. 2) and contained poly(A) (data not shown), they were not infectious. Since Toto5 has only a single extra G at the 5' terminus, we suspected that our inability to produce infectious transcripts might be due to the presence of one or more lethal mutations in the Sindbis virus cDNA clone. Since Toto5 contains a number of unique restriction sites in the Sindbis virus sequences, we used these sites to replace defined intervals of the Sindbis insert of Toto5 with cDNA derived from an independent HRsp cDNA clone. One of the resulting clones is called Toto50 (Fig. 1). Similarly, Toto10 and Toto1000 contain large regions which have been replaced with cDNA derived from Sindbis virus strain HR. In vitro runoff transcripts of Toto10, Toto50, Toto1000 (Fig. 2), and λToto1101 (see Materials and Methods) produce infective centers when transfected into CEF, suggesting that Toto5 contains one or more lethal mutations in the replaced regions (see below). Table 1 shows that the infective centers must be derived from RNA transcripts of the cDNA clone, since the DNA template is required only for the transcription step and is dispensable after transcription, when infective center formation becomes sensitive to RNase A. Under these conditions, the DNA is not infectious. The cap analog, $m^7G(5')ppp(5')G$, was included during transcription so that the resulting transcripts would contain a 5' cap (34). The specific transfectivity of the capped transcripts is about 10-fold less than that of 49S RNA (1×10^5 to 4×10^5 PFU/μg) extracted from Sindbis virions, even when the fraction of apparently full-length transcripts was accounted for. The lower specific infectivity of the in vitro transcripts could be due to nonviral nucleotides at the termini of the transcripts (see below) or the presence of incomplete, premature falloff products from transcription, despite the observation that some of the transcripts appear full length on agarose gels.

TABLE 1. Infectiousness of in vitro transcripts of Toto1000

Conditions[a]	RNA (PFU/μg)[b]
Complete [$m^7G(5')ppp(5')G$]	4.0×10^4
$m^7G(5')ppp(5')A$	1.1×10^4
No cap analog	1.3×10^2
DNase I before transcription	0[c]
DNase I after transcription	1.0×10^4
RNase A after transcription	0[c]

[a] Complete SP6 transcription reaction [including $m^7G(5')ppp(5')G$; see Materials and Methods] except for the modifications listed. Dilutions of the transcription mixes were used directly for transfection.

[b] PFU produced per μg of transcribed RNA. Titrations were done in the range of 0.1 ng to 1 μg of RNA. Values of PFU/μg were extrapolated from titrations in the range of 1 to 10 ng of RNA.

[c] Less than 1 PFU in the entire transcription reaction (the usual yield was 1 to 1.2 μg of transcripts when the template was not pretreated with DNase I).

FIG. 2. In vitro transcripts. RNAs isolated from the transcription reactions described in Table 1 were denatured with glyoxal and DMSO and electrophoresed on a 1% agarose gel. Lanes: 1 to 3, transcription products made in the presence of $m^7G(5')ppp(5')A$, $m^7G(5')ppp(5')G$, and no cap, respectively; 4, RNase A digestion after transcription; 5, DNase I digestion after transcription; 6, DNase I digestion before transcription. The markers are indicated and correspond to Sindbis virion RNA (11.7 kb) and a 4.1-kb SP6 premature transcription product (present in minor amounts in lanes 1 to 3 and 5) which comigrates with Sindbis virus 26S RNA (unpublished observation).

Although the in vitro transcripts are expected to initiate with G, we find little difference in the specific transfectivity of transcripts made in the presence of the cap analogs $m^7G(5')ppp(5')G$ and $m^7G(5')ppp(5')A$. The transcripts made in the presence of $m^7G(5')ppp(5')G$ are indeed capped, as demonstrated by analysis of the 5' ends (34) and by the fact that the specific transfectivity of transcripts made in the absence of cap analogs is 100-fold lower. Direct evidence for incorporation of the $m^7G(5')ppp(5')A$ cap analog was not obtained since the Gp spot obscured the $m^7G(5')ppp(5')Ap$ spot in our two-dimensional separations. Additional nucleotides at the 5' end of the transcripts seem to be deleterious, since Toto30 transcripts, identical to Toto50 transcripts except for having 8 extra G-'s at the 5' terminus, were not infectious (<1 infectious center per μg of RNA).

Properties of virus derived from transcripts of the cDNA clones. Virus stocks derived from transfection with in vitro transcripts have efficiencies of plating at 30, 37, and 40°C that are indistinguishable from the parental Sindbis virus strains. Toto50, like its parental Sindbis virus HRsp strain, gave small plaques. Plaque sizes of Toto10 and Toto1000, which are hybrids of Sindbis virus HRsp and HR (Fig. 1), were intermediate between those of Sindbis virus HRsp and HR. Presumably, one or more determinant(s) affecting plaque size maps in the *Cla*I (nt 2713) to *Bss*HII (nt 9804) interval (which encompasses most of nsP2 through to near the end of E2).

RNA of virus derived from infectious transcripts. Both the intracellular, virus-specific RNA species from transfected cells and the virion RNAs of purified virus derived from in vitro transcripts are indistinguishable from that of Sindbis virus by gel electrophoresis after denaturation (results not shown). Transfection efficiencies of virion RNAs of Toto-derived stocks were comparable to 49S virion RNA of the parental Sindbis virus.

We analyzed virion RNAs labeled in vivo with ^{32}P, derived from either HRsp or Toto1000, by two-dimensional chromatography after complete digestion with RNase T2.

The patterns were indistinguishable. However, because of a high background of unidentified nucleosides, neither $m^7G(5')ppp(5')Ap$, $m^7G(5')ppp(5')Gp$, nor pppGp could be unambiguously identified (data not shown). Thus, if transcripts containing an extra G residue are infectious, it is unknown whether this residue is eliminated in subsequent amplification in vivo. The 3'-terminal nucleotides were analyzed in the same manner after enzymatic labeling of the transcripts or virion RNAs with [5'-^{32}P]pCp and RNA ligase, purification on oligo(dT) cellulose, and digestion with RNase T2. The HRsp and Toto1000-derived virion RNAs gave identical patterns, with only A being labeled, whereas the transcripts from Toto1000 contained heterogeneous 3' termini (data not shown). This heterogeneity is presumably due to alternative runoff of the SP6 polymerase at the 3' overhang generated by *Sst*I cleavage (49). It is not known whether the absence of heterogeneous 3'-terminal nucleotides in Toto1000 virion RNAs results from elimination of extra bases during replication or selective replication of transcripts without extra nucleotides [possibly produced by falloff of the SP6 polymerase in the poly(A) tract].

Proteins of virus derived from infectious transcripts. The intracellular virus-specific proteins in cells infected with HRsp, HR, Toto10, Toto50, and Toto1000 are compared in Fig. 3. The structural protein patterns are essentially identical, with PE2, E1, and C clearly resolved. These proteins have been shown to be immunoprecipitable with antisera which are monospecific for each of the virion structural proteins (data not shown). Of note is a strain variation affecting the migration of PE2. PE2 of HRsp migrates slightly faster than PE2 from HR, and as shown in Fig. 3, the PE2 of virus derived from Toto10 and Toto1000 comigrates with the HR PE2, whereas the PE2 of virus derived from Toto50 migrates faster and comigrates with the HRsp PE2, reflecting the source of the PE2 cDNA sequences.

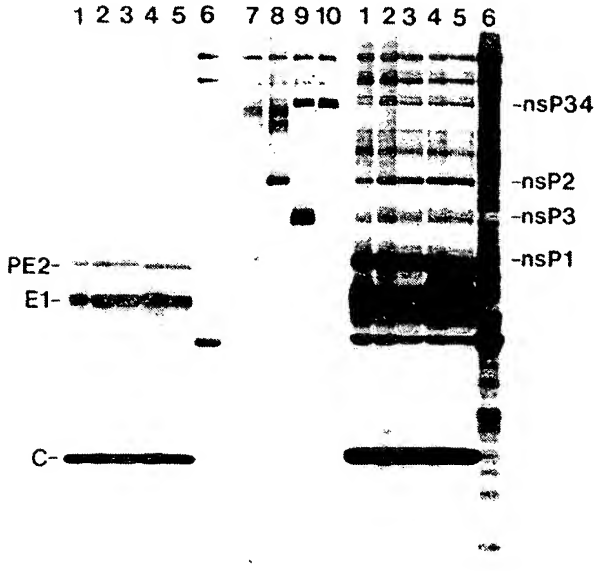

FIG. 3. Structural and nonstructural proteins from parental and in vitro-derived Sindbis strains. CEF monolayers infected with Sindbis virus strains HR, Toto10, Toto1000, HRsp, or Toto50 or mock infected (lanes 1 to 6, respectively) were pulse-labeled with L-[^{35}S]methionine from 3 to 4 h post-infection. Lysates were run on a 10% sodium dodecyl sulfate-polyacrylamide gel. Immunoprecipitates of a Sindbis virus-infected lysate with antisera specific for nsP1, nsP2, nsP3, and nsP4 were run in lanes 7 to 10, respectively. The positions of structural protein precursors and nonstructural proteins are indicated in the left and right margins, respectively. A longer exposure of lanes 1 to 6, to intensify the bands of the nonstructural proteins, is shown at the right of the figure.

The nonstructural proteins made by virus derived from Toto10, Toto50, and Toto1000 are indistinguishable from those of parental Sindbis virus strains. Although only nsP2, nsP3, and nsP4 can be identified in Fig. 3, the presence of nsP1 (which comigrates with PE2) and nsP4 (present in very small quantities and migrating slightly faster than nsP3), as well as that of nsP2, nsP3, and nsP34, has been verified by immunoprecipitation (G. Li, unpublished data) with monospecific antisera to nsP1, nsP2, nsP3, and nsP4 (W. R. Hardy and J. H. Strauss, manuscript in preparation).

Mapping of Toto5 defect. As mentioned above, the full-length Sindbis virus cDNA clone, Toto5, did not yield infectious RNA transcripts. We suspected that the Sindbis virus sequences in Toto5 contained a lethal mutation(s), perhaps generated during cDNA cloning. This theory was tested by the following strategy, which serves as an example of how an infectious clone can be used to map a specific phenotypic marker (in this case a lethal mutation). Individual segments of Toto5, flanked by unique restriction sites, were replaced with corresponding segments from independent cDNA clones of Sindbis virus HRsp or HR. Of a number of replacement clones tested, infectious in vitro transcripts were obtained when the *Cla*I (nt 2713)-*Spe*I (nt 5262) interval of Toto5 was replaced by that from HRsp cDNA or when the *Cla*I (nt 2713)-*Avr*II (nt 4280) interval was replaced by that from Toto1000 (Table 2). Infectious transcripts were not obtained with replacement of other regions (results not shown). Thus, Toto5 contains one or more lethal mutations in the *Cla*I (nt 2713)-*Avr*II (nt 4280) region. Since this interval does not contain additional unique restriction sites, subclones of it were made, such that some of the sites in the interval are now unique in the subclones. These sites were then used for substituting smaller fragments of HRsp cDNA into Toto5 sequences, after which the *Cla*I-*Avr*II fragment was recloned into Toto5, resulting in Toto5 derivatives containing small sequence replacements. Of a number of such derivatives tested, only the *Cla*I (nt 2713)-*Pvu*II (nt 3103) segment rescued Toto5 (clone Toto5CP; Table 2). Sequence analysis of this region showed that Toto5 has 2 base changes relative to Toto50 and Toto1000, at positions 2824 (a C to T change leading to substitution of nsP2 Ala-382 of Toto50 by Val in Toto5) and 2992 (a T to C change leading to substitution of nsP2 Leu-438 of Toto50 by Pro in Toto5). The sequence of Sindbis virus (74) at position 2992, derived from the same cDNA clone used to construct Toto5, is that of the mutant and must be amended to a U. The two base changes are on either sides of a *Nco*I site (nt 2976), which was used to construct Toto5CN and Toto5NT, which have single mutations at nucleotides 2824 and 2992, respectively. Neither clone gave infectious in vitro transcripts (Table 2). We conclude that Toto5 contains two lethal point mutations.

Marker rescue of the temperature-sensitive mutation of *ts*2. To demonstrate the utility of this approach for mapping *ts* mutations, we replaced the capsid sequences of Toto1000 with cDNA containing the *ts*2 mutation to produce a plasmid called Toto *ts*2.1 (see Materials and Methods). *ts*2 is in RNA^+ complementation group C. Sequence analysis of cDNA clones derived from *ts*2 as well as from a temperature-insensitive revertant suggested that the *ts*2 phenotype resulted from a C to U transition at position 701 of the 26S mRNA, such that serine is substituted for proline at residue

TABLE 2. Clones used to map mutations in Toto5[a]

Clone	Toto5 sequence replaced[b]	Rescue[c]
Toto50	*Cla*I 2713-*Spe*I 5262	+
Toto5CS	*Cla*I 2713-*Spe*I 5262	+
Toto5CA	*Cla*I 2713-*Avr*II 4280	+
Toto5CP	*Cla*I 2713-*Pvu*II 3103	+
Toto5CN	*Cla*I 2713-*Nco*I 2976	−
Toto5BN	*Bgl*II 2288-*Nco*I 2976	−
Toto5NT	*Nco*I 2976-*Tth*111I 3912	−
Toto5PT	*Pvu*II 3103-*Tth*111I 3912	−
Toto5Bs	*Bst*XI 3441-*Bst*XI 4175	−
Toto5TA	*Tth*111I 3912-*Avr*II 4280	−

[a] See Materials and Methods for construction of these clones.
[b] Donor sequences were from HRsp cDNA, except that HR cDNA was used for Toto5CS and Toto5CA.
[c] Transcripts of the clone were infectious (+) or noninfectious (−). Base changes in Toto5 relative to Toto50 or Toto1000 are at nt 2824 and nt 2992.

218 of the capsid protein (27). At the nonpermissive temperature (40°C), *ts*2 is defective in cotranslational cleavage of the capsid protein from the nascent structural polyprotein translated from 26S mRNA, resulting in the accumulation of a 130-kDa polyprotein. Monolayers were transfected with dilutions of RNA transcribed from Toto *ts*2.1 and incubated at either 30°C (the permissive temperature) or 40°C (the nonpermissive temperature). Plaques were observed at 30°C but not at 40°C. The virus stock derived from these infectious transcripts was clearly temperature sensitive, having an efficiency of plating at 40°C/30°C of $<2.7 \times 10^{-4}$. We examined the ability of this virus to complement representative *ts* mutants from several other complementation groups. The results in Table 3 show that the virus derived from Toto *ts*2.1 complements all four of the RNA$^-$ complementation groups but does not, as expected, complement *ts*2.

Figure 4 shows the Sindbis virus proteins extracted from cells infected with HRsp, *ts*2, or virus derived from Toto10, Toto1000, or Toto *ts*2.1 and pulse-labeled at the permissive and nonpermissive temperatures. The patterns of both *ts*2 and Toto *ts*2.1 are essentially similar to those of the parental viruses at 30°C, but at 40°C, both viruses produce a prominent species of about 130 kDa characteristic of *ts*2 and with greatly diminished quantities of the cleaved structural proteins. These polypeptides are virus specific, as demonstrated by their absence from patterns of mock-infected monolayers (Fig. 4) and by immunoprecipitation with antisera specific for the structural proteins (data not shown). It is of interest that while both Toto1000 and *ts*2, parents of Toto *ts*2.1, produce large plaques at 30°C, the virus derived from Toto *ts*2.1 has significantly smaller plaques. These different plaque phenotypes of the *ts*2 mutation placed on different genetic backgrounds raise the possibility that during selection or propagation of *ts*2, secondary mutations were selected on the basis of either larger plaque morphology or a selective growth advantage or both.

TABLE 3. Complementation analysis of virus derived from Toto *ts*2.1

Virus	Complementation index[a] with complementation group:					
	A (*ts*24)	B (*ts*11)	F (*ts*6)	G (*ts*18)	C	
					*ts*2	Toto *ts*2.1
*ts*2	3	306	219	27	1	1
Toto *ts*2.1	7	212	77	32	1	1

[a] Complementation index at 40°C (73) defined as yield of the mixed infection divided by the sum of the yields of the individual infections. Numbers are rounded to the nearest integer.

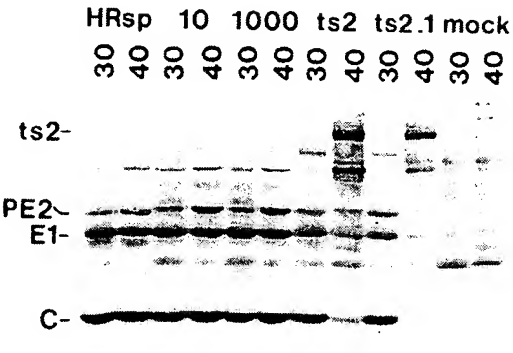

FIG. 4. Proteins made by *ts*2- and Toto*ts*2.1-derived virus. Virus-infected (10, Toto10; 1000, Toto1000; ts2, Sindbis virus *ts*2 mutant; ts2.1, Toto*ts*2.1) or mock-infected (mock) cells were incubated at either 30 or 40°C and pulse-labeled with L-[^{35}S]methionine at the same temperatures from either 7 to 8 h (30°C) or 6 to 7 h (40°C) postinfection. Lysates were run on a 10% sodium dodecyl sulfate-polyacrylamide gel. The positions of C, PE2, E1, and the protein characteristic of the *ts*2 mutant (ts2; ca. 130 kDa) are indicated in the left margin.

In vitro mutagenesis of Toto1000: formal evidence for infectious in vitro transcripts. We inserted a 6-base-pair TCTAGA *Xba*I linker in the *Rsa*I site 14 nt 3′ of the 26S mRNA transcription start (56, 62). Transcription of this clone, called Toto1002, produced infectious RNA. The virus derived from Toto1002 retains the *Xba*I recognition sequence (Fig. 5), providing formal proof that viruses recovered after transfection of cells are indeed derived from in vitro transcripts. Using the assays described above, we found that the virus is essentially wild type except for a slight underproduction of 26S mRNA relative to 49S RNA.

DISCUSSION

We constructed full-length Sindbis virus HRsp and HRsp-HR hybrid cDNA clones that can be transcribed in vitro to produce infectious transcripts. Cells transfected with the transcripts produce virions that are indistinguishable from Sindbis virus and that retain strain-specific phenotypes reflecting their genetic origin. As has been found for other viruses whose virion RNAs are normally capped (1, 16), capping of in vitro-synthesized Sindbis virus transcripts enhanced their infectivity. Most transcripts synthesized in the presence of m^{7}G(5′)ppp(5′)G are capped and include an extra G residue at the 5′ terminus. In addition, most of the transcripts contain extra 3′ terminal nucleotides. The specific infectivity (PFU/μg of RNA) of the transcripts is about 10% of that of virion RNA. The RNA recovered from Sindbis virions derived from the Toto clones appears to have at least the same 3′ termini as RNA from HR or HRsp virus. Thus, if molecules containing these extra nucleotides are infectious, the extra nucleotides are somehow selectively deleted during virus replication. The eight extra G residues

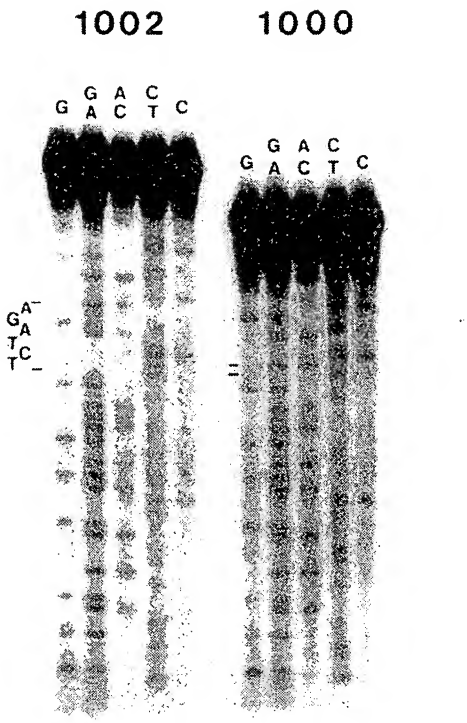

FIG. 5. Sequence of 26S mRNA 5′ untranslated region of Toto1000 and Toto1002. Discrete primer extension products of intracellular RNA from either Toto1000- (1000) or Toto1002- (1002) infected cells corresponding to the 5′ end of 26S RNA were isolated and sequenced (see Materials and Methods). Dashes in the Toto1000 ladder indicate the *Rsa*I site used for insertion of the *Xba*I linker in Toto1002. The linker sequence in the Toto1002 ladder is indicated, i.e., 3′-AGATCT-5′.

at the 5′ terminus of Toto30 led to inactive transcripts. Thus, Sindbis virus seems to be more sensitive to extraneous 5′-terminal sequences than are certain other RNA viruses. In the case of poliovirus cDNA clones transcribed with T7 RNA polymerase, the in vitro transcripts showed a 50-fold increase in specific infectivity (to 5% of that of virion RNA; 81) when 58 extra nucleotides at the 5′ terminus (leaving 2) and 619 extra nucleotides at the 3′ terminus (leaving 7) were removed. In vitro transcripts of cDNA clones from another picornavirus, human rhinovirus 14, are infectious even though they contain 21 additional 5′-terminal nucleotides (52). For black beetle virus, RNA 2 transcripts containing 20 extra 5′ nucleotides are infectious, but in this case, their removal does not increase specific infectivity (16). It is possible that engineering Sindbis virus in vitro transcripts with proper 5′ and 3′ termini may yield specific infectivities closer to those of virion RNA.

Mapping of mutant phenotypes. The cDNA clones of Sindbis virus can be used to define precisely the sequence changes responsible for the phenotype of any Sindbis virus variant by the strategy of exchanging segments of the wild-type clone with cDNA of the variant and determining the phenotype of the resulting clones (33, 38, 54, 59). Complex phenotypes due to multiple sequence changes (e.g., *ts*24; 65, 66) may be identified as such and dissected into single changes whose individual contributions can be determined. The mapping of the two lethal mutations of Toto5 illustrates this approach. The strategy is feasible whenever two strains of virus are closely related enough to share usable restriction sites for exchanging segments. Although Sindbis virus HRsp was derived from HR and subsequently propagated separately, and although HRsp and HR are known to differ at a number of nucleotide positions, we have not found any differences in the restriction maps of their cDNAs.

The infectious Sindbis virus cDNA clones may be used to map a number of interesting phenotypes of Sindbis virus. These phenotypes include mutants which affect virion morphogenesis (72), host range (35), virulence in neonatal mice (17, 53), enhanced neurovirulence in adult mice (26), cytopathogenicity (84), actinomycin D resistance (3), immunodominant epitopes on the envelope glycoproteins, and the ability to grow in low concentrations of methionine in mosquito cells (20). We have also begun to map temperature-sensitive mutations in each of the four RNA$^-$ complementation groups.

An important advantage of this approach is that any mutation that is mapped is also preserved as a DNA clone, with a correspondingly much lower mutation rate (32). The mutation is also placed upon a known genetic background. This placement makes possible the study of subtle effects of the mutation and of the interaction between a mutation and a particular genetic background and allows the facile construction of viruses with multiply defined mutations. The smaller plaque size of virus derived from Toto *ts*2.1 when compared with the *ts*2 or the Toto1000 parents provide initial evidence that the genetic background can be important.

Study of structure-function relationships via site-directed mutagenesis. The cDNA clones may be mutagenized by any of a number of methods to generate transcripts with novel mutations, i.e., lethal, viable or conditional, which can be studied both in vivo and in vitro (5, 7, 19, 28, 45, 51, 64). The characterization of these mutants, in conjunction with the traditionally derived mutants, will further our understanding of the molecular biology of Sindbis virus. In addition to Toto1002 described here, we have constructed a set of single- and multiple-codon insertion mutations of the nonstructural protein genes and are characterizing the replication of the corresponding mutant viruses. The structural proteins of Sindbis virus are better understood, and current experiments include the targeted mutagenesis of the capsid protein to define the amino acid residues responsible for its autoprotease activity (27; C. Hahn and J. H. Strauss, personal communication).

Thus far, essentially all of the revertants of Sindbis virus *ts* mutants derived by chemical mutagenesis (single-base substitutions) are true revertants resulting in restoration of the wild-type sequence. The insertion-deletion or multiple-base-change mutations that now can be introduced into the Sindbis virus genome should be less easily revertable, thus facilitating the selection of revertants with compensating mutations elsewhere in the genome. Mapping and characterization of such second-site revertants should be extremely valuable in elucidating functional interactions between the nonstructural proteins and of the interactions of the nonstructural proteins with *cis*-acting regulatory sequences. We have obtained revertants from a number of codon-insertion mutations in the nonstructural region and are screening them for true second-site revertants. Similar approaches may be taken to study viral maturation to help define the interactions of PE2 with E1, of E2 with E1, and of capsid protein with the cytoplasmic extensions of the envelope proteins or with 49S RNA.

Other applications. The cDNA clones described here consist of functional cDNA copies of the nonstructural and structural protein genes of Sindbis virus. These sequence modules may be inserted into existing gene expression vectors to express large quantities of the corresponding proteins for in vivo and in vitro studies, as well as to provide *trans* complementation for the amplification and study of lethal mutations. A vaccinia virus recombinant that expresses the Sindbis virus structural proteins has been described previously (61). The structural proteins have also been expressed in yeast cells (85).

Finally, given the rapid and high level of expression of its structural proteins, Sindbis virus can be used as a self-replicating gene expression vector. We have shown that Sindbis virus defective-interfering genomes can be used to express the bacterial chloramphenicol acetyltransferase (*cat*) gene (42). We show elsewhere that Sindbis virus, like bromegrass mosaic virus (22) and tobacco mosaic virus (78), can be used to express efficiently the *cat* gene (C. Xiong et al., manuscript in preparation).

ACKNOWLEDGMENTS

We thank Arash Grakoui and Edith Lenches for expert technical assistance; Steve A. Chervitz for participation in transcription experiments of supercoiled plasmid DNA; Chang S. Hahn and W. Reef Hardy for providing the *ts*2 cDNA clone and antisera to the nonstructural proteins, respectively; Vince Cannistraro and David Kennell for valuable advice on synthesis of [5′-^{32}P]pCp and 3′-end labeling of RNAs; and Milton Schlesinger and Sondra Schlesinger for helpful suggestions on the manuscript.

This work was supported by a Biomedical Research Support grant; Public Health Service grants AI24134, AI20612, and AI10793 from the National Institutes of Health; grant DMB86-17372 from the National Science Foundation; a grant from the Pew Memorial Trust; and the Monsanto/Washington University Biomedical Research Contract. C.M.R. is a Pew Scholar in the Biomedical Sciences.

LITERATURE CITED

1. **Ahlquist, P., R. French, M. Janda, and L. S. Loesch-Fries.** 1984. Multicomponent RNA plant virus infection derived from cloned viral cDNA. Proc. Natl. Acad. Sci. USA **81**:7066–7070.
2. **Arias, C., J. R. Bell, E. M. Lenches, E. G. Strauss, and J. H. Strauss.** 1983. Sequence analysis of two mutants of Sindbis virus defective in the intracellular transport of their glycoproteins. J. Mol. Biol. **168**:87–102.
3. **Baric, R. S., L. J. Carlin, and R. E. Johnston.** 1983. Requirement for host transcription in the replication of Sindbis virus. J. Virol. **45**:200–205.
4. **Bell, J. R., E. G. Strauss, and J. H. Strauss.** 1979. Purification and amino acid compositions of the structural proteins of Sindbis virus. Proc. Natl. Acad. Sci. USA **97**:287–294.
5. **Bernstein, H. D., P. Sarnow, and D. Baltimore.** 1986. Genetic complementation among poliovirus mutants derived from an infectious cDNA clone. J. Virol. **60**:1040–1049.
6. **Brun, G., and N. Plus.** 1980. The viruses of *Drosophila*. p. 625–702. *In* M. Ashburner and T. R. F. Wright (ed.), The genetics and biology of *Drosophila*, vol. 2. Academic Press, Inc., New York.
7. **Bujarski, J. J., P. Ahlquist, T. C. Hall, T. W. Dreher, and P. Kaesberg.** 1986. Modulation of replication, aminoacylation and adenylation *in vitro* and infectivity *in vivo* of BMV RNAs containing deletions within the multifunctional 3′ end. EMBO J. **5**:1769–1774.
8. **Burge, B. W., and E. R. Pfefferkorn.** 1966. Isolation and characterization of conditional-lethal mutants of Sindbis virus. Virology **30**:204–213.
9. **Burge, B. W., and E. R. Pfefferkorn.** 1966. Complementation between temperature-sensitive mutants of Sindbis virus. Virology **30**:214–223.
10. **Burge, B. W., and E. R. Pfefferkorn.** 1968. Functional defects of temperature-sensitive mutants of Sindbis virus. J. Mol. Biol. **35**:193–205.
11. **Butler, E. T., and M. J. Chamberlain.** 1982. Bacteriophage SP6-specific RNA polymerase: isolation and characterization of the enzyme. J. Biol. Chem. **257**:5772–5778.
12. **Clark, H. F., M. M. Cohen, and P. D. Lunger.** 1973. Comparative characterization of a C-type virus-producing cell line (VSW) and a virus-free cell line (VH2) from *Vipera russelli*. J. Natl. Cancer Inst. **51**:645–654.
13. **Collmer, C. W., and J. M. Kaper.** 1986. Infectious RNA transcripts from cloned cDNAs of cucumber mosaic viral satellites. Biochem. Biophys. Res. Commun. **135**:290–296.
14. **Cress, D. E., M. C. Kiefer, and R. A. Owens.** 1983. Construction of infectious potato spindle tuber viroid cDNA clones. Nucleic Acids Res. **11**:6821–6835.
15. **Dalgarno, L., D. W. Trent, J. H. Strauss, and C. M. Rice.** 1986. Partial nucleotide sequence of the Murray Valley encephalitis virus genome: comparison of the encoded polypeptides with yellow fever virus structural and nonstructural proteins. J. Mol. Biol. **187**:309–323.
16. **Dasmahapatra, B., R. Dasgupta, K. Saunders, B. Selling, T. Gallagher, and P. Kaesberg.** 1986. Infectious RNA derived by transcription from cloned cDNA copies of the genomic RNA of an insect virus. Proc. Natl. Acad. Sci. USA **83**:63–66.
17. **Davis, N. L., F. J. Fuller, W. G. Dougherty, R. A. Olmstead, and R. E. Johnston.** 1986. A single nucleotide change in the E2 glycoprotein gene of Sindbis virus affects penetration rate in cell culture and virulence in neonatal mice. Proc. Natl. Acad. Sci. USA **83**:6771–6775.
18. **Dawson, W. O., D. L. Beck, D. A. Knorr, and G. L. Grantham.** 1986. cDNA cloning of the complete genome of tobacco mosaic virus and production of infectious transcripts. Proc. Natl. Acad. Sci. USA **83**:1832–1836.
19. **Dreher, T. W., J. J. Bujarski, and T. C. Hall.** 1984. Mutant viral RNAs synthesized *in vitro* show altered aminoacylation and replicase template activities. Nature (London) **311**:171–175.
20. **Durbin, R. K., and V. Stollar.** 1985. Sindbis virus mutants able to replicate in methionine-deprived *Aedes albopictus* cells. Virology **144**:529–533.
21. **England, T. E., and O. C. Uhlenbeck.** 1978. 3′-terminal labelling of RNA with T4 RNA ligase. Nature (London) **275**:560–561.
22. **French, R., M. Janda, and P. Ahlquist.** 1986. Bacterial gene inserted in an engineered RNA virus: efficient expression in monocotyledonous plant cells. Science **231**:1294–1297.
23. **Fuller, S. D.** 1987. The T=4 envelope of Sindbis virus is organized by interaction with a complementary T=3 capsid. Cell **48**:923–934.
24. **Gerlach, W. L., J. M. Buzayan, I. R. Schneider, and G. Bruening.** 1986. Satellite tobacco ringspot virus RNA: biological activity of DNA clones and their *in vitro* transcripts. Virology **151**:172–185.
25. **Griffin, D. E.** 1986. Alphavirus pathogenesis and immunity, p. 209–249. *In* S. Schlesinger and M. J. Schlesinger (ed.), The Togaviridae and Flaviviridae. Plenum Publishing Corp., New York.
26. **Griffin, D. E., and R. T. Johnson.** 1977. Role of the immune response in recovery from Sindbis virus encephalitis in mice. J. Immunol. **118**:1070–2075.
27. **Hahn, C. S., E. G. Strauss, and J. H. Strauss.** 1985. Sequence analysis of three Sindbis virus mutants temperature-sensitive in the capsid protein autoprotease. Proc. Natl. Acad. Sci. USA **82**: 4648–4652.
28. **Ishikawa, M., T. Meshi, F. Motoyoshi, N. Takamatsu, and Y. Okada.** 1986. *In vitro* mutagenesis of the putative replicase genes of tobacco mosaic virus. Nucleic Acids Res. **14**: 8291–8305.
29. **Kang, C., and C.-W. Wu.** 1987. Studies on the SP6 promoter using a new plasmid vector that allows gene insertion at the transcription initiation site. Nucleic Acids Res. **15**:2279–2294.
30. **Kaplan, G., J. Lubinski, A. Dasgupta, and V. R. Racaniello.** 1985. *In vitro* synthesis of infectious poliovirus RNA. Proc. Natl. Acad. Sci. USA **82**:8424–8428.
31. **Kielian, M., and A. Helenius.** 1986. Entry of Alphaviruses. p.

91–119. *In* S. Schlesinger and M. J. Schlesinger (ed.), The Togaviridae and Flaviviridae. Plenum Publishing Corp., New York.
32. **Kohara, M., S. Abe, S. Kuge, B. L. Semler, T. Komatsu, M. Arita, H. Itoh, and A. Nomoto.** 1986. An infectious cDNA clone of the poliovirus Sabin strain could be used as a stable repository and inoculum for the oral polio live vaccine. Virology **151**:21–30.
33. **Kohara, M., T. Omata, A. Kameda, B. L. Semler, H. Itoh, E. Wimmer, and A. Nomoto.** 1985. In vitro phenotypic markers of a poliovirus recombinant constructed from infectious cDNA clones of the neurovirulent Mahoney strain and the attenuated Sabin 1 strain. J. Virol. **53**:786–792.
34. **Konarska, M. M., R. A. Padgett, and P. A. Sharp.** 1984. Recognition of cap structure in splicing *in vitro* of mRNA precursors. Cell **38**:731–736.
35. **Kowal, K. J., and V. Stollar.** 1981. Temperature-sensitive host-dependent mutants of Sindbis virus. Virology **114**:140–148.
36. **Krieg, P. A., and D. A. Melton.** 1984. Functional messenger RNAs are produced by SP6 *in vitro* transcription of cloned cDNAs. Nucleic Acids Res. **12**:7057–7070.
37. **Laemmli, U. K.** 1970. Cleavage of structural proteins during the assembly of the head of bacteriophage T4. Nature (London) **227**:680–685.
38. **La Monica, N., C. Meriam, and V. R. Racaniello.** 1986. Mapping of sequences required for mouse neurovirulence of poliovirus type 2 Lansing. J. Virol. **57**:515–525.
39. **Laskey, R. A., and A. D. Mills.** 1975. Quantitative film detection of ^{3}H and ^{14}C in polyacrylamide gels by fluorography. Eur. J. Biochem. **56**:335–341.
40. **Leake, C. J., M. G. R. Varma, and M. Pudney.** 1977. Cytopathic effect and plaque formation by arboviruses in a continuous cell line (XTC-2) from the toad *Xenopus laevis*. J. Gen. Virol. **35**:335–339.
41. **Leder, P., D. Tiemeier, and L. Enquist.** 1977. EK2 derivatives of bacteriophage lambda useful in the cloning of DNA from higher organisms: the λgtWES system. Science **196**:175–177.
42. **Levis, R., H. Huang, and S. Schlesinger.** 1987. Engineered defective interfering RNAs of Sindbis virus express bacterial chloramphenicol acetyltransferase in avian cells. Proc. Natl. Acad. Sci. USA **84**:4811–4815.
43. **Levis, R., B. G. Weiss, M. Tsiang, H. Huang, and S. Schlesinger.** 1986. Deletion mapping of Sindbis virus DI RNAs derived from cDNAs defines the sequences essential for replication and packaging. Cell **44**:137–145.
44. **Lindqvist, B. H., J. Di Salvo, C. M. Rice, J. H. Strauss, and E. G. Strauss.** 1986. Sindbis virus mutant *ts*20 of complementation group E contains a lesion in glycoprotein E2. Virology **151**: 10–20.
45. **Loesch-Fries, L. S., N. P. Jarvis, K. J. Krahn, S. E. Nelson, and T. C. Hall.** 1985. Expression of alfalfa mosaic virus RNA 4 cDNA transcripts *in vivo* and *in vitro*. Virology **146**:177–187.
46. **Lutz, C. T., W. C. Hollifield, B. Seed, J. M. Davie, and H. V. Huang.** 1987. Syrinx 2A: an improved lambda phage vector designed for screening DNA libraries by recombination *in vivo*. Proc. Natl. Acad. Sci. USA **84**:4379–4383.
47. **Maniatis, T., E. F. Fritsch, and J. Sambrook.** 1982. Molecular cloning: a laboratory manual. Cold Spring Harbor Laboratory, Cold Spring Harbor, N.Y.
48. **Maxam, A. M., and W. Gilbert.** 1980. Sequencing end-labeled DNA with base-specific chemical cleavages. Methods Enzymol. **65**:499–560.
49. **Melton, D. A., P. A. Krieg, M. R. Rebagliati, T. Maniatis, K. Zinn, and M. R. Green.** 1984. Efficient *in vitro* synthesis of biologically active RNA and RNA hybridization probes from plasmids containing a bacteriophage SP6 promoter. Nucleic Acids Res. **12**:7035–7056.
50. **Meshi, T., M. Ishikawa, F. Motoyoshi, K. Semba, and Y. Okada.** 1986. *In vitro* transcription of infectious RNAs from full-length cDNAs of tobacco mosaic virus. Proc. Natl. Acad. Sci. USA **83**:5043–5047.
51. **Miller, W. A., T. W. Dreher, and T. C. Hall.** 1985. Synthesis of brome mosaic virus subgenomic RNA *in vitro* by internal initiation on (−)-sense genomic RNA. Nature (London) **313**:68–70.
52. **Mizutani, S., and R. J. Colonno.** 1985. *In vitro* synthesis of an infectious RNA from cDNA clones of human rhinovirus type 14. J. Virol. **56**:628–632.
53. **Olmsted, R. A., R. S. Baric, B. A. Sawyer, and R. E. Johnston.** 1984. Sindbis virus mutants selected for rapid growth in cell culture display attenuated virulence in animals. Science **225**: 424–426.
54. **Omata, T., M. Kohara, S. Kuge, T. Komatsu, S. Abe, B. L. Semler, A. Kameda, H. Itoh, M. Arita, E. Wimmer, and A. Nomoto.** 1986. Genetic analysis of the attenuation phenotype of poliovirus type 1. J. Virol. **58**:348–358.
55. **Omata, T., M. Kohara, Y. Sakai, A. Kameda, N. Imura, and A. Nomoto.** 1984. Cloned infectious complementary DNA of the poliovirus Sabin 1 genome: biochemical and biological properties of the recovered virus. Gene **32**:1–10.
56. **Ou, J.-H., C. M. Rice, L. Dalgarno, E. G. Strauss, and J. H. Strauss.** 1982. Sequence studies of several alphavirus genomic RNA's in the region containing the start of subgenomic RNA. Proc. Natl. Acad. Sci. USA **79**:5235–5239.
57. **Ou, J.-H., E. G. Strauss, and J. H. Strauss.** 1981. Comparative studies of the 3′ terminal sequences of several alphavirus RNAs. Virology **109**:281–289.
58. **Pierce, J. S., E. G. Strauss, and J. H. Strauss.** 1974. Effect of ionic strength on the binding of Sindbis virus to chick cells. J. Virol. **13**:1030–1036.
59. **Pincus, S. E., and E. Wimmer.** 1986. Production of guanidine-resistant and -dependent poliovirus mutants from cloned cDNA: mutations in polypeptide 2C are directly responsible for altered guanidine sensitivity. J. Virol. **60**:793–796.
60. **Racaniello, V. R., and D. Baltimore.** 1981. Cloned poliovirus complementary DNA is infectious in mammalian cells. Science **214**:916–919.
61. **Rice, C. M., C. A. Franke, J. H. Strauss, and D. E. Hruby.** 1985. Expression of Sindbis virus structural proteins via recombinant vaccinia virus: synthesis, processing, and incorporation into mature Sindbis virions. J. Virol. **56**:227–239.
62. **Rice, C. M., and J. H. Strauss.** 1981. Synthesis, cleavage, and sequence analysis of DNA complementary to the 26S messenger RNA of Sindbis virus. J. Mol. Biol. **150**:315–340.
63. **Rice, C. M., and J. H. Strauss.** 1982. Association of Sindbis virion glycoproteins and their precursors. J. Mol. Biol. **154**: 325–348.
64. **Sarnow, P., H. D. Bernstein, and D. Baltimore.** 1986. A poliovirus temperature-sensitive RNA synthesis mutant located in a noncoding region of the genome. Proc. Natl. Acad. Sci. USA **83**:571–575.
65. **Sawicki, D. L., and S. G. Sawicki.** 1985. Functional analysis of the A complementation group mutants of Sindbis HR virus. Virology **144**:20–34.
66. **Sawicki, S. G., and D. L. Sawicki.** 1986. The effect of loss of regulation of minus-strand RNA synthesis on Sindbis virus replication. Virology **151**:339–349.
67. **Sawicki, S. G., D. L. Sawicki, L. Kääriäinen, and S. Keränen.** 1981. A Sindbis virus mutant temperature-sensitive in the regulation of minus-strand RNA synthesis. Virology **115**:161–172.
68. **Schlesinger, M. J., and S. Schlesinger.** 1986. Formation and assembly of Alphavirus glycoproteins, p. 121–148. *In* S. Schlesinger and M. J. Schlesinger (ed.), The Togaviridae and Flaviviridae. Plenum Publishing Corp., New York.
69. **Schlesinger, S., and M. J. Schlesinger (ed.).** 1986. The Togaviridae and Flaviviridae. Plenum Publishing Corp., New York.
70. **Semler, B. L., A. J. Dorner, and E. Wimmer.** 1984. Production of infectious poliovirus from cloned cDNA is dramatically increased by SV40 transcription and replication signals. Nucleic Acids Res. **12**:5123–5141.
71. **Simon, A. E., and S. H. Howell.** 1987. Synthesis *in vitro* of infectious copies of the virulent satellite of turnip crinkle virus. Virology **156**:146–152.
72. **Strauss, E. G., C. R. Birdwell, E. M. Lenches, S. E. Staples, and J. H. Strauss.** 1977. Mutants of Sindbis virus. II. Characterization of a maturation-defective mutant, *ts*103. Virology **82**: 122–149.

73. **Strauss, E. G., E. M. Lenches, and J. H. Strauss.** 1976. Mutants of Sindbis virus. I. Isolation and partial characterization of 89 new temperature-sensitive mutants. Virology **74**:154–168.
74. **Strauss, E. G., C. M. Rice, and J. H. Strauss.** 1984. Complete nucleotide sequence of the genomic RNA of Sindbis virus. Virology **133**:92–110.
75. **Strauss, E. G., and J. H. Strauss.** 1980. Mutants of alphaviruses: genetics and physiology, p. 393–426. *In* R. W. Schlesinger (ed.), The Togaviruses. Academic Press, Inc., New York.
76. **Strauss, E. G., and J. H. Strauss.** 1986. Structure and replication of the alphavirus genome, p. 35–90. *In* S. Schlesinger and M. J. Schlesinger (ed.), The Togaviridae and Flaviviridae. Plenum Publishing Corp., New York.
77. **Tabler, M., and H. L. Sänger.** 1985. Infectivity studies on different potato spindle viroid (PSTV) RNAs synthesized *in vitro* with the SP6 transcription system. EMBO J. **4**:2191–2199.
78. **Takamatsu, N., M. Ishikawa, T. Meshi, and Y. Okada.** 1987. Expression of bacterial chloramphenicol acetyltransferase gene in tobacco plants mediated by TMV-RNA. EMBO J. **6**:307–311.
79. **Taniguchi, T., M. Palmieri, and C. Weissmann.** 1978. Qβ DNA-containing hybrid plasmids giving rise to Qβ phage formation in the bacterial host. Nature (London) **274**:223–228.
80. **Taylor, R. M., H. S. Hurlbut, T. H. Work, J. R. Kingston, and T. E. Frothingham.** 1955. Sindbis virus: a newly recognized arthropod-transmitted virus. Am. J. Trop. Med. Hyg. **4**:844–862.
81. **van der Werf, S., J. Bradley, E. Wimmer, F. W. Studier, and J. J. Dunn.** 1986. Synthesis of infectious poliovirus RNA by purified T7 RNA polymerase. Proc. Natl. Acad. Sci. USA **83**:2330–2334.
82. **Visvader, J. E., A. C. Forster, and R. H. Symons.** 1985. Infectivity and *in vitro* mutagenesis of monomeric cDNA clones of citrus exocortis viroid indicates the site of processing of viroid precursors. Nucleic Acids Res. **13**:5843–5855.
83. **Weislander, L.** 1979. A simple method to recover intact high molecular weight RNA and DNA after electrophoretic separation in low gelling temperature agarose gels. Anal. Biochem. **98**:305–309.
84. **Weiss, B., R. Rosenthal, and S. Schlesinger.** 1980. Establishment and maintenance of persistent infection by Sindbis virus in BHK cells. J. Virol. **33**:463–474.
85. **Wen, D., and M. J. Schlesinger.** 1986. Regulated expression of Sindbis and vesicular stomatitis virus glycoproteins in *Saccharomyces cerevisiae*. Proc. Natl. Acad. Sci. USA **83**: 3639–3643.

Proc. Natl. Acad. Sci. USA
Vol. 88, pp. 5139–5143, June 1991
Medical Sciences

Infectious RNA transcribed from stably cloned full-length cDNA of dengue type 4 virus

(dengue virus/infectious transcripts/virus genetics)

CHING-JUH LAI, BANGTI ZHAO, HIROYUKI HORI, AND MICHAEL BRAY

Molecular Viral Biology Section, Laboratory of Infectious Diseases, National Institute of Allergy and Infectious Diseases, National Institutes of Health, Bethesda, MD 20892

Communicated by Robert M. Chanock, March 1, 1991

ABSTRACT **Dengue virus is an enveloped positive-strand RNA virus with a genome ≈11 kilobases in length. The four serotypes of dengue virus are currently the most important members of the flavivirus family in terms of geographical distribution and the incidence of infection in humans. In this communication we describe successful cloning of a stable full-length cDNA copy of dengue type 4 virus that can be used as the template for *in vitro* transcription of infectious RNA. Evidence is presented that dengue virus recovered from permissive cells transfected with the *in vitro* RNA transcripts retained a mutation that was engineered into full-length cDNA. The properties of the virus produced by cells transfected with infectious RNA transcripts of dengue cDNA resembled those of the virus from which the cDNA clone was derived. The dengue virus recombinant DNA system should prove helpful in gaining a better understanding of the molecular biology of dengue viruses and should facilitate the development of a safe and effective live vaccine for use in humans.**

The family *Flaviviridae* contains some 68 viruses most of which are arthropod-borne and cause disease of varying severity in humans or animals. The four dengue virus serotypes (types 1–4) of the flavivirus family form a distinct antigenic subgroup known as the dengue complex. In terms of geographic distribution and incidence of infection, dengue viruses rank highest among flaviviruses (1). Although typical dengue illness is moderately severe, mortality is usually low. However, a life-threatening form of dengue disease with hemorrhagic fever or shock syndrome can occur under certain circumstances in young children. Because an effective vaccine against dengue is still not available, the World Health Organization has designated the dengue viruses a priority area for accelerated vaccine development. Dengue viruses, like other flaviviruses, contain a positive-strand RNA genome and three virus-coded structural proteins: the capsid (C) protein, the membrane (M) protein, and the envelope (E) glycoprotein. Virion RNA is capped at the 5′ end but a poly(A) sequence is not present at the 3′ end (2, 3). Virion RNA is infectious when inoculated into experimental animals or into cells in culture (4–6). Sequence information obtained from molecular cloning of nearly all major strains of flaviviruses has contributed much to our current understanding of flavivirus gene organization, expression, and replication (7). Sequence analysis showed that the dengue type 4 virus genome contains 10,646 nucleotides (nt); the first 101 nt at the 5′ end and the last 384 nt at the 3′ end are noncoding and the remaining sequences code for a 3386-amino acid polyprotein in the order of C-preM-E-NS1-NS2A-NS2B-NS3-NS4A-NS4B-NS5 (where the NS proteins are nonstructural proteins) (8, 9). Several strategies of proteolytic cleavage are employed to process the polyprotein into individual proteins. For example, cleavage between C and preM, preM and E, or E and NS1 is mediated by a host-cell signal peptidase ("signalase") (10, 11). Cleavage between NS1 and NS2A is effected by NS2A and requires an 8-amino acid sequence at the carboxyl terminus of NS1 (12, 13). It appears that NS3 is a viral protease; however, it was recently observed that both NS2B and NS3 are required for the proteolytic processing of most of the remaining nonstructural proteins (14–16).

Genetic analysis of positive-strand RNA viruses has been greatly facilitated by the use of recombinant DNA techniques. It was shown that cloned full-length cDNA of poliovirus is infectious for susceptible cells in culture (17). Subsequent studies showed that RNA transcripts produced *in vitro* from a poliovirus cDNA template were more infectious than the cDNA itself (18). RNA transcripts produced by *in vitro* transcription of cloned full-length cDNA derived from several other positive-strand RNA viruses (19–21) and, more recently, from yellow fever virus (22) have also been demonstrated to be infectious. One of the objectives of our dengue research has been to construct cloned full-length dengue virus cDNA that could serve as a template for infectious RNA transcripts. This would allow us to introduce specific mutations into the dengue virus genome at the cDNA level and isolate dengue virus mutants for biological studies and potential use in a live virus vaccine for humans. In this study we describe the construction and cloning of a stable full-length dengue cDNA copy in a strain of *Escherichia coli* using the pBR322 plasmid vector. RNA molecules produced by *in vitro* transcription of the full-length cloned DNA template were infectious, and progeny virus recovered from transfected cells was indistinguishable from the parental virus from which the cDNA clone was derived.

MATERIALS AND METHODS

Cloning Subfragment and Full-Length cDNA of Dengue Virus. DNA segments spanning nearly the entire genome were initially cloned from a cDNA library of dengue type 4 virus strain 814669 (virus kindly supplied by W. Brandt, Walter Reed Army Institute of Research, Washington) (23). These cDNA clones, used to establish the dengue type 4 sequence, were joined to form full-length clone 1A by shared restriction enzyme sites: namely, pF19 *Hin*dIII^{44}–*Sst* I^{1931}, pE19 *Sst* I^{1931}–*Sst* I^{3033}, pD20 *Sst* I^{3033}–*Hae* II^{4189}, pC20 *Hae* II^{4189}–*Hae* II^{5881}, pA9 *Hae* II^{5881}–*Xba* I^{7725}, pA28 *Xba* I^{7725}–*Hin*dIII^{9829}, and pB81 *Hin*dIII^{9829}–*Hae* II^{10608}. The 5′ and 3′ subfragments used for replacement in the full-length clone were constructed from other independently isolated cDNA clones: clone 2 of the 5′ half-fragment was joined by pF34 *Hin*dIII^{44}–*Sst* I^{1931}, pS15 *Sst* I^{1931}–*Sst* I^{3033}, pD16 *Sst* I^{3033}–*Spe* I^{3338}, and pD17 *Spe* I^{3338}–*Eco*RI^{5125}; clone B of the 3′ half-fragment was joined by pD13 *Bst*BI^{5069}–*Nco* I^{6332}, pX6

The publication costs of this article were defrayed in part by page charge payment. This article must therefore be hereby marked "*advertisement*" in accordance with 18 U.S.C. §1734 solely to indicate this fact.

Abbreviation: nt, nucleotide(s).

Exhibit D

Nco I^{6332}–*Xba* I^{7725}, and pK2 *Xba* I^{7725}–*Hae* II^{10608}; and clone C of the 3′ subfragment by pD13 *Bst*BI^{5069}–Nco I^{6332}, pX10 *Nco* I^{6332}–*Xba* I^{7725}, and pK1 *Xba* I^{7725}–*Hae* II^{10608}.

The SP6 promoter sequence was positioned upstream of the 5′ end of the dengue sequence as follows: the 287-base-pair (bp) *Sau*3A1 fragment of pGEM-3 (nt 2618–37) (Promega) containing the SP6 promoter sequence (nt 2809–2867) was inserted at the *Bgl* II site created from the *Pst* I site of pBR322. A dengue cDNA fragment (nt 1–88) flanked by the *Pst* I cleavage sequence at its 5′ end and the *Bgl* II cleavage sequence at its 3′ end was inserted between the *Pst* I and *Bgl* II sites downstream of the promoter sequence. Additional sequence between the SP6 transcription-initiating G residue and the first nucleotide of the dengue sequence was removed by oligonucleotide-directed mutagenesis in an M13 cloning vector. Also, in the pBR322 plasmid, the cleavage sequence GGTACC for *Asp*718 was engineered immediately following the dengue 3′ end sequence. *E. coli* strain HB101 was used for cloning dengue sequences from the cDNA library and for cloning intermediate-length cDNA. Strains HB101 and DH5α were employed in the initial attempt to clone full-length cDNA. Successful cloning of full-length dengue cDNA was accomplished with *E. coli* strain BD1528 (*thy A, met*$^-$, *nadBF, ung*$^-$, *gal*$^-$, *supE, supF, nsdR*$^-$, *hsdM*$^+$; originally from B. Duncan, obtained through D. Nathans, Johns Hopkins University, Baltimore).

***In Vitro* Transcription.** Plasmid containing full-length dengue cDNA was linearized by cleavage with *Asp*718 (Boehringer Mannheim) followed by phenol extraction and ethanol precipitation. The linearized DNA template (2 μg) was added to a transcription reaction mixture (50 μl) containing 40 mM Tris (pH 7.5), 6 mM $MgCl_2$, 10 mM NaCl, 10 mM dithiothreitol, 50 units of RNasin, and 0.5 mM each NTP (Promega). To incorporate a cap structure at the 5′ end of RNA transcripts, m^7G(5′)ppp(5′)G (0.5 mM) was also added to the reaction mixture, which was incubated at 37°C for 1 hr (24). The RNA product was analyzed by agarose gel electrophoresis in Tris/borate buffer containing 0.1% SDS. RNA transcripts were visualized and quantitated by ethidium bromide staining. The transcription product was also treated with DNase or RNase to confirm that the infectious moiety of the transcription product was RNA.

RNA Transfection. Simian $LLCMK_2$ cells were grown in medium 199 supplemented with 10% fetal bovine serum. For transfection, subconfluent $LLCMK_2$ cells in a 24-well plate were rinsed once with serum-free medium 199 and then covered with 0.3 ml of serum-free medium per well. The transfection mixture containing DNase-treated *in vitro* RNA transcripts (0.1–1 μg) or virion RNA (0.01–0.1 μg) in 17 μl of 0.02 mM Hepes buffer (pH 7.05) and 6 μl of Lipofectin (Bethesda Research Laboratories) was mixed thoroughly and added to the medium. After incubation at 37°C for 12–18 hr, medium 199 plus 10% fetal bovine serum was added. Eight days after transfection, cells were trypsinized and transferred to a 6-well plate or to a chamber slide for an additional 2 days of incubation in the growth medium. Cells in the chamber slide were tested by immunofluorescence to detect the presence of dengue antigens. Infected cells in the culture plate were collected together with the fluid medium, lysed by freezing and thawing, and used as the source of recovered dengue virus.

Dengue Virus Characterization. Parental and recovered dengue viruses were characterized for plaque phenotype on $LLCMK_2$ cells (25). To analyze dengue virus proteins, confluent $LLCMK_2$ cells in a 6-well plate were infected with parental or recovered virus at 0.2 plaque-forming unit per cell in medium 199 containing 2% fetal bovine serum. Six days after infection cells were metabolically labeled with [^{35}S]methionine (50 μCi per well; specific activity, 600 Ci/mmol; 1 Ci = 37 GBq) in methionine-free medium for 2 hr and the lysate was prepared in RIPA buffer for radioimmunoprecipitation using dengue virus hyperimmune mouse ascitic fluid (12). The immunoprecipitate was analyzed by SDS/12% PAGE (9).

RESULTS

Initial Attempt to Clone Full-Length Dengue DNA in Plasmid pBR322 Containing the SP6 Promoter. A series of dengue cDNA inserts had been cloned at the *Pst* I site of pBR322 that spanned the entire length of the dengue type 4 virus genome (8, 9). These cDNA inserts were joined at shared restriction enzyme sites to form a full-length dengue DNA copy (1A) by using the same *Pst* I cloning site of pBR322. For *in vitro* transcription, the SP6 polymerase promoter sequence was placed at the 5′ end preceding the dengue sequence. The DNA structure for the predicted 5′ sequence of RNA transcripts is shown in Fig. 1. The A residue of the first dengue nucleotide was positioned immediately following the normal SP6 polymerase transcription-initiating G residue. The m^7G cap structure that is present at the 5′ end of the virion RNA was provided by incorporation of m^7G(5′) pppG(5′) as a cap analog in the transcription reaction. Thus, the DNA template would yield an m^7G-capped dengue RNA transcript containing an additional G residue at the 5′ terminus. To produce run-off transcripts, the template was linearized at the unique *Asp*718 cleavage site immediately following the 3′ end of the dengue sequence. As shown in Fig. 1, five additional nucleotides are present in the template strand preceding the *Asp*718 cleavage site. If transcription proceeded to the last nucleotide, the RNA transcripts would contain these five additional residues at the 3′ terminus.

In the earlier experiments in which *E. coli* HB101 was employed as the host for transformation, we observed that full-length dengue cDNA was often unstable in the plasmid. Thus, dengue cDNA underwent rearrangement and many colonies had to be screened to isolate a clone of DNA with the predicted restriction enzyme digestion pattern. In an attempt to solve this problem, we examined stability of clone 1A plasmid produced in other strains of *E. coli*. The highly transformation-competent strain DH5α and strain BD1528 used in bisulfite-induced mutagenesis were compared with

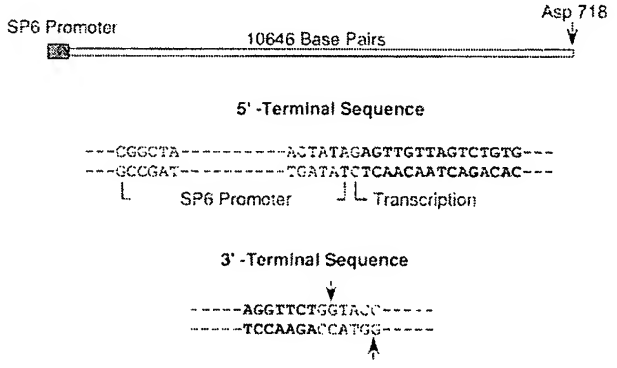

FIG. 1. Terminal sequences of cloned full-length dengue virus cDNA used for transcription of infectious RNA. The full-length dengue virus cDNA (10,646 nt long) was cloned with the adjacent SP6 promoter sequence (filled box) at the 5′ end and the unique *Asp*718 cleavage sequence (arrow) at the *Pst* 1 site of pBR322 plasmid. Note that there is one additional C residue at the position between 10,448 and 10,449 and one additional G residue between 10,470 and 10,471, both of which were missing in the published dengue type 4 sequence (8). The template sequences for the predicted 5′ terminus and 3′ terminus of the RNA transcript are also shown. The SP6 polymerase transcription-initiating G is retained and is located preceding the 5′ dengue sequence shown in bold letters. The *Asp*718 cleavage sequence GGTACC is positioned immediately following the 3′ dengue sequence also shown in bold letters.

strain HB101. We found that strain DB1528 produced transformants exhibiting a colony size 3–4 times larger than HB101 transformants. More important was the observation that transformants of DB1528 generally yielded a plasmid with the predicted restriction enzyme pattern, suggesting that *E. coli* DB1528 was the strain of choice to produce stable clones of full-length dengue DNA. However, *in vitro* RNA transcripts made from such a full-length dengue DNA clone (1A) were not infectious when tested by transfection of permissive cells in culture, whereas dengue virion RNA used as the positive control at a 100-fold lower concentration yielded infectious dengue virus as detected by indirect immunofluorescence assay.

Replacement of Dengue DNA Segments in the Full-Length Construct with Independently Derived DNA Clones. We reasoned that the failure to produce an infectious RNA transcript from the cloned dengue virus cDNA template might be due to the presence of one or more deleterious mutations in the full-length cDNA clone 1A. Such mutations could presumably arise from cloning of a defective genomic RNA in the virus stock or from a copying error during cloning and/or propagation of the plasmid. In an attempt to correct the defect in cDNA clone 1A, we replaced dengue DNA segments that might contain such deleterious mutations with the corresponding segments from independently cloned dengue cDNA. We adopted the strategy of cloning the 5′ and 3′ halves of the dengue cDNA sequence separately. The unique *Bst*BI site at nt 5069 was used to divide the full-length dengue sequence into two fragments, each representing ≈50% of the genome. A unique *Asp*718 site was introduced at the *Pst* I site of pBR322 downstream of the *Bst*BI site of the dengue sequence. For convenience, the 5′ fragment of the first full-length clone containing the SP6 promoter was designated 5′-1 and the remaining 3′ sequence between the *Bst*BI and *Asp*718 sites was designated 3′-A. A plasmid containing the second 5′ fragment, 5′-2, was constructed from a second set of dengue cDNA inserts. This plasmid was also suitable for use as a cloning vector for insertion of a 3′ fragment to yield a full-length DNA construct. Two additional 3′ fragments flanked by *Bst*BI and *Asp*718 sites, 3′-B and 3′-C, were also constructed from an independent series of dengue cDNA inserts (Fig. 2). Replacement of the 3′ fragment in the first full-length clone 1A with 3′-B or 3′-C fragments yielded two other full-length clones, 1B and 1C. Similarly, substitution of the 5′-2 fragment into three other full-length DNA constructs yielded full-length DNA clones 2A, 2B, and 2C. In this manner, six full-length cDNA combinations were available for analysis.

Initial Evidence for Infectivity of RNA Transcripts Produced *in Vitro*. RNA transcripts produced from the six cloned full-length dengue DNA templates were tested for infectivity

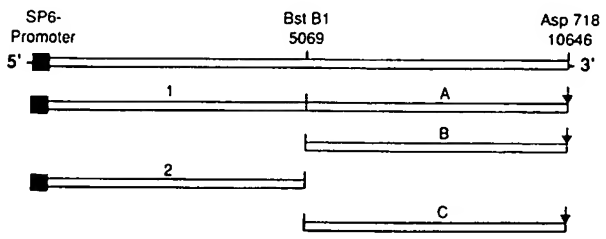

FIG. 2. Full-length dengue cDNA clones. The diagram depicts the full-length dengue cDNA clone containing the SP6 promoter sequence at the 5′ end and an *Asp*718 cleavage site at the 3′ end as shown in Fig. 1. The *Bst*BI cleavage site at nt 5069 separates the dengue genome into the 5′ and 3′ half-fragments. Replacement of these fragments in full-length clone 1A with the corresponding 5′-2, 3′-B, or 3′-C fragments that were constructed from an independent set of cDNA clones gives rise to five other full-length combinations as shown.

by transfection of simian LLCMK$_2$ cells. Dengue virus-infected cells were readily observed by an indirect immunofluorescence assay 10 days following transfection with 2A RNA. In contrast, RNA transcripts from the five other full-length DNA clones were negative by this assay, indicating that these cDNA clones contained one or more lethal mutations that were not detected by restriction enzyme analysis. Confirmation of the infectivity of the RNA transcripts of clone 2A was provided by recovery of dengue virus from the medium or the cell lysate of 2A RNA-transfected cells. The titer of dengue virus present in the transfected cell lysate was 10^5 plaque-forming units/ml. Treatment of 2A RNA transcripts with DNase I did not affect infectivity, whereas RNase treatment completely abolished infectivity (data not shown). In these experiments the infectivity of RNA transcripts was not analyzed by plaque assay. Instead, the production of infectious virus in cell culture was sought after an extended incubation that permitted virus amplification. When assayed in this manner by indirect immunofluorescence the minimum concentration required for infectivity was 1 ng for virion RNA and 10 ng for 2A RNA transcripts. Thus, specific infectivity was estimated to be 100 infectious units/μg of 2A RNA or 1000 infectious units/μg of virion RNA. These values were 10–100 times less than those observed for yellow fever virus (22), suggesting that dengue RNA transfection is relatively less efficient or that one or more attenuating but nonlethal mutations are present in clone 2A. In any event, these analyses indicated that the RNA transcripts made from clone 2A were infectious following transfection of permissive cells in culture.

Additional Evidence for Infectivity of RNA Transcripts. To provide additional evidence that infectious dengue virus was produced by cells transfected with clone 2A RNA transcripts, we introduced two silent mutations into full-length dengue clone 2A DNA (G3473 → T and C3476 → A) that created a new *Pst* I site at nt 3476. These mutations created a reporter sequence but did not alter the amino acid sequence. RNA transcripts were then prepared from reengineered 2A(P) DNA, containing the new *Pst* I cleavage site, and complete removal of the DNA template was effected by exhaustive digestion with DNase I. These transcripts were then used for transfection of cells. The transfected cells produced infectious dengue virus designated 2A(P). Genomic RNA extracted from progeny virus derived from 2A or 2A(P) was reverse-transcribed using appropriate primers and the cDNA product was employed as a template for a polymerase chain reaction (PCR) to generate a DNA fragment between nt 3193 and 4536. A DNA band was observed at a gel position predicted for the 1343-bp fragment produced by PCR (Fig. 3). *Pst* I digestion of the PCR DNA product from 2A(P) virus yielded two fragments that were 280 and 1063 bp long as predicted by the presence of the *Pst* I cleavage sequence. The control PCR DNA product of virus recovered from 2A RNA was insensitive to *Pst* I digestion. This observation indicated that progeny virus 2A(P) was derived from the RNA transcripts of mutant 2A(P) DNA containing the engineered *Pst* I site.

Dengue Virus Recovered from Infectious RNA Transcribed *in Vitro*. The progeny dengue virus recovered from the lysate of cells transfected with RNA transcripts produced from clone 2A or clone 2A(P) was compared with parental wild-type virus for ability to produce plaques on LLCMK$_2$ cell monolayers. Six days after infection, both progeny virus and parental virus produced characteristic dengue plaques. Although the parental virus previously subjected to passage in mosquito cells produced both small and large plaques, both progeny viruses recovered from LLCMK$_2$ cells yielded mostly large plaques. It is not known whether the mixed plaque morphology of the wild-type virus on LLCMK2 cells was the result of passage in mosquito cells, leading to

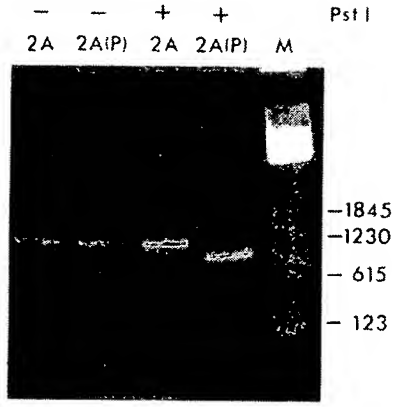

FIG. 3. Dengue virus recovered from infectious RNA contains the genomic sequence of the DNA template. Progeny dengue virus was recovered from $LLCMK_2$ cells transfected with DNase-treated RNA transcribed from clone 2A DNA (wild-type control) or from clone 2A (P) DNA containing an engineered *Pst* I site at nt 3476 of the dengue sequence. The recovered dengue virus was then grown in C6/36 mosquito cells. Medium from infected C6/36 cells was collected and virion RNA was extracted from the pelleted virus. Virion RNA was used for reverse transcription and the cDNA product was used as template to produce the 1343-bp dengue virus cDNA fragment (nt 3193–4536) by PCR using the appropriate primers. *Pst* I digestion of the PCR product is shown. Lane M shows the 123-bp DNA ladder as size markers.

emergence of plaque morphology mutants. The more uniform plaque morphology of the viruses recovered from cells transfected with full-length RNA transcripts probably reflects the clonal origin of the clone 2A- or 2A(P)-derived virus. Dengue-specific proteins produced by progeny virus-infected cells and by parental virus-infected cells were also compared. Fig. 4 shows the profile of protein bands including dengue virus preM, E, NS1, NS3, and other, unassigned, dengue-specific

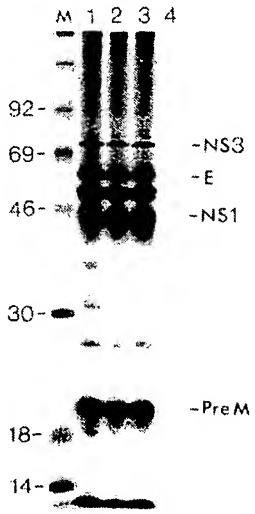

FIG. 4. Comparison of dengue virus proteins from $LLCMK_2$ cells infected with recovered virus or parental virus. [^{35}S]Methionine-labeled cell lysates were prepared for immunoprecipitation with dengue virus hyperimmune mouse ascitic fluid. The immunoprecipitates were separated by electrophoresis in SDS/12% polyacrylamide gel (acrylamide/*N,N'*-methylenebisacrylamide weight ratio, 60:1.6). Lanes: 1, cells infected with parental dengue virus; 2, cells infected with dengue virus recovered from clone 2A DNA; 3, cells infected with dengue virus recovered from clone 2A(P) DNA; 4, mock-infected cells; M, protein size markers (sizes in kilodaltons at left). Dengue virus proteins preM, E, NS1, and NS3 are indicated.

bands that were precipitated by dengue virus hyperimmune ascitic fluid. The size and relative intensity of each dengue protein appeared to be similar for progeny viruses and parental virus. Taken together, these results indicate that the recovered dengue viruses were similar to the virus from which the cDNA clone was derived.

DISCUSSION

We constructed stable full-length dengue type 4 virus cDNA clones that were used as templates for production of RNA transcripts that were evaluated for infectivity in cell culture. Evidence is presented that dengue virus was recovered upon transfection of permissive cultured cells with the *in vitro* RNA transcripts of one of six full-length DNA clones tested. To our knowledge, this represents the first demonstration that full-length flavivirus cDNA can be stably cloned and propagated in a cloning vector. In the case of yellow fever virus, the full-length cDNA used for successful production of infectious RNA transcripts was obtained by *in vitro* ligation of two separately cloned DNA segments (22). Instability of plasmid full-length dengue type 4 virus cDNA was initially observed when *E. coli* HB101 was used. Subsequent evaluation of plasmid dengue cDNA stability in other strains of *E. coli* showed that full-length dengue cDNA could be stably amplified in *E. coli* strain BD1528.

The full-length cDNA clone 1A, constructed from DNA segments that were used to establish the dengue type 4 virus sequence, did not yield infectious RNA transcripts. Replacement of the DNA segment in the region between the *Hin*dIII and *Bst*BI sites (nt 44–5069) with a corresponding DNA segment obtained from another set of independent clones from the same cDNA library corrected the defect, as infectious RNA was transcribed from the resulting full-length clone 2A. The failure of 1A DNA to serve as a template for infectious RNA transcripts was probably a manifestation of one or more deleterious mutations that were not detected by restriction enzyme analysis. Such mutations did not apparently affect expression of the encoded polyprotein, since recombinant vaccinia viruses containing sequences for one or more proteins from this region each produced properly processed and functional dengue proteins (15, 23, 26). It should be possible to further localize the site of lethal mutation(s) by using smaller DNA segments for substitution in a manner analogous to the marker rescue study originally performed to map the mutation sites of temperature-sensitive mutants of simian virus 40. (27). Comparison of the sequence in the functionally active segment with the established dengue type 4 sequence should clarify the nature of the deleterious mutation(s). One or more deleterious mutations also occurred in the 3′ region between *Bst*BI and *Asp*718 sites (nt 5069–10,646), as two other separately cloned DNA segments in this 3′ region failed to produce infectious RNA when used together with the functional 5′ sequences to construct a full-length DNA clone. A possibly deleterious mutation in the 3′ sequence of cloned yellow fever DNA was reported (22). This change apparently did not occur in dengue virus in the 3′ region of 2A cDNA, which was stably cloned.

The reduced specific infectivity of dengue virus RNA transcribed *in vitro* might be explained by nonviral 5′ and 3′ sequences if internal sequences were otherwise identical to the virion RNA. The predicted 5′ terminus of RNA transcripts contains an additional G following the added m^7G cap. This additional 5′ sequence was also present in the yellow fever RNA transcripts, which exhibited 2–3% of the specific infectivity of virion RNA (22). Additional nucleotides are also present in the 5′ sequence of infectious RNA transcribed *in vitro* from cDNA of other RNA viruses including poliovirus (18), hepatitis A virus (20), and Sindbis virus (21). In each case, the specific infectivity of the *in vitro* RNA transcripts

was also lower than that of virion RNA. The presence of additional nucleotides at the 3′ terminus might also reduce the specific infectivity of *in vitro* transcribed dengue RNA. While it is possible to remove additional nucleotides at the 3′ template by exonuclease digestion, as was carried out for the yellow fever cDNA template, we found that additional nucleotides present in the 3′ template of dengue cDNA did not abolish the infectivity of the RNA product.

Recovered dengue virus showed a more uniform plaque morphology than did the parental dengue virus, which had been propagated several times in C6/36 mosquito cells. This is not surprising, because recovered virus probably represents a clonal population of the original virus stock. Nonetheless, analysis of dengue proteins produced by recovered virus and by parental virus showed an identical profile. The terminal sequences of virion RNA from recovered virus were not verified by direct analysis. Conceivably, specific sequence recognition and initiation of flavivirus RNA replication coupled with specific packaging of virion RNA could provide a mechanism for precise trimming of the additional nucleotides present in transfecting RNA. For these reasons, it is possible that virion RNA of recovered dengue virus contains authentic terminal sequences despite the fact that additional nucleotides are present in RNA transcripts.

The successful recovery of dengue virus from cloned cDNA-derived RNA transcripts has implications for molecular analysis of dengue virus as well as the development of new dengue vaccine strategies. It is now possible to introduce mutations into dengue cDNA by site-directed mutagenesis and recover dengue virus for biological studies such as identification of regulatory elements involved in transcription, replication, and packaging of dengue RNA, as well as elucidation of the mechanism of polyprotein processing. Molecular techniques now become available for analysis of the antigenic structure of dengue envelope glycoprotein and other protective antigens and for characterization of other viral structural and nonstructural proteins to better understand their functional role in viral replication and possible involvement in dengue immunopathogenesis.

One immediate application of our current findings is in the area of vaccine development. Restriction of dengue virus replication should cause attenuation. For example, it should be possible to produce a panel of dengue viruses that are restricted in viral replication to a varying degree as a consequence of suboptimal polyprotein processing. The polyprotein NS1–NS2A cleavage site has been chosen as the first target for constructing dengue virus mutants that are restricted because of inefficient cleavage (M. Pethel and C.-J.L., unpublished observations). Similarly, it may be possible to isolate dengue virus mutants containing deletions in the coding regions as well as in the 3′ or 5′ noncoding region that result in reduced replicative capacity. Deletion mutants would offer the theoretical advantage of being less subject to reversion of phenotype than amino acid substitution mutants. Dengue virus deletion mutants with altered properties such as temperature sensitivity or reduced virulence could be subjected to further evaluation in monkeys for evidence of attenuation prior to initiation of clinical trials in volunteers. Because of the concern about immune enhancement as the underlying cause for severe dengue (1), the current strategy for immunization against dengue favors the use of a vaccine preparation that contains all four dengue serotypes. In this regard, the full-length cDNA of dengue type 4 virus could be used as a vector for engineering chimeric dengue viruses that contain the DNA sequence coding for the structural proteins of one of the three other serotypes that are substituted for the corresponding DNA sequence of dengue type 4 virus. Such chimeric dengue viruses prepared from the other serotypes would share a common sequence of type 4 nonstructural proteins and the 5′ and 3′ noncoding regions of type 4 if the appropriate mutations conferring satisfactory attenuation could be engineered in these type 4 regions. In this manner it may be possible to construct chimeric dengue viruses of type 1, type 2, and type 3 antigenic specificity that could be included in a live quadrivalent dengue vaccine.

We are grateful to Dr. R. Chanock for encouragement and support of the dengue virus research program; to Drs. B. Falgout and L. Markoff and other staff members in the Section for helpful discussions; to Ms. M. Pethel for providing the dengue cDNA sequences with the silent mutation; to Mr. T. Popkin for expert photographic work; and to Mr. T. Heishman for excellent editorial assistance.

1. Halstead, S. B. (1988) *Science* **239**, 476–481.
2. Vezza, A. C., Rosen, L., Repik, P., Dalrymple, J. & Bishop, D. H. L. (1980) *Am. J. Trop. Med. Hyg.* **29**, 643–652.
3. Wengler, G., Wengler, G. & Gross, H. J. (1978) *Virology* **89**, 423–437.
4. Ada, G. & Anderson, S. G. (1959) *Nature (London)* **183**, 799–800.
5. Nakamura, M. (1961) *Nature (London)* **191**, 624.
6. Stollar, V., Schlesinger, R. W. & Stevens, T. M. (1967) *Virology* **33**, 650–658.
7. Chambers, T. J., Hahn, C. S., Galler, R. & Rice, C. M. (1990) *Annu. Rev. Microbiol.* **44**, 649–688.
8. Mackow, E., Makino, Y., Zhao, B., Zhang, Y. M., Markoff, L., Buckler-White, A., Guiler, M., Chanock, R. & Lai, C. J. (1987) *Virology* **159**, 217–228.
9. Zhao, B., Mackow, E., Buckler-White, A., Markoff, L., Chanock, R. M., Lai, C. J. & Makino, Y. (1986) *Virology* **155**, 77–88.
10. Markoff, L. (1989) *J. Virol.* **63**, 3345–3352.
11. Ruiz-Linares, A., Cahour, A., Després, P., Girard, M. & Bouloy, M. (1989) *J. Virol.* **63**, 4199–4209.
12. Falgout, B., Chanock, R. M. & Lai, C. J. (1989) *J. Virol.* **63**, 1852–1860.
13. Hori, H. & Lai, C. J. (1990) *J. Virol.* **64**, 4573–4577.
14. Chambers, T. J., Weir, R. C., Grakouri, A., McCourt, D. W., Bazan, J. F., Fletterick, R. J. & Rice, C. M. (1990) *Proc. Natl. Acad. Sci. USA* **87**, 8898–8902.
15. Falgout, B., Pethel, M., Zhang, Y. M. & Lai, C. J. (1991) *J. Virol.* **65**, 2467–2475.
16. Preugschat, F., Yao, C.-W. & Strauss, J. H. (1990) *J. Virol.* **64**, 4364–4374.
17. Racaniello, V. R. & Baltimore, D. (1981) *Science* **214**, 916–919.
18. Van der Werf, S., Bradley, J., Wimmer, E., Studier, F. W. & Dunn, J. J. (1986) *Proc. Natl. Acad. Sci. USA* **83**, 2330–2334.
19. Mizutani, S. & Colonno, R. J. (1985) *J. Virol.* **56**, 628–632.
20. Cohen, J. I., Ticehurst, J. R., Feinstone, S. M., Rosenblum, B. & Purcell, R. H. (1987) *J. Virol.* **61**, 3035–3039.
21. Rice, C. M., Levis, R., Strauss, J. H. & Huang, H. V. (1987) *J. Virol.* **61**, 3809–3819.
22. Rice, C. M., Grakouri, A., Galler, R. & Chambers, T. J. (1989) *The New Biologist* **1**, 285–296.
23. Zhao, B., Prince, G., Horswood, R., Eckels, K., Summers, P., Chanock, R. & Lai, C. J. (1987) *J. Virol.* **61**, 4019–4022.
24. Konarska, M. M., Padgett, R. A. & Sharp, P. A. (1984) *Cell* **38**, 731–736.
25. Bancroft, W. H., McCown, J. M., Lago, P. M., Brandt, W. E. & Russell, P. K. (1979) *Pan Am. Health Organ. Sci. Publ.* **375**, 175–178.
26. Bray, M., Zhao, B., Markoff, L., Eckels, K. H., Chanock, R. M. & Lai, C. J. (1989) *J. Virol.* **63**, 2853–2856.
27. Lai, C. J. & Nathans, D. (1974) *Virology* **60**, 466–475.